Master's thesis

NTNU
Norwegian University of Science and Technology
Faculty of Information Technology and Electrical Engineering
Department of Electric Power Engineering

Fanny Skirbekk

# Transformer insulation stressed by power converters

Master's thesis in Energy and Environmental Engineering
Supervisor: Kaveh Niayesh
Co-supervisor: Hans Kristian Meyer and Øystein Hestad
June 2021

NTNU
Norwegian University of Science and Technology

Fanny Skirbekk

# Transformer insulation stressed by power converters

Master's thesis in Energy and Environmental Engineering
Supervisor: Kaveh Niayesh
Co-supervisor: Hans Kristian Meyer and Øystein Hestad
June 2021

Norwegian University of Science and Technology
Faculty of Information Technology and Electrical Engineering
Department of Electric Power Engineering

NTNU
Norwegian University of
Science and Technology

# Preface

This master thesis has been performed at the Department of Electric Power Engineering at the Norwegian University of Science and Technology (NTNU) in Trondheim in the spring of 2021. This project is part of the "FastTrans – Insulation stressed with fast rise time voltages from power electronics"-project, an ongoing research project at SINTEF Energy Research.

The objective of this project has been to study the partial discharges generated in two different transformer insulation systems, i.e. the degradation of the two insulation systems, when stressed by a bipolar voltage pulse compared to a sinusoidal voltage stress.

I would like to thank my supervisor, professor Kaveh Niayesh at NTNU, for his useful feedback and support throughout my work, and my co-supervisor, Øystein Hestad at SINTEF Energy Research, for his support throughout my work.

A huge thanks to my second co-supervisor, Hans Kristian Hygen Meyer at SINTEF Energy Research, for his feedback and help with solving various problems throughout the project, and his assistance when learning to use the different measuring equipment in the lab.

I would also like to thank Lars Lundgaard, Knut Brede Liland, Dag Linhjell, and Torstein Grav Aakre at SINTEF Energy Research and Ivan Semenov at NTNU for their help with solving various problems in the lab, and explaining how the different apparatus work.

Lastly, I would like to thank the people at NTNU's mechanical and electrical workshops for their help when constructing the test object.

Trondheim, June 16$^{th}$ 2021

Fanny Skirbekk

# Sammendrag

For å kunne ta i bruk flere fornybare energikilder i kraftsystemet, med så lite effekttap som mulig, blir stadig mer kraftelektronikk tatt i bruk i kraftsystemet. Kraftelektronikkomformere brukes primært til å skru av og på halvlederbrytere for å oppnå ønsket spenningsform. Dette medfører flere og større spenningspulser, noe som potensielt kan skade den elektriske isolasjonen i kraftsystemet. Partielle utladninger kan føre til ødeleggelse og aldring av isolasjonsystem. Å studere de partielle utladningene i et isolasjonsystem kan derfor gi en god indikasjon på isolasjonens tilstand.

Målet med dette prosjektet har vært å studere de partielle utladningene i to ulike transformatorisolasjonsystemer for å få en bedre forståelse av hvordan transiente spenninger påvirker isolasjonen sammenlignet med sinusformede spenninger. Nytro 10XN, en mineralolje som det er vanlig å bruke i transformatorisolasjon, ble brukt som isolasjonsvæske i det ene systemet. Midel 7131, en biologisk nedbrytbar syntetisk ester som er på vei til å bli et populært alternativ til Nytro i transformatorisolasjon, ble brukt som isolasjonsvæske i det andre systemet. Isolasjonsystemene ble utsatt for en sinusformet spenning for å se hvordan de oppførte seg under "normale" omstendigheter, og en bipolar spenningspuls for å se hvordan systemene oppførte seg når de ble utsatt for raske repeterende spenningspulser.

De partielle utladningene ble detektert og målt ved hjelp av fotomultiplikatorrør og en strømtransformator, for begge spenningsformene. I målingene med den sinusformede spenningen ble Omicron MPD 600 og et høyhastighet videokamera brukt i tillegg. Hovedfokuset har vært på å finne tennspenningen for de partielle utladningene i de to isolasjonssystemene ved de to ulike spenningsformene. I tillegg ble mønstrene i de målte signalene for partielle utladninger og den synlige aldringen av isolasjonen studert.

Tennspenningen for de partielle utladningene, for begge isolasjonsystemene, var mye lavere da systemene ble utsatt for en bipolar spenningspuls. Tennspenningen for hulromsutladninger var omtrent tre ganger høyere da systemene ble utsatt for en sinusformet spenning. Tennspenningen for overflateutladninger var omtrent dobbelt så stor da systemene ble utsatt for en sinusformet spenning. Noen mindre forskjeller mellom de to isolasjonsystemene ble også observert.

De målte tennspenningene indikerer at partielle utladninger, som kan medføre nedbrytning og aldring av isolasjonsystemet, opptrer ved lavere spenninger dersom isolasjonsystemet blir utsatt for raske repeterende pulser sammenlignet med en sinusformet spenning. Resultatene støtter dermed hypotesen om at raske repeterende spenningspulser er mer skadelige for transformatorisolasjon enn det sinusformede spenninger er.

# Abstract

In order to include more renewable power sources in the grid, with as little power loss as possible, an increasing number of power electronics are being integrated as well. The switching of the power electronics leads to more and larger transients, which might harm the electrical insulation. Partial discharges (PDs) can lead to degradation and ageing of the insulation system. Studying the PDs occurring in the insulation can therefore give a good indication to the state of the insulation.

The objective of this project has been to study the partial discharges in two different transformer insulation systems, in order to gain a better understanding of how transient voltage stresses affect the insulation compared to sinusoidal voltage stresses. Nytro 10XN, a mineral oil that is commonly used in transformer insulation, was used as the insulation liquid in one of the systems. Midel 7131, a biodegradable synthetic ester that is becoming a popular alternative to Nytro for use in transformer insulation, was used as the insulation liquid in the other system. The insulation systems were stressed by a sinusoidal voltage in order to see how the systems behave under "normal" conditions, and by a bipolar voltage pulse in order to see how they behave when stressed by fast repetitive voltage pulses.

The PDs have been detected and measured using photomultiplier tubes (PMTs) and a current transformer for both voltage stresses. For the measurements with a sinusoidal voltage stress, Omicron MPD 600 and a high-speed video camera was used as well. Finding the partial discharge inception voltage (PDIV) for the two insulation systems under the two different voltage stresses has been the main focus. The patterns in the PD-plots and the visible ageing on the insulation caused by the PDs have also been studied.

The PDIV was found to be much lower, for both insulation systems, when the systems were stressed by a bipolar voltage pulse. The PDIV for void discharges was approximately three times higher when the systems were stressed by a sinusoidal voltage. The PDIV for surface discharges was approximately twice as high when the insulation systems were stressed by a sinusoidal voltage. Some slight differences were observed between the behaviour of the two insulation systems.

The difference in PDIV suggests that PDs, which might lead to deterioration and ageing of the insulation systems, occur at lower voltages if the insulation system is stressed by fast repetitive voltage pulses compared to if it is stressed by a sinusoidal voltage. The results have therefore reaffirmed the hypothesis that fast repeating voltage pulses are more harmful to transformer insulation than a sinusoidal voltage.

# Contents

# List of Figures

# List of Tables

# List of Abbreviations

| | |
|---|---|
| AC | Alternating current |
| DC | Direct current |
| DUT | Device under test |
| HV | High voltage |
| MOSFET | Metal–oxide–semiconductor field-effect transistor |
| PD | Partial discharge |
| PDEV | Partial discharge extinction voltage |
| PDIV | Partial discharge inception voltage |
| PMT | Photomultiplier tube |
| PRPDA | Phase resolved partial discharge analysis |

# 1 Introduction

In Norway, the amount of installed and produced solar and wind power in the power grid has increased almost exponentially in the last five years, see Figure 1i and Figure 1ii. This increase in installed and produced power from renewable power sources is not only the trend in Norway, it is also the trend globally, see Figure 1iii. The increased use of renewable power sources is an important part of making the power grid, and subsequently every process that uses power from the grid, more sustainable and better for the environment. This is important in order to prevent drastic climate change and environmental damage.

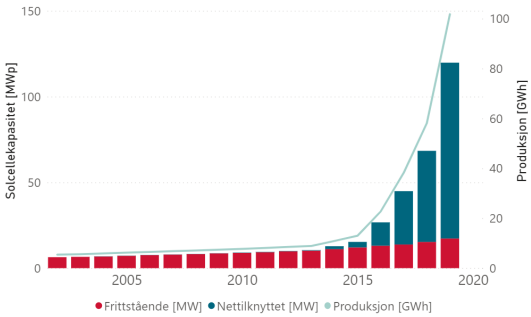


*(i) The capacity and production of solar energy in Norway, 2002-2019. The figure is from [1]. The left y-axis is the capacity in MWp, the right y-axis is the production in GWh. Red bar: Unconnected [MW]. Blue bar: Connected to the grid [MW]. Grey line: Production [GWh].*

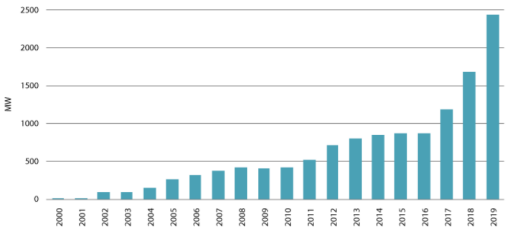


*(ii) The total installed wind power in Norway, 2000-2019. The figure is from [2]. The y-axis is installed power in MW. The x-axis represents the years 2000-2019.*

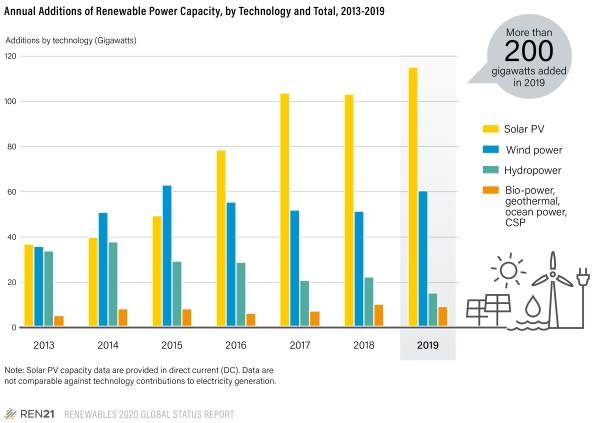


*(iii) The annual additions of renewable power capacity globally, 2013-2019. Yellow bar: Solar PV. Blue bar: Wind power. Grey/Green bar: Hydropower. Orange bar: Bio-power, geothermal, ocean power, CSP. The figure is from [3].*

*Figure 1: The amount of installed and produced renewable power has increased in recent years, both in Norway and globally [1], [2], [3].*

In order to use these renewable power sources in the grid, with as little power loss as possible,

more power electronics have to be integrated in the grid as well. To reduce the power losses as much as possible, power electronics are developed for ever higher voltages and faster switching. This is an important development for the environment, but this change in the power system is not without its problems.

The power grid consists of a variety of different power equipment. All of these components are vital for the power grid to function. In order for these components to function properly, they need to have their electrical insulation intact. The increased use of power electronics changes the behaviour of the grid because the switching leads to more and larger voltage transients. Large and frequent transients are known to be harmful for electrical insulation materials. So, the increased use of power electronics in the grid poses a potential threat to the electrical insulation of the power components, and thus a potential threat to the entire grid itself. How the fast and frequent switching of the voltage affect different insulation systems and materials should therefore be studied in order to determine the consequences of the increased use of power electronics.

For this master thesis, transformer insulation was used because transformer oil is transparent, making it possible to measure the light emitted from the discharges caused by the voltage stress. The behaviour of the insulation was studied both when stressed by a bipolar voltage pulse, i.e. a transient voltage stress, and when stressed by a sinusoidal voltage. The sinusoidal voltage stress was used in order to mimic "normal" conditions, since this is the type of voltage the components in the power grid typically are designed to withstand. Two different transformer insulation systems were studied, pressboard impregnated and submerged in Nytro 10XN and pressboard impregnated and submerged in Midel 7131, in order to compare these insulation systems.

The bipolar voltage pulse is expected to be more damaging for the insulation systems than the sinusoidal voltage. The two insulation systems are expected to behave fairly similarly to each other.

## 1.1 Structure of the report

The objective of this master thesis has been to study the partial discharges (PDs) in two different transformer insulation systems, in order to gain a better understanding of how transient voltage stresses affect the insulation compared to sinusoidal voltage stresses. Finding the partial discharge inception voltage (PDIV) for the two insulation systems under the two different voltage stresses has been the main focus. The patterns in the PD-plots and the visible ageing on the insulation caused by the PDs have also been studied.

In chapter 2, the theoretical background for the measurements is presented. The method, including the lab set-ups, test object, and how the measurements were performed, is presented in chapter 3. The results are presented in chapter 4, followed by the discussion of the results in chapter 5. The conclusion is found in chapter 6, and suggestions for further work are given in chapter 7.

# 2 Theory

In the project preceding this thesis [4] the state of the art and related work were reviewed, and the relevant background material was identified. The presentation from the project report has been added below. A short section on partial discharge measurements for very-high frequency and ultra-high frequency signals has been added, since this topic is relevant for this thesis. A more thorough explanation of how phase resolved partial discharge analysis (PRPDA) plots can be interpreted has also been added.

## 2.1 Oil-paper insulated transformers

Combining oil and paper to make electrical insulation is the most common method for insulating transformers [5]. This type of insulation has many advantages, like high breakdown strength, good cooling and no cavities (if the liquid has filled all of the cavities in the paper) [6]. There are also some disadvantages to this insulation system, namely that it is sensitive to pollution (moisture, particles etc.), difficult to repair, and that the liquid can be inflammable [6].

Several different liquids can be used as the oil-part of the transformer insulation. The choice of liquid is based on economic and technical considerations, as when choosing what insulation system to use [6]. Economic considerations are here meant in a wider sense, including potential costs related to environmental damage.

The dominating liquid for transformer insulation, both in the past and present, is mineral oil [7]. Since mineral oil has been dominating for a long time, there is some data and knowledge about how this insulation behaves [7]. Other liquids are, however, becoming more popular and are now being used for a variety of transformers, increasing the knowledge of how these liquids behave. Especially esters, both synthetic and natural, and silicon oil are being used as alternative fluids [7]. There are several reasons why mineral oil has gotten competition from other liquids in recent years, where environmental reasons are the most prominent.

### 2.1.1 Nytro 10XN vs Midel 7131

Nytro 10XN is a mineral oil that is commonly used in transformer insulation. It is transparent and colorless, and is composed of different types of hydrocarbons [7].

Midel 7131 is a biodegradable synthetic ester. This colorless and transparent liquid is derived from chemicals, with a very stable chemical structure because the acid-groups in the molecules usually are saturated [7], see Figure 2. Midel is becoming a popular alternative to Nytro for use in transformer insulation.

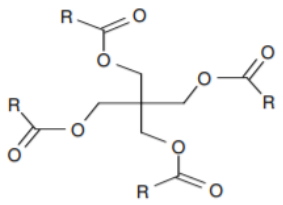


*Figure 2: The molecular structure of a synthetic ester. The figure is from [7].*

In the following paragraphs, different aspects of

Nytro 10XN and Midel 7131 are compared.

**Biodegradability:**
Biodegradability is defined as the liquid's ability to be metabolised, i.e. degraded, by the microbes that naturally inhabit soil and water, should there be a spillage or leakage of the liquid into the surrounding area [7]. It is advantageous, from an environmental point of view, for insulation liquids to degrade and disappear by themselves. It is also preferable from an economic point of view, since it reduces the need for expensive clean up operations [7].

One advantage in using Midel, or another synthetic ester, instead of a mineral oil is that it is classified as readily biodegradable, whilst Nytro is classified as slow to biodegrade [7]. Two criteria have to be satisfied in order for a substance to be classified as readily biodegradable:

- When the degradation has exceeded 10%, 60% of the degradation has to occur within the next 10 days [7].
- Minimum 60% of the biodegradation has to occur within the $28^{\text{th}}$ day of the test [7].

The OECD 301 series of tests is used for classifying the biodegradability of different insulation liquids [7]. The biodegradability of mineral oil and synthetic ester, as well as natural ester and silicone oil, is visualised in Figure 3.

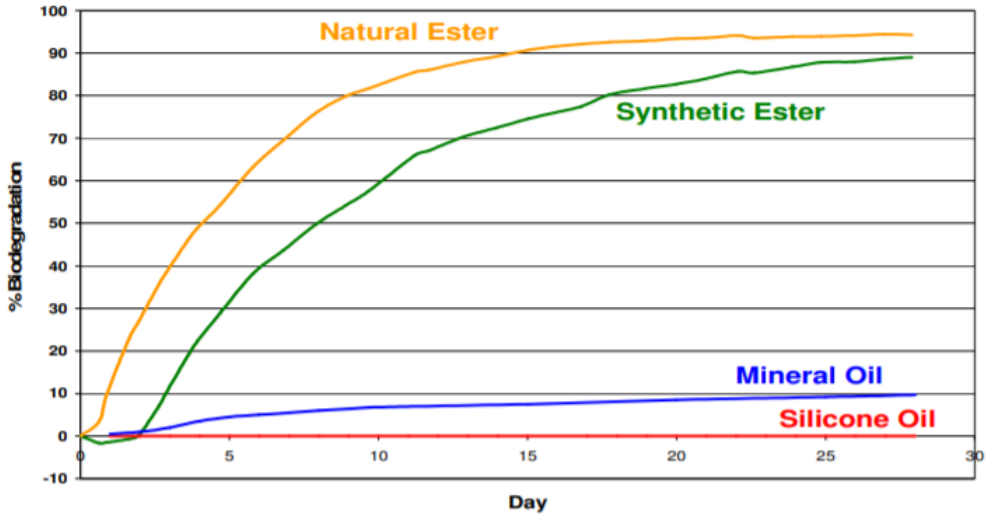


*Figure 3: Biodegradation of different insulation liquids. The figure is from [7].*

**Flash point:**
The liquids used in liquid-paper insulation can be inflammable, as mentioned previously. This is a concern, especially in installations placed in populated areas, in tunnels, on ships and in other locations where fire safety is of utmost importance. The potential costs of a fire in transformer oil includes the risk of human lives, damage to property, down-time costs, insurance claims, and time and cost of transformer replacement [7].

The lowest temperature where a liquid forms enough vapour to "flash", i.e. temporarily ignite, is defined as the flash point [8]. The fire point is a temperature above the flash point at which the vapour formed by the liquid is sufficient to support combustion [8]. Using insulation with high flash point and fire point is therefore preferable. Synthetic esters, like Midel, are better than mineral oils like Nytro also in this regard: Both the flash point and the fire point are significantly higher for synthetic esters compared to mineral oil, see Table 1 [7].

*Table 1: Flash point and fire point for mineral oil and synthetic ester [7].*

| | **Mineral oil** | **Synthetic ester** |
|---|---|---|
| **Flash point** | 160°C - 170°C | >250°C |
| **Fire point** | 170°C - 180°C | >300°C |

**Electrical properties:**
Despite both flash point and biodegradability being important factors to consider when choosing insulation materials, the electrical properties of the materials used in electrical insulation systems are by far the most important factor. There has been some research on the electrical properties of the different insulation liquids, but there is still a lot that is currently unknown and uncertain.

Nytro 10XN and Midel 7131 have different dielectric constants, i.e. different relative permittivity. According to [9], Midel 7131 and kraft paper impregnated in Midel 7131 have higher relative permittivities than transformer oil (Nytro) and kraft paper impregnated in transformer oil, see Table 2.

*Table 2: Relative permittivity of Midel 7131 and transformer oil, both alone and when used to impregnate kraft paper [9].*

| **Insulation material** | **Relative permittivity** |
|---|---|
| Transformer oil | 2.24 |
| Transformer oil/paper | 3.69 |
| Midel 7131 | 3.29 |
| Midel 7131/paper | 4.20 |

The viscosity of the two oils also differs, which might affect electrical properties like charge density, although this is unlikely according to [10], and ageing factors like heating. The heating will be affected by the viscosity because the cooling of transformers is done by heat transfer (convection) from the oil to the surrounding area [10]. The heat transfer will be less efficient for fluids with higher viscosity [7], [10]. Mineral oil usually has lower viscosity than synthetic esters.

Esters were found to generate more charges when circulating in the transformer [10], i.e. to have a higher charge density than mineral oil. The cause of this is unclear, but it might be connected to the molecular structure of the oils [10]. Whether this constitutes a problem for high voltage transformers or not, is unclear, since the amount of these charges ending up on the pressboard is unknown [10]. Charge accumulation on cellulose is, however, known to initiate partial discharges (more on partial discharges in section 2.2) [10].

According to [9], the breakdown voltages of Midel and Nytro are fairly similar, which one that has the higher value depends on the voltage stress, and whether the liquid is alone or in an insulation system. The partial discharge inception voltage, explained in section 2.2, was also found to be fairly similar for the two liquids [7].

Despite the inception voltage being similar, the partial discharge patterns that occur when the voltage stress is increased above the voltage inception level have been found to differ between mineral oil and Midel [11]. Midel was found to result in more and larger discharges than the mineral oil [11]. But there is still more research that needs to be done on this subject in order to be sure of the different behavior of Midel and Nytro.

### 2.1.2 Moisture in the insulation

Liquid-paper insulation is, as previously mentioned, sensitive to moisture. According to [6], the rate of ageing of oil-impregnated paper is approximately proportional to the moisture content of the insulation. This is because the dielectric strength of the material is reduced by the increase in moisture content, as Figure 4 illustrates. From this it can be seen that the breakdown voltage is reduced with increased relative moisture content, regardless of the type of insulation liquid.

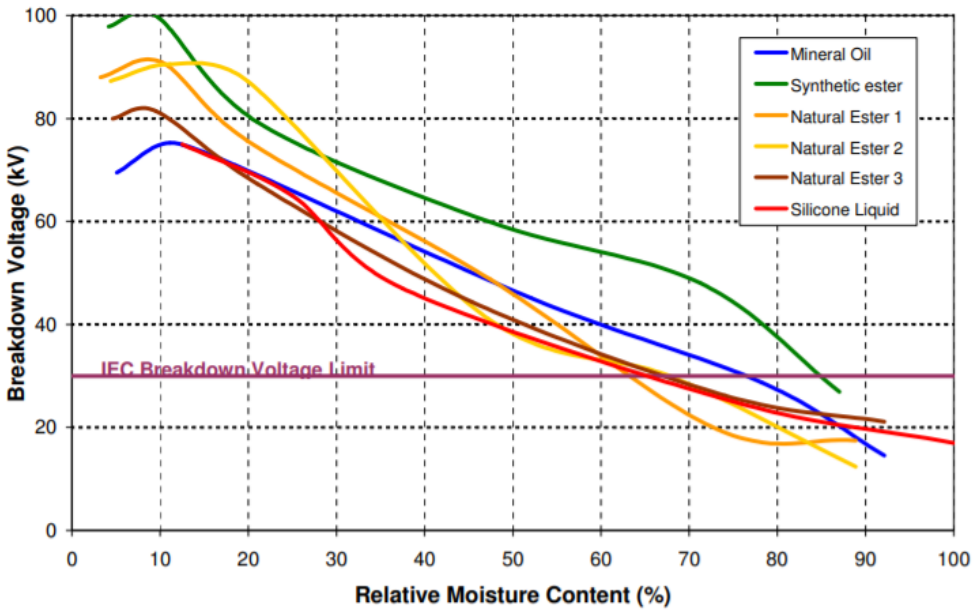


*Figure 4: The breakdown voltage of different liquids, as a function of the relative moisture content. The figure is from [7].*

Before use, the moisture and gas should therefore be removed from the paper by using a combination of heat and vacuum [6]. Dried and degassed oil should then be used to impregnate the paper, thereby preventing moisture and gas from entering the dried paper [6]. There might still be some moisture and gas in the system after this procedure, but as long as the moisture content is below 0.5% the insulation is considered to be dry [12].

Moisture content of 2-3% is considered to be middle dry, and 4-5% is considered to be wet [12].

The insulation should be kept in a closed environment in order to prevent moisture from entering the system [6]. Nevertheless, some moisture might still enter the system. The moisture content of transformer insulation should therefore be measured regularly while the transformer is in service, in order to prevent the insulation from ageing due to moisture.

## 2.2 Partial discharges

A partial discharge, PD, is a local breakdown that does not completely bridge between two conductors, see Figure 5. This includes both external discharges, e.g. corona and streamers, and internal discharges, e.g. void-discharges [13]. Over time, the partial discharges will lead to deterioration and ageing of the insulation.

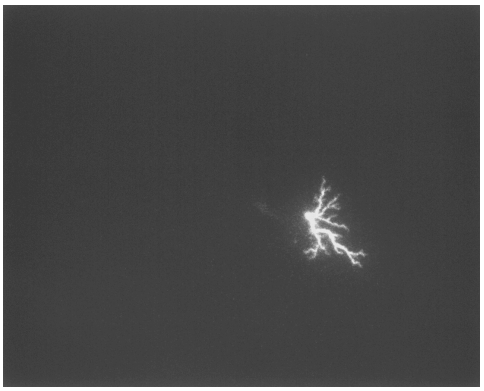

*Figure 5: A partial discharge occurring along the interface between Nytro-impregnated pressboard and Nytro.*

The severity and speed of the deterioration depends on several different factors including: The type of insulation, the strength of the electric field, the type of discharge, the size of the discharge, and the recurrence rate of the PDs [13].

**Requirements for PDs to occur:**
In order for a partial discharge to occur, the withstand strength of the insulation has to be low enough for the insulation to break down [13]. This is highly dependent on the type of insulation material used and the state of the insulation. A gas-filled cavity in the oil-paper-insulation will, for instance, have a lower withstand strength than the insulation surrounding it. The thickness of the paper and the type of liquid used will also affect the withstand strength of a liquid-paper insulation system.

An electric field that is strong enough for a local electron avalanche to occur is also required for partial discharges to happen [13]. Sharp points, metal particles, and free charges all contribute to this, since they enhance their surrounding electric field. Nevertheless, it is important to remember that partial discharges are a stochastic phenomenon. Whether a PD will occur or not can therefore not be determined solely by the withstand strength and the electric field, the stochastic nature of the PDs have to be taken into account as well.

**Inception and extinction voltage:**
The voltage amplitude at which the partial discharges start occurring is called the partial discharge inception voltage (PDIV). When the voltage amplitude is reduced to the partial discharge extinction voltage (PDEV), the partial discharges stop [6]. The inception voltage is usually higher than the extinction voltage. Both limits will depend on the insulation system, the electrical stresses and the stochastic nature of the PDs.

**PDs in oil-paper insulation:**
In a liquid-paper insulation system, the paper usually has higher permittivity than the liquid part of the insulation [6]. This results in the liquid part of the insulation getting a higher stress than the paper part of the insulation system, since the dielectric strength of the liquid is lower than that of the paper [6]. Partial discharges are therefore more likely to occur in the liquid part of the insulation, either in liquid-filled cavities in the paper, or as streamers in the oil or streamers along the surface of the paper on the interface between the paper and the liquid [6]. If the PDs occur over a longer period of time, erosion of the paper-surface or the walls of the cavity might begin [6]. This erosion might develop into pits, and eventually electric trees might start to form from these pits [6]. Eventually, this might lead to breakdown.

If the oil-paper insulation and electrode are placed in a similar way to the configurations depicted in Figure 6c, then the PDs will probably not occur directly underneath the electrode since the oil-layer under the electrode is very thin and very thin layers of oil have high dielectric strength [6].

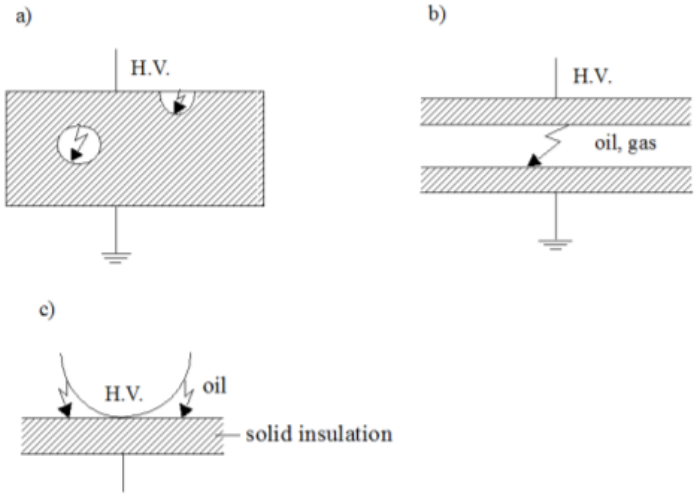


*Figure 6: Partial discharges in different oil-paper configurations. The figure is from [6].*

### 2.2.1 Types of PD

There are several different types of partial discharges. According to [14] they can be divided into the six groups depicted in Figure 7. The two following types of partial discharges are the two types that are most likely to occur in oil-paper insulation.

**Void discharges:**
Void discharges are discharges that occur inside a gas or liquid filled void in solid insulation, or inside a gas-filled bubble in a liquid. Voids usually have strong internal electric fields due to the different dielectric properties of the material inside and outside of the void. The strong electric field increases the chances for PDs. These discharges usually occur at the rising edge of the voltage [13].

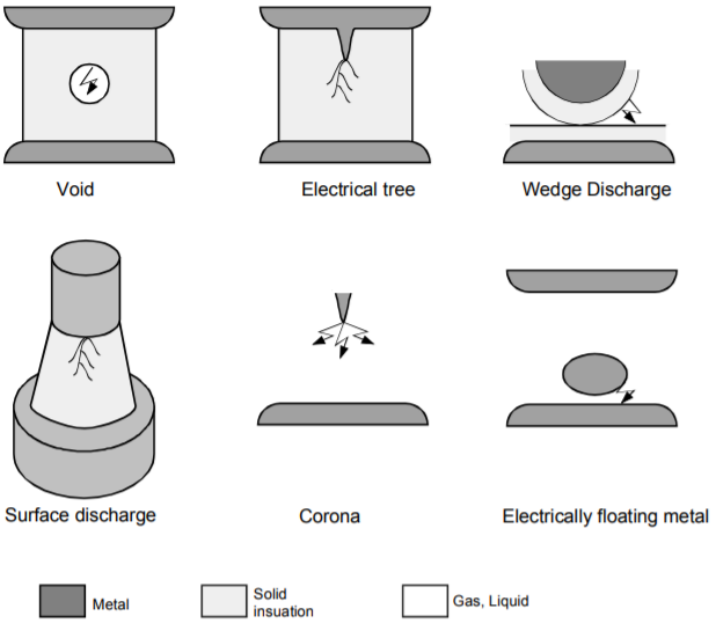


*Figure 7: Types of partial discharges. The figure is from [14].*

**Surface discharges:**
Surface discharges are a type of streamers, and occur on the interface between the solid insulation and the gas/liquid insulation [13]. They are often caused by impurities in the insulation liquid and sharp points on the electrodes [15]. These discharges usually occur close to the peak of the voltage [13]. Typically, surface discharges require a stronger and more inhomogeneous external electric field than void discharges in order to occur. This is because surface discharges occur on the surface, which subsequently does not have an internal field that can help cause PDs.

According to [16], the branching of the streamers, i.e. the phenomena of streamers dividing into different branches, is proportional to the relative permittivity of the solid insulation, and inversely proportional to the thickness of the solid insulation. The permittivity of the solid insulation might therefore affect the behavior of the streamers.

**Characterising partial discharges:**
One common way of characterising partial discharges is by recording and counting the pulses relative to the phase of the voltage, and to find the extinction and inception voltage [15]. The partial discharges can then be analysed using phase resolved partial discharge analysis, PRPDA [15]. The phase location, repetition rate and magnitude of the partial discharges are analysed when PRPDA is used [15]. The result can be plotted, and the type of PD can be determined based on the plot because different types of PD have different PRPDA signatures [15].

According to [17], the degradation of insulation systems due to partial discharges can be described by using the following three measurements:

1. The phase angle (of the voltage) where the PD occurs. This indicates the ignition and extinction conditions of the defect with regard to the electric field.
2. The magnitude trend of the PD can be used as an indication of the rate of dielectric deterioration.
3. The number of pulses gives an indication of the severity of the defect. Periods of continuous PD activity are considered to be more harmful than periods of irregular activity.

All three quantities can, as mentioned, be found from a PRPDA plot, and together they can be used to characterize and better understand the PD activity [17].

Another interesting aspect to observe in PRPDA plots is whether there are any symmetries between the two half periods of the voltage in the plot. There are three types of symmetry that can occur in a PRPDA plot: magnitude, shape, and phase [17]. Magnitude symmetry is when the PDs have the same magnitude in the positive and negative half period. Shape symmetry means that the shape/pattern created by the PDs is the same in both half periods. Magnitude and shape symmetry are indications of the defect, i.e. the place where the PDs occur, being physically symmetrical [17]. Phase position symmetry is when the PDs occur at the "same" phase angles in the two half periods, e.g. the peak is at the "same" phase angle in the two half periods. This is an indication that the field conditions for PD are similar for both positive and negative polarities [17].

Void discharges can usually be seen as a band between the zero crossing and the voltage peak, often increasing in magnitude as the voltage increases (absolute value). The pattern can therefore end up looking a bit like rabbit ears or grass bending in the wind. If the void is symmetrical, then magnitude and phase symmetry of the PDs can be expected from the PRPDA plot.

Surface discharges will, as mentioned, normally occur near the peak of the voltage. In the PRPDA plot, this can be observed as "clouds" of PDs starting right before and ending right after the voltage peak, for both half periods.

## 2.3 Measuring partial discharges

Partial discharges are one of the most important ageing- and failure-mechanisms in insulation systems [13]. Measuring the PDs is therefore very useful for condition assessment and quality control. Partial discharges are measured in Coulomb, C.

When a partial discharge occurs, locally stored energy in the insulation is transformed into other forms of energy, see Figure 8 [13]. It is these other forms of energy that are measured when a partial discharge is measured, since PDs can not be measured directly. Which process that should be measured and observed depends on the system that is being studied, because different geometries and defects result in different phenomena and signatures [13]. The choice of measuring technique also depends on the location of the measurements, e.g. different methods are preferred in the field where there is a lot of noise, compared to in a controlled lab environment. Light emission and current pulses, as well as the magnetic field

induced in a current transformer by the current pulse, are the PD phenomena that will be studied in this report.

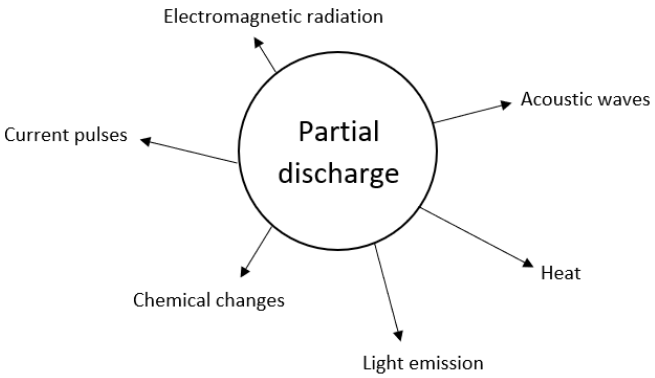


*Figure 8: The other forms of energy that the local energy is transformed into when partial discharges occur [13]. Reproduced from [14].*

### 2.3.1 Current pulses

When a partial discharge occurs, the voltage will drop over the area with the PD [6]. This results in a current pulse that can be observed at the connected terminals [13]. In order to measure this pulse it is common to use a measuring impedance. The measuring impedance is placed in parallel with the test object. The voltage that the current pulse generates across the measuring impedance can then be measured [13]. Based on this voltage, the apparent charge of the partial discharge can be calculated. The apparent charge is defined as the charge that is required from the external circuit for restoring the voltage across the test object when a partial discharge has occurred [6].

This method works well for systems with low frequency voltages. For high frequency voltages, however, it is difficult to distinguish the partial discharges from the harmonics in the system voltage, and other methods should consequently be used instead [13].

**The abc-equivalent:**
The principle of how the electrical signal from void discharges can be detected, if the insulation is stressed by an AC voltage, is shown by the abc-equivalent, see Figure 9. The idea behind this model is that the void, the insulation in parallel with the void and the insulation in series with the void can be described by a network of capacitances [6], [13]. In the abc-model, $a$ is the capacitance representing the insulation in parallel with the cavity, $b$ represents the capacitance of the insulation in series with the cavity, and $c$ represents the capacitance of the cavity itself [6], [13]. $c$ is much smaller than $b$, which is smaller than $a$: $c << b < a$. The voltage source is represented by a Thévenin equivalent with voltage $u(t)$ and impedance $Z_i$.

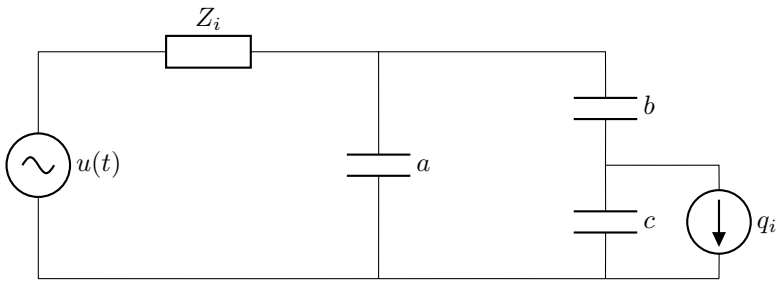


*Figure 9: The abc-equivalent. Reproduced from [6].*

When a discharge occurs, the voltage across the void will drop rapidly from the ignition voltage, $U_{s0}$, to the remnant voltage, $U_{r0}$:

$$\Delta U = U_{s0} - U_{r0} \tag{1}$$

This is equivalent to a charge, $q_i$, being applied over $c$ from the external circuit [6]. The current in the external circuit, caused by the partial discharge, can be considered to be zero during the discharge time, if the assumption that $Z_i$ is mainly inductive and without parallel capacitance is used [6]. During the discharge time, the equivalent circuit is as in Figure 10.

However, the charge, $q_i$, across $c$ cannot be observed from the external circuit. But a small voltage drop across $a$, the insulation in parallel, can be measured:

$$\Delta U_a = \frac{b}{a+b} \cdot \Delta U \approx \frac{b}{a} \cdot \Delta U \tag{2}$$

A transient current from the external circuit restores the voltage across the test object right after the partial discharge has occurred [6]. The aforementioned apparent charge represents this transient current:

$$q_a = \Delta U_a \cdot \left( a + \frac{bc}{b+c} \right) \approx \Delta U_a \cdot a \tag{3}$$

By combining Equation 2 and Equation 3, the apparent charge can be represented by the capacitance in series with the void multiplied with the voltage drop across the void during the partial discharge:

$$q_a = b \cdot \Delta U \tag{4}$$

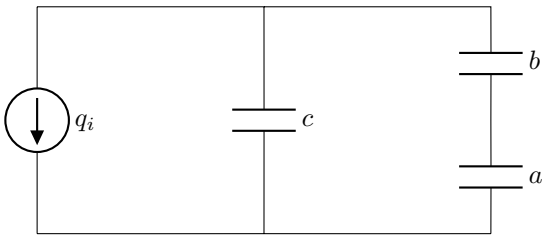


*Figure 10: The abc-equivalent during the partial discharge. Reproduced from [6].*

### 2.3.2 Magnetic field induced by the current pulse

As mentioned in section 2.3.1, the PD results in a voltage drop which results in a current pulse. If a current transformer is connected around the conductor where the current pulse flows, the current pulse will induce a magnetic field, and hence also a current, in the current transformer.

A high frequency current transformer should be used, since the signal from the partial discharge contains high frequencies. For this project, a current transformer with bandwidth 1200 Hz to 500 MHz was used.

The signal from the current transformer can then be sent to a spectrum analyzer. By sweeping over a large spectrum of frequencies and using the hold max function on the spectrum analyzer, the dominating frequency within the partial discharge signal can be determined. The frequency that dominates the voltage signal in the system can be avoided. Thus, this method works well both for systems with low frequency voltages and for systems with high frequency voltages.

When the dominating frequency has been determined, the spectrum analyzer can be used as a bandpass filter. The desired part of the input-signal is then folded down in frequency by using the spectrum analyzer as a down-converter. This is done by using the spectrum analyzer's zero span-function whilst filtering the signal. This makes it easier for equipment with limited bandwidth to interpret the signal. The signal can then be sent to for instance an oscilloscope, where the signal can be studied further.

### 2.3.3 Light emission

If the partial discharge occurs outside the solid part of the insulation, for instance as a streamer, the PD can be observed by the light emission it is causing.

The photons that are emitted can be detected by a photomultiplier tube (PMT). A PMT is a measuring device that counts all of the photons entering the photomultiplier tubes [18]. The PMT converts radiation from the visible, infrared and ultraviolet regions of the electromagnetic spectrum into electrical signals by using photo-emission and then amplifying the signals by using secondary emission [18], i.e. it converts the photons from the PD into electrical signals. These electrical signals can then be used to calculate the apparent charge of the partial discharge.

The light emission can also be observed by a camera. It is, however, only possible to observe and not to measure the PDs if one uses a camera to detect the light emission. If a camera is to be used for PD measurements, it has to be able to record the low-light and fast phenomena that partial discharges are. For this project, a Lambert HiCAM 500 was used. This is a high-speed video camera that can, with a signal to noise ratio of 10, record a single photon [19]. And it is possible to gate the camera's two image intensifier stages with shutter times down to 40 ns [19].

Measuring and observing the light emission from partial discharges only works if the discharges occur in transparent, or somewhat transparent, insulation materials, i.e. on the

surface of solid insulation and inside transparent liquids and gases. Thus, streamers are easily observed by the light emission, whilst void discharges inside cavities in the solid insulation are impossible to measure by the emitted light.

This technique, measuring the light emission in order to measure the partial discharges, works both for low and high frequency voltages, since the light emission is independent of the voltage shape.

# 3 Method

## 3.1 Measurement set-up

Two different set-ups were used: One for measurements with a sinusoidal shaped source voltage, and one where the voltage source produced a bipolar voltage pulse.

### 3.1.1 Sinusoidal voltage

A resonance test circuit was used in order to study the partial discharges in insulation samples subjected to sinusoidal high voltage waves, with minimal required power and harmonic distortion. A resonance circuit does not require reactive power from the source since the impedance of the circuit, as seen from the source, is purely resistive at resonance [20]. The resonance frequency can be varied by either varying the high voltage coupling capacitance or by using compensation reactors, or both [20]. The resonance frequency of the set-up was found to be 30Hz.

Figure 11 depicts the test circuit used to perform the measurements with the sinusoidal voltage stress. This circuit has been discussed and explained in detail in [15] and [20]. A picture of the lab set-up is included in Figure 12.

Both the high voltage part of the circuit and the test object were placed inside a metal cabinet that works as a Faraday cage, as seen from Figure 11 and Figure 12. The two PMTs are placed on the outside of the cabinet, with a tube going into the cabinet through a hole in order to register the photons. The two PMTs were placed on opposing sides of the cabinet, as Figure 11 and Figure 12 suggest. The signals from the two PMTs were then sent to a coincidence circuit, where the two signals were combined into one and sent to the PD measuring system.

The Lambert HiCAM 500 camera, marked as iCCD in Figure 11, was place directly above the test object, with the lens pointing down towards the test object, as seen from Figure 12. The focus of the camera was adjusted to be the top of the pressboard in the test object. TimeViewer and Lambert Intensifier Control Software were used to control the camera and take pictures. The voltage amplitude and frequency were controlled by the Tektronix AFG3052C signal generator situated outside of the cabinet, see Figure 11 and Figure 12.

The MagneLab current transformer (serial number 24530) used for the measurements is not depicted in Figure 11, but can be seen from Figure 12. It was placed above the test object, i.e. on the low voltage side of the test object. The current transformer could measure signals between 1200 Hz and 500 MHz. The current transformer was connected to a spectrum analyzer, see Figure 12, which was used to filter the signal from the current transformer, as described in section 2.3.2. The signal was then sent from the spectrum analyzer to an oscilloscope, see Figure 12, in order to study the signal.

Omicron MPD 600 was used to measure the electric signal caused by the PDs, i.e. the current pulse. This device measured the voltage over the coupling capacitance, C, see Figure 11. The two PMTs were used to measure the light emitted by the PDs.

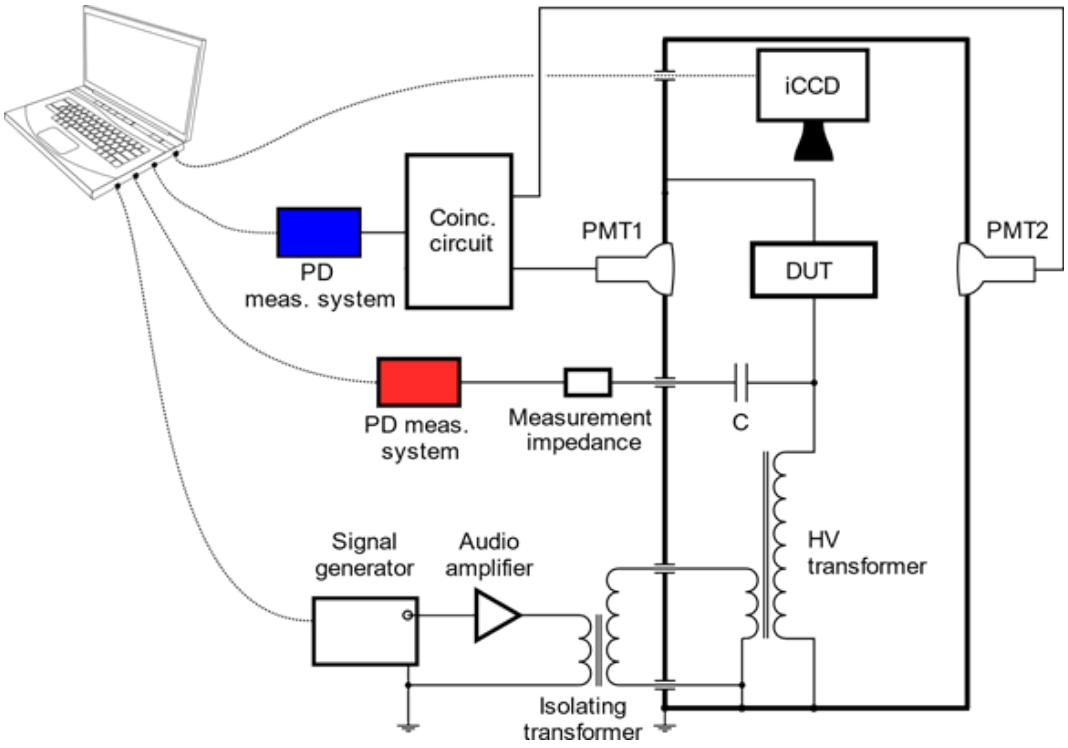


*Figure 11: The circuit used for the measurements with the sinusoidal voltage. The DUT is the device under test, i.e. the test object. The figure was made by Dr. Ivan Semenov at the Department of Electric Power Engineering at NTNU.*


*Figure 12: The lab set-up for the measurements with a sinusoidal voltage stress. 1: The coincidence circuit for the PMT signals. 2a&b: The coolers for the PMTs. 3: The Lambert HiCAM 500 camera. 4: The Omicron MPD 600. 5a&b: The power sources for the PMTs. 6: The signal generator. 7: The computer (just outside of the picture). 8: The oscilloscope. 9a&b: The PMTs. 10: The current transformer. 11: The test object. 12: The spectrum analyzer. 13: The HV transformer.*

The measurements from the PMTs and Omicron were sent to a computer outside of the cabinet. The Omicron software, MPD and MI 1.6.7.1, was used to collect the data, both from the Omicron and the PMT. Both the charge of the test object, which is dependent on the capacitance, and the voltage were calibrated in order to make the Omicron system interpret the measured values correctly. They were calibrated one at a time, by sending in a known signal (either voltage or charge, depending on what was to be calibrated), and then comparing this with the measured value. By dividing the known value with the measured value, a division factor, $d$, was obtained which could be used to calculate the correct value in future tests,

$$q_{\text{real value, test}} = \frac{q_{\text{meas. value, calibration}}}{q_{\text{real value, calibration}}} \cdot q_{\text{meas. value, test}} = d \cdot q_{\text{meas. value, test}} \tag{5}$$

#### 3.1.1.1 Omicron MPD 600:

The Omicron MPD 600 uses the IEC 60270 standard for measuring PDs, and was used for measuring the electrical signal generated by the PD pulse. It measured the voltage over the coupling capacitance, C, see Figure 11. This signal was then integrated and divided by the resistance in order to obtain the size of the PD [21], using the formula

$$q = \frac{1}{R} \int_{t1}^{t2} u(t)dt \tag{6}$$

The frequency integration used by the Omicron system was at 250 kHz ± 150 kHz.

The photons observed by the PMTs were converted into an electrical signal. This signal was also sent into the Omicron system where it was integrated using Equation 6.

### 3.1.2 Bipolar voltage pulse

Figure 13 depicts the circuit used for the measurements with the bipolar voltage pulse. The circuit has been discussed and explained in detail in [22]. Figure 14 shows how the measuring devices were connected with the circuit in Figure 13. A picture of the lab set-up is included in Figure 15.

The pulse source was based on a solid state switch which switched between two different DC voltages. This was used to generate a symmetric square wave, with zero DC offset. In order to make it comparable to the sinusoidal set-up, the frequency of the signal was set to 30 Hz, and the generated pulse was symmetric and bipolar. The solid state switch was a Behlke HTS 651-03 GSM using MOSFET technology [22]. The switch, two capacitor banks, charging resistors and current limiting resistors were situated in a metal cabinet, see Figure 15. Both the cooler for the switch and the power source for the internal control electronics of the switch were located in a box on the outside of the cabinet. The source cabinet was connected to the experiment cabinet through an enclosed connection, see Figure 13. In order to get voltage amplitudes large enough to get PDs, the current limiting resistance in the battery was set to 2 kΩ. The rise time of the voltage pulse was therefore between 200 and 400 ns, depending on the voltage amplitude, since the capacitance of the test object was low [22].

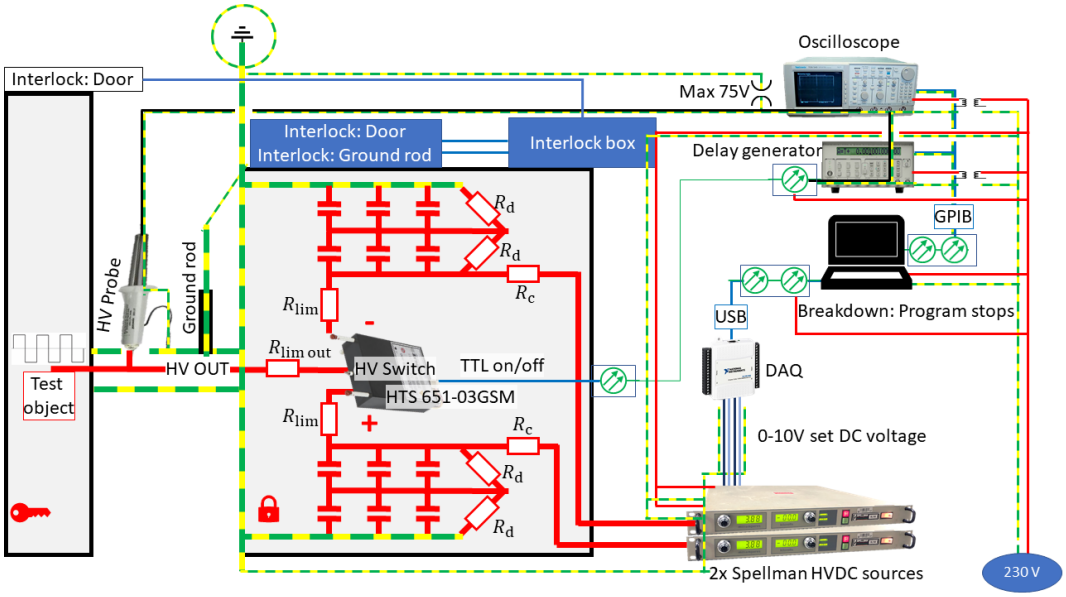


*Figure 13: The circuit used for the measurements with the bipolar voltage pulse. This circuit diagram does not show the set-up of the devices used to measure the partial discharges, for that part of the circuit see Figure 14. The figure was made by Dr. Torstein Grav Aakre at SINTEF Energy Research.*

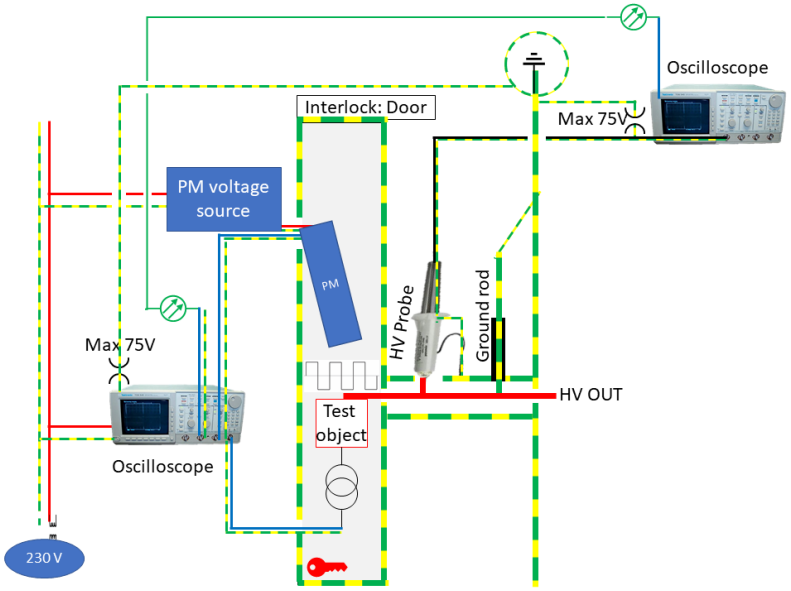


*Figure 14: The measurement set-up used for the measurements with the bipolar voltage pulse. The spectrum analyzer is not included in this figure. It was connected between the current transformer and the oscilloscope, and used as a filter as explained in section 2.3.2. The figure was made by Dr. Torstein Grav Aakre at SINTEF Energy Research.*

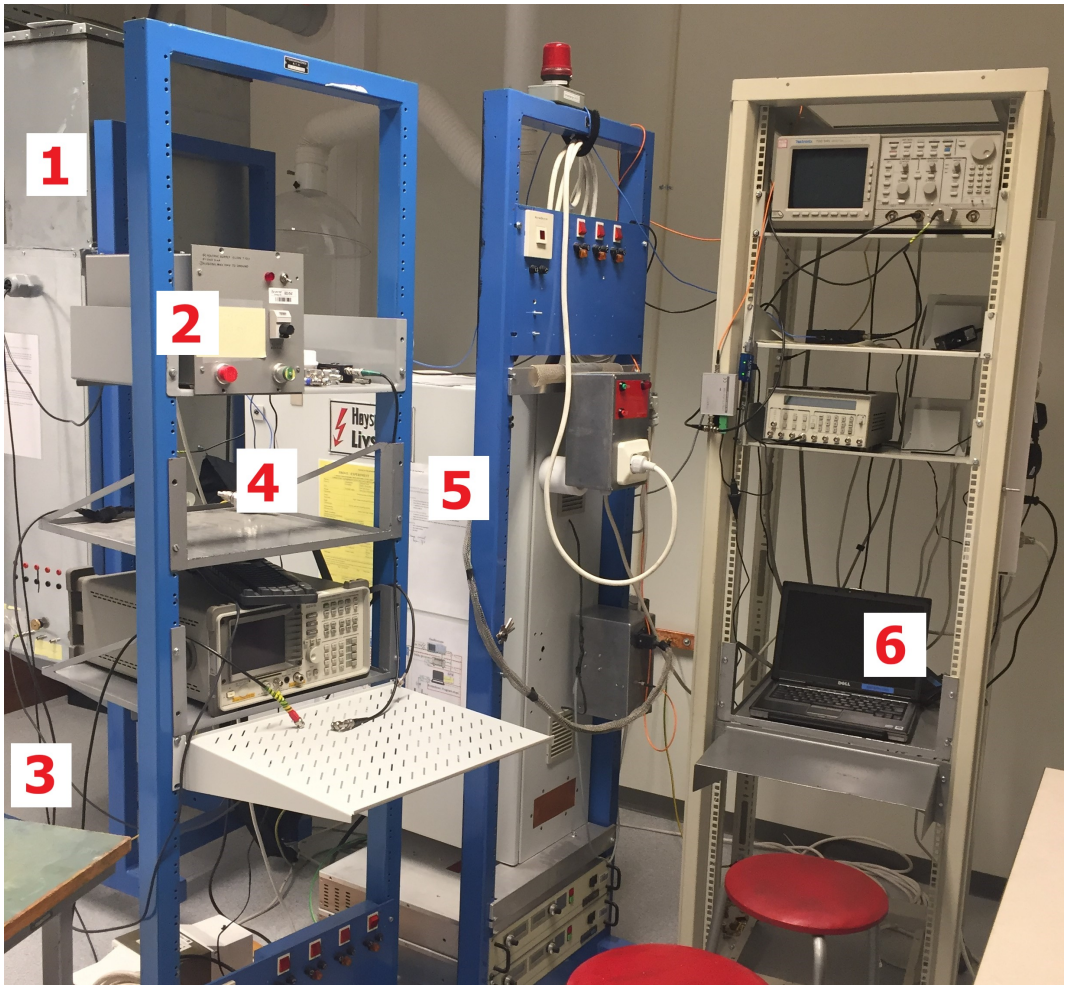


*Figure 15: The lab set-up for the measurements with a bipolar voltage pulse. 1: The test cabinet. 2: The voltage source for the PMT. 3: The spectrum analyzer was placed here. 4: The oscilloscope was placed here. 5: The cabinet with the voltage switch. 6: The computer used to control the voltage.*

The PMT was placed above the test object, as seen from Figure 14 and Figure 16. The tube/opening of the PMT was pointing down towards the test object in order to observe any light emitted from PDs. The signal from the PMT was sent to an oscilloscope, see Figure 14.

The MagneLab current transformer (serial No. 24530) was connected below the test object, i.e. on the low voltage side of the test object, as seen from Figure 14 and Figure 16. The current transformer could measure signals between 1200 Hz and 500 MHz. The current transformer was connected to a spectrum analyzer, which was used to filter the signal from the current transformer, as described in section 2.3.2. The signal was then sent from the spectrum analyzer to an oscilloscope, in order to study the signal, see Figure 15.

The oscilloscope that received the signals from the PMT and the current transformer also received a low voltage version of the voltage pulse, see Figure 14, making it possible to observe where on the voltage shape the PDs occurred.

### 3.1.3 Reducing the noise

Having the measurement results disturbed and altered by noise is undesirable, and several measures were taken in order to try and prevent as much of the noise as possible. In order to make the two set-ups as similar as possible, so that any potential noise would be the same and the results would be comparable, the same current transformer, spectrum analyzer, and oscilloscope were used in both set-ups. The PMTs were, however, different.

In order to prevent dark currents, i.e. the currents the PMT produces without incident photons, the PMTs in the sinusoidal set-up were cooled with PMT cooling units and water cooling. Unfortunately, these cooling methods were not available in the bipolar voltage pulse set-up.

Since the Lambert HiCAM 500 camera has a long exposure time and the PMTs detect photons, they are both highly sensitive with regard to light. In order to prevent unwanted light from entering the camera and the PMTs, the two cabinets used for testing had as few holes and gaps as possible (whilst still being able to take wires in and out). In the sinusoidal set-up this was done by adding rubber seals around the cabinet door and covering the holes around the wires with tape, resulting in it being completely dark inside the cabinet. In the voltage pulse set-up, there were still some gaps light could enter through, despite having tried to cover them all up. A black curtain was therefore used to try and cover up the small gaps around the HV probe (for placement of the probe, see Figure 13). Additionally, the main light in the room was switched off when performing measurements with the voltage pulse set-up, leaving the screens, the red signal-light, and a small lamp facing away from the cabinet as the only light sources in the room.

Two PMTs were used in the sinusoidal set-up. This made it possible to use a coincidence circuit to compare the signals from the two PMTs, and only register the PD signals that both of the PMTs registered, making the results more reliable. Additionally, Omicron MPD 600 was used as a gate for the signal from the two PMTs in the sinusoidal set-up. I.e. whenever a PD was detected by both PMTs, it would only be registered if a PD was detected by the Omicron MPD 600 as well. This was done to further increase the reliability of the results

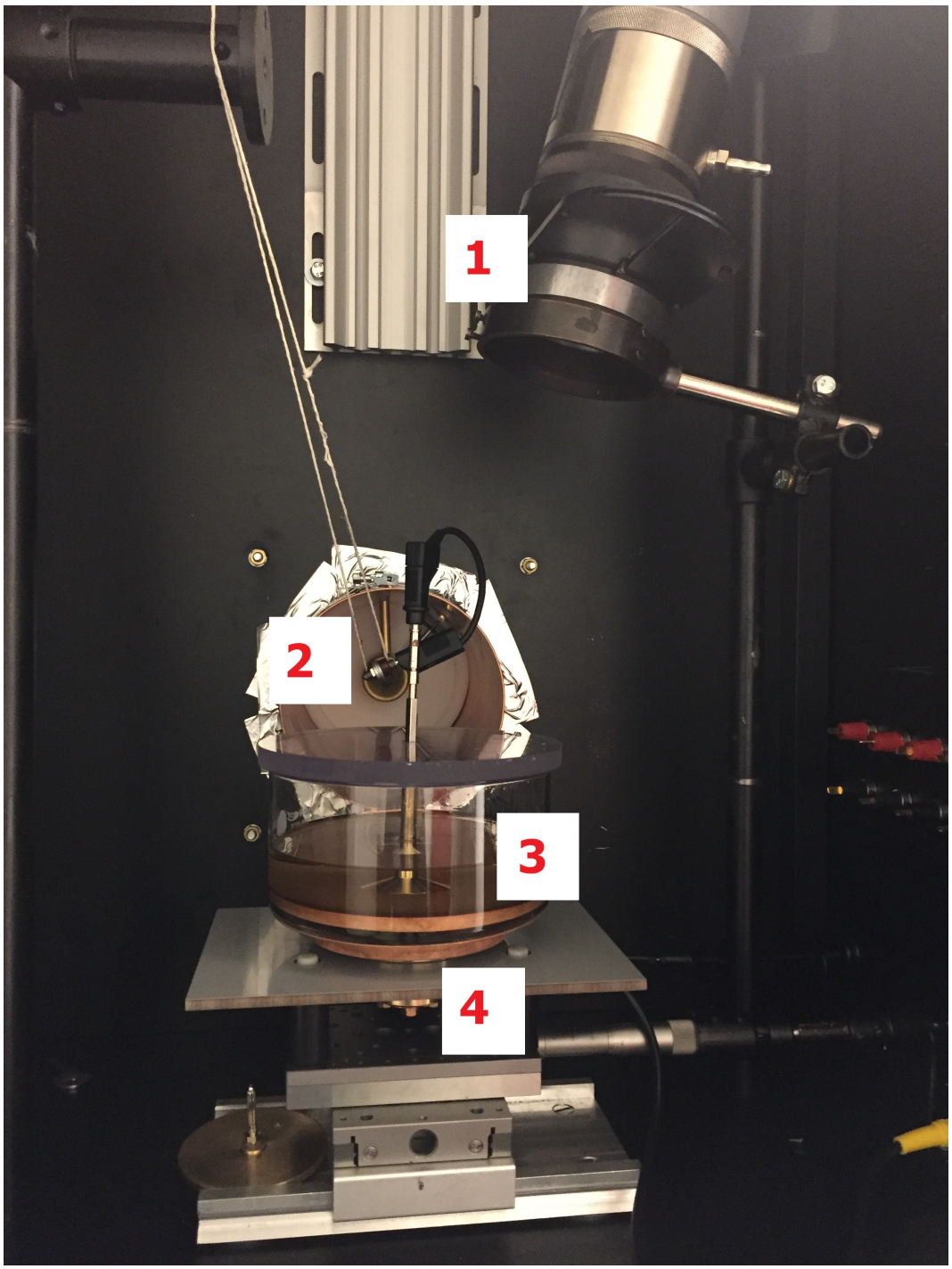


*Figure 16: The inside of the test cabinet used for the measurements with a bipolar voltage pulse. 1: The PMT. 2: The connection between the switching cabinet and the test cabinet. 3: The test object. 4: The current transformer was placed right below the small shelf.*

from the PMT.

In order to reduce the noise on the electrical signals in the sinusoidal set-up, the circuit was set up avoiding ground loops, and 50 Ω cables and terminations were used where possible [15].

## 3.2 The test object

In the following section, the different aspects and parameters of the test object will be explained and discussed. The section starts with the pressboard samples, followed by the dishes used during the measurements, before ending with the top-electrodes used for the measurements.

### 3.2.1 The pressboard samples

#### 3.2.1.1 The diameter of the pressboard samples

In the project preceding this thesis [4], the partial discharge inception voltage for streamers was very close to the breakdown voltage for the test object. This resulted in it being difficult to study the streamers properly, since breakdown was to be avoided. In order to avoid this problem, the diameter of pressboard circles used was increased from 62 mm, i.e. the diameter of the samples used in [4], to approximately 140 mm. The increased diameter increases the distance the streamer have to cover in order to result in breakdown. I.e. the breakdown voltage is increased by the increase in diameter of the pressboard circles.

#### 3.2.1.2 The thickness of the pressboard samples

As mentioned in section 3.2.1.1, the partial discharge inception voltage (PDIV) for streamers and the breakdown voltage for the test object used during the project preceding this thesis [4] were very close.

Partial discharges are largely dependant on the electric field; the stronger the electric field is, the more likely PDs are to occur. The electric field strength in the test object depends, among other factors, on the thickness of the pressboard sample. A thick pressboard sample will help create a weaker electric field than a thin pressboard sample. The 2 mm thick pressboard used for the test in the project preceding this thesis [4] was therefore substituted with a 0.5 mm thick pressboard, in order to increase the electric field strength and reduce the PDIV.

Unfortunately, the thin pressboard sheets were only produced on rolls, so the sheets were not completely flat. Neither heat nor pressure could flatten them out completely. This resulted in a lot of complications. It made it more difficult to remove air bubbles from underneath the pressboard sample before running a measurement. Another problem was that the PDs now started at very low voltages, about 5-6 $kV_{peak}$, and this was registered by both electrical measurements and the PMTs, yet nothing could be seen by the camera. The

most likely explanation being that the streamers were occurring underneath the pressboard, rather than on top of the pressboard. Due to these complications, the thin pressboard were substituted with the original 2 mm thick pressboard, which worked a lot better.

Due to a limited number of available 2 mm thick pressboard sheets, the pressboard impregnated in Nytro 10XN was from another batch than the one impregnated in Midel 7131. The main difference was that the surface of the Midel-impregnated pressboard was completely smooth, whilst the surface of the Nytro-impregnated pressboard was slightly uneven. This is assumed to have little to no impact on the results.

#### 3.2.1.3 Preparing the pressboard samples

The high-density pressboard samples were dried in a heating-cabinet before being impregnated with the oil. First, the samples were placed in a glass container in a heating cabinet at 40°C. The temperature was increased to 90°C after 24 hours, and left for another 48 hours.

The glass container with the pressboard samples was then removed from the cabinet, and a glass lid was placed on top. The container was then connected to both a vacuum pump and a bottle of oil at 90 °C through two different valves in the lid, see Figure 17. The warm oil was added whilst the glass container was under vacuum, making the oil impregnate the pressboard samples.

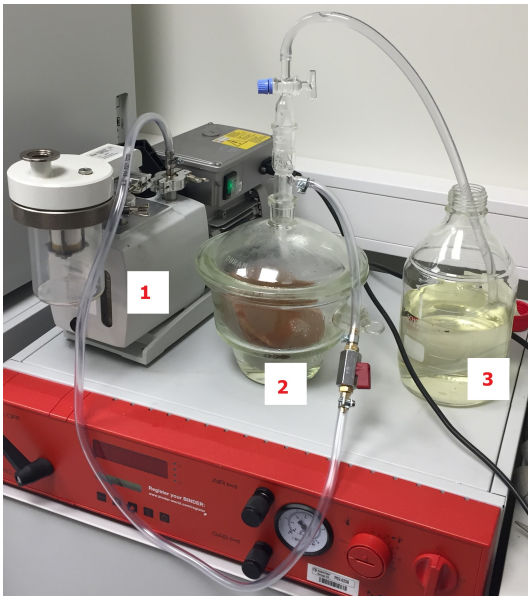


*Figure 17: 1: The vacuum pump. 2: The glass container with the pressboard samples. 3: The bottle with the warm oil.*

When measurements were to be performed, a pressboard sample was placed in the dish used for measurements and oil was poured onto it. The dish was put under vacuum for at least 15 minutes in order to remove any air bubbles. During this process, the pressboard sample was slightly tilted, whilst still being fully submerged in the oil, in order to let the air bubbles out as swiftly as possible.

#### 3.2.1.4 Moisture content

Moisture increases the speed of the deterioration and ageing of the liquid-paper insulation system, as discussed in section 2.1.2. In order to perform a correct analysis of the results of the measurements, the moisture content of the samples should therefore be known. This is because a dry transformer and a wet transformer are expected to behave differently; the wet

transformer will, according to the theory, get PDs at lower voltages than the dry transformer.

The moisture in the insulation system is distributed between the paper and liquid in a state of equilibrium [6]. The pressboard-part of the insulation system holds a lot more moisture than the oil-part of the insulation, since cellulose is highly hygroscopic [6]. The moisture content in the pressboard is therefore assumed to be the moisture content in the entire system. Thus, only the moisture content in the pressboard samples was measured.

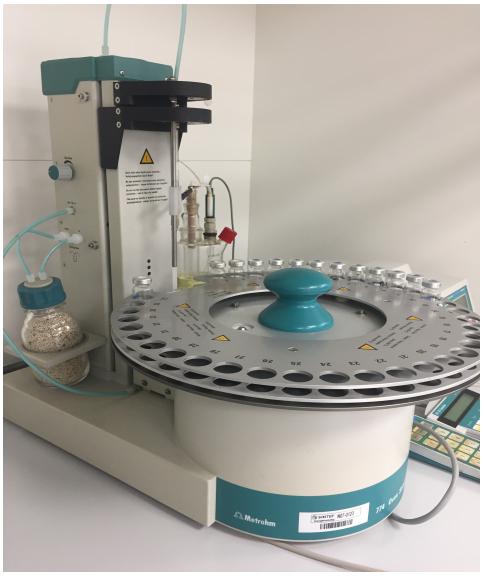

*Figure 18: The Coulometer was used to measure the moisture content in the pressboard samples.*

The moisture in the pressboard samples was measured using the Karl Fischer titration method. This is a method that determines both the bonded and the free water in the sample, using coulometric and volumetric titration [23].

In order to measure the moisture in the pressboard sample, three pieces were cut from it. These three pieces were taken from different parts of the sample, in order to make the results more reliable: one piece from the middle of the sample, one from the edge, and one from the opposing edge of the sample. Three air samples were gathered as well, in order to account for the moisture in the air, see Figure 19.

All six samples were then put in the Coulometer to measure the water content, see Figure 18. Afterwards, the pressboard pieces were dried and weighed. The weight of the pieces was then used to calculate the water content.

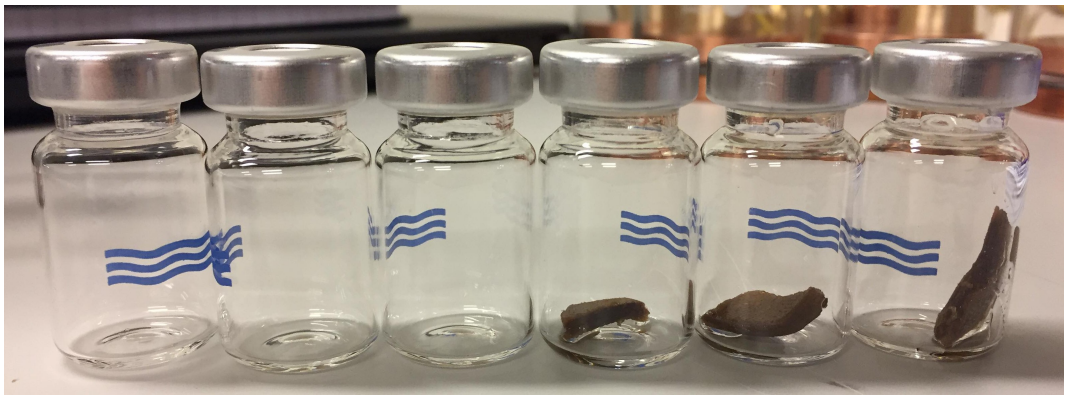

*Figure 19: 6 samples for measuring the moisture. 3 with air, 3 with oil-impregnated pressboard.*

### 3.2.2 The dishes used for the measurements

The dishes used for the measurements are depicted in Figure 20. The dishes had a 140 mm diameter. There were two electrodes connected to each other through the bottom of the dish. These electrodes both had an 110 mm diameter. The pressboard sample was placed on top of these two electrodes, and submerged in the insulation liquid. In the sinusoidal set-up, the bottom electrodes were on the high voltage side of the transformer, see Figure 11. In the voltage pulse set-up, the bottom electrodes were grounded, see Figure 16. The bottom electrodes were made to have smaller diameters than the dish itself. This would increase the distance the streamer discharges would have to cover in order to result in a breakdown, and therefore reduce the probability of breakdowns.

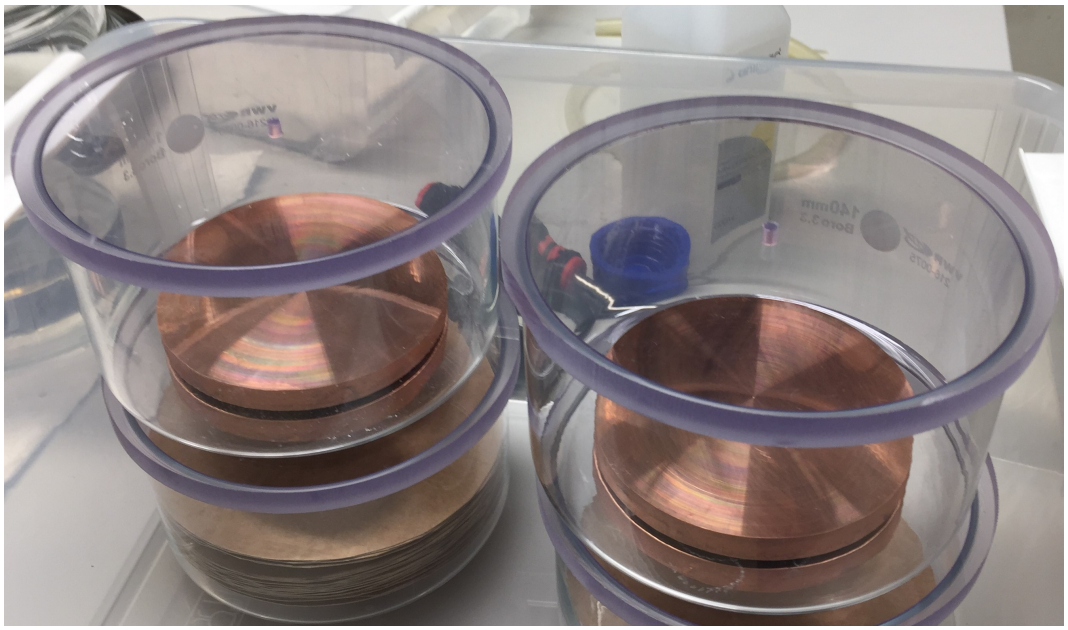

*Figure 20: The dishes (diameter = 140 mm) used for the measurements. A large electrode (diameter = 110 mm) was placed on each side of the bottom of the dish, and connected to each other through a hole in the bottom of the dish. A plexiglass lid is placed on top of each dish.*

The dish with the impregnated pressboard and oil, as described in section 3.2.1.3, was placed inside the cabinet with a smaller electrode placed on top of the pressboard, see section 3.2.3, and a lid on top of the dish to prevent moisture from entering the system and to help keep the top-electrode centered.

### 3.2.3 Electrodes

The partial discharge activity depends on the electric field, as mentioned in section 2.2. In order to study the effect of different electric fields, two differently shaped brass electrodes were supposed to be used: one with a rounded edge and one with a sharp edge, see Fig-

ure 21. The sharp edged electrode creates a more inhomogeneous electric field than the round electrode. Hence, the electric field is stronger when the sharp edged electrode is used. It is therefore expected to be more partial discharges when using the sharp edged electrode compared to the round electrode. The breakdown voltage is assumed to be similar for both electrodes since the breakdown depends more on the voltage amplitude than on the electric field.

The top electrode was grounded in the sinusoidal voltage set-up, and on the high voltage side of the insulation in the bipolar voltage set-up, see Figure 11 and Figure 16. The bottom of the sharp edged electrode had a 30 mm diameter. The diameter of the widest part of the round electrode was 36 mm. Both electrodes were 20 mm high.

In the project preceding this thesis, both electrodes were used [4]. The sharp edged electrode was found to result in more PDs, and was therefore prioritised during the master thesis. Due to time constraints, only the sharp edged electrode was used.

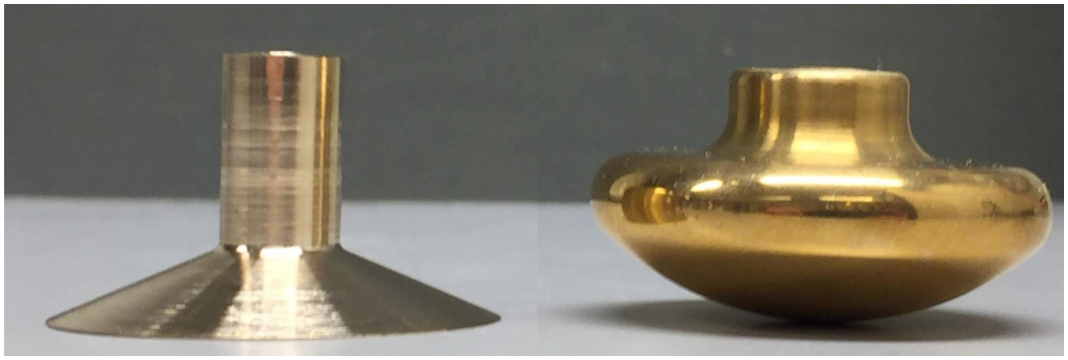

*Figure 21: The electrodes. The electrode on the left was used as the sharp edged electrode (bottom diameter = 30 mm), the electrode on the right was supposed to be used as the round electrode (diameter at of the widest part = 36 mm). Both electrodes were 20 mm high.*

## 3.3 Performing the measurements

When performing a measurement, the dish with the impregnated pressboard and oil, as described in sections 3.2.1.3 and 3.2.2, was placed inside the test cabinet with the small electrode placed on top of the pressboard, see section 3.2.3, and a lid on top of the dish to prevent moisture from entering the system and to help keep the top-electrode centered, see Figure 22.

The signal generator in the sinusoidal set-up was set to a frequency of 30 Hz and high load impedance, as described in section 3.1.1. The voltage signal in the voltage pulse set-up was also set to a frequency of 30 Hz, as explained in section 3.1.2.

In order to find the main frequency component of the partial discharge, the voltage amplitude in the bipolar voltage pulse set-up was set to a voltage with lots of PDs. This voltage was found by increasing the voltage until both the current transformer and the PMT detected PD pulses. The main frequency component of the partial discharge was then found using

the spectrum analyzer. This frequency, 157 MHz, was then used as the center frequency for the filter. The same center frequency, 157 MHz, was used in the sinusoidal set-up because streamer discharges were expected to occur in the systems, and the frequency of these discharges should not be affected by the shape of the applied voltage. It is also easier to compare the results when the measurements have been performed under the same conditions. The band width of the filter was set to 8 MHz for both lab set-ups.

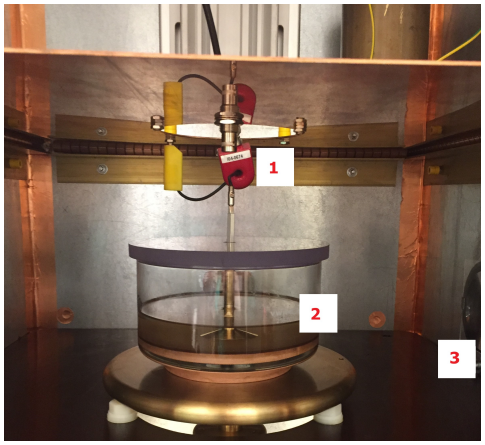


*(i) The test object inside the test cabinet used for the measurements with a sinusoidal voltage. 1: The current transformer. 2: The test object. 3: One of the PMTs.*

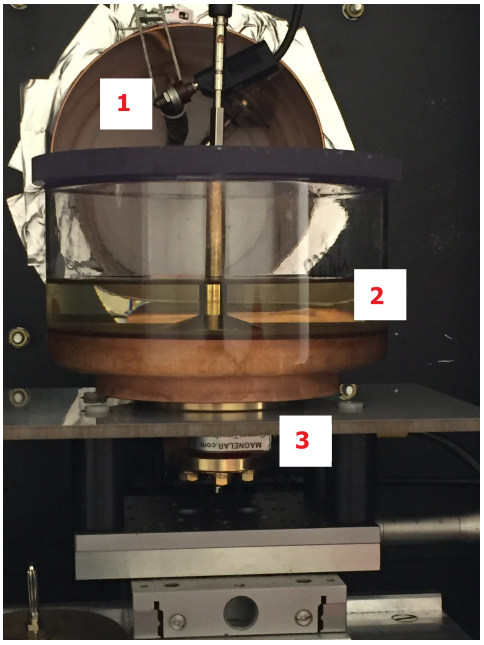


*(ii) The test object inside the test cabinet used for the measurements with a bipolar voltage pulse. 1: The connection between the switching cabinet and the test cabinet. 2: The test object. 3: The current transformer.*

*Figure 22: The test object inside the test cabinets.*

Data from the PMT in the bipolar voltage set-up and from the current transformer in both set-ups were collected using an oscilloscope. The envelope function on the oscilloscope was used to collect the data. By doing this, the largest value detected at each time step/part of the voltage was collected. The data file could then be exported from the oscilloscope to a memory stick as soon as the envelope-function had been running for the determined amount of time. The use of the envelope function gave a suggestion of a PD pattern. It is, however, not possible to count the number of PDs based on the collected data from the oscilloscope, since the envelope function made pulses overlap. The Omicron collected data continuously throughout the experiments.

The aim of the measurements was to gain a better understanding of how the two insulation systems, one impregnated with Nytro 10XN and one impregnated with Midel 7131, behave under different voltage stresses. This was studied by observing the partial discharges that occurred in the insulation systems when the systems were stressed by different voltage stresses. The partial discharge inception voltage (PDIV) can give a good indication of how

harmful a particular type of stress is to the insulation system. One of the aims of the measurements was therefore to find the PDIV for the two insulation systems, when stressed by the different voltage shapes, using the different measuring devices in the set-ups.

The PDIV was found by starting at a low voltage, one without PDs. This start voltage was set to 7 $kV_{peak}$ and 8 $kV_{peak}$ in the sinusoidal and bipolar voltage pulse set-up, respectively. The voltage was then increased stepwise, by 1 $kV_{peak}$ per step. The voltage amplitude was kept at each step for 1 min, and the data was collected using the envelope function on the oscilloscope, as explained above. Exporting the data files from the oscilloscope took up to 15 minutes. This resulted in the voltage being kept at each step, and the insulation systems being subjected to each voltage amplitude, for significantly longer than the minute data was collected for. Whether PDs had occurred or not were registered manually as well. The voltage was increased until the PDs were detected clearly by all of the different measuring devices. All of the measuring series were performed in this way.

### 3.3.1 Time constraints

Only four measurements were performed, one for each combination of insulation system and voltage stress. One important reason for this is that a lot of time was spent trying to straighten out the aforementioned 0.5 mm thick pressboard, and performing measurements on it. These tests were, as mentioned, not a success, and led to a lot of wasted time and effort. Changing to 2 mm thick pressboard meant a lot of extra waiting time as well, since the samples had to be cut out, dried and impregnated before use. A few test-rounds had to be performed as well, in order to check that the different measuring devices in the set-ups worked as expected. To top it all of, the lab set-up for the bipolar voltage pulse was not ready to be used until the last week in April. This all led to time constraints, which is why I only had time to perform four proper measurements. Nevertheless, the results from these measurements are still valuable and interesting. The differences between the two voltage stresses were distinct, so these four measurements are enough to make some interesting observations and to form a conclusion. The results will be presented and discussed in the following chapters.

# 4 Results

## 4.1 Sinusoidal voltage

This section consists of the results and observations from the measurements performed on the two different insulation systems stressed by a sinusoidal voltage. A brief discussion of the signal delay of the current transformer signal, which affects some of the results in this section, is presented first. Then the results for the Nytro 10XN impregnated insulation system are presented, followed by the results for the Midel 7131 impregnated insulation system. Something went wrong while collecting the data from the PMTs in the sinusoidal set-up. The only data from the PMT that can be included in this section is therefore the PDIV found by the PMT.

### 4.1.1 Signal delay

The signal from the current transformer was filtered through a spectrum analyzer before reaching the oscilloscope, as explained in section 3.3. This caused a delay of the current transformer signal, compared to the voltage measurement that went straight to the oscilloscope. Since the same current transformer, spectrum analyzer, and oscilloscope were used both in the set-up with the sinusoidal voltage and in the set-up with the bipolar voltage pulse, the delay of the current transformer signal was the same in both set-ups and for both insulation systems.

The switching transient in the set-up with the bipolar voltage pulse made it possible to find the length of the signal delay, see section 4.2.1.2. The delay was found to be approximately 4 µs. In order to compensate for this, the signal from the current transformer was shifted 4 µs to the left in the post-processing of the data.

### 4.1.2 Nytro 10XN

In this section the results and observations from the measurements performed on the Nytro 10XN impregnated insulation system stressed by a sinusoidal voltage will be presented. First, the phase resolved partial discharge analysis (PRPDA) plot based on results from the Omicron MPD 600 will be presented. This is followed by the PDs detected by the current transformer, the partial discharge inception voltage (PDIV), and the visible ageing of the pressboard. Lastly, some pictures of PDs taken by a high speed camera are presented.

Note that since the signal from the current transformer was collected from an oscilloscope using the envelope-function on the oscilloscope (the envelope function holds the highest pulses at each point on the voltage shape), it is not possible to tell how many pulses the current transformer detected at a given point on the voltage shape. It is only possible to determine the size of the largest pulse at each point and where on the voltage curve the pulses occurred.

The moisture content in the pressboard sample used in the measurements was below 1% the whole time. Since 1% is between the defined limits of dry and middle dry, see section 2.1.2,

the insulation system is considered to be dry to middle dry.

#### 4.1.2.1 Phase resolved partial discharge analysis (PRPDA)

Figure 23 is the phase resolved partial discharge analysis (PRPDA) plot from the test performed using the 2 mm thick pressboard impregnated in Nytro 10XN in order to find the partial discharge inception voltage (PDIV). The PRPDA plot in Figure 23 is based on the PDs detected and measured by the Omicron MPD 600. A sharp-edged top-electrode was used, see section 3.2.3. The applied sinusoidal voltage had amplitudes varying from 21 $kV_{peak}$ to 40 $kV_{peak}$.

The y-axis in the plot in Figure 23 represents the apparent charge of the partial discharges in pC, and the scale of this axis is logarithmic. The x-axis in the same figure represents the phase angle of the applied voltage in degrees. The shape of the applied voltage itself is shown as a black curve (a sinusoidal wave) in Figure 23. The color map represents the pulse count, i.e. the number of PDs that occurred per phase angle and apparent charge, starting at dark blue (few pulses) and ending at dark red (many pulses).

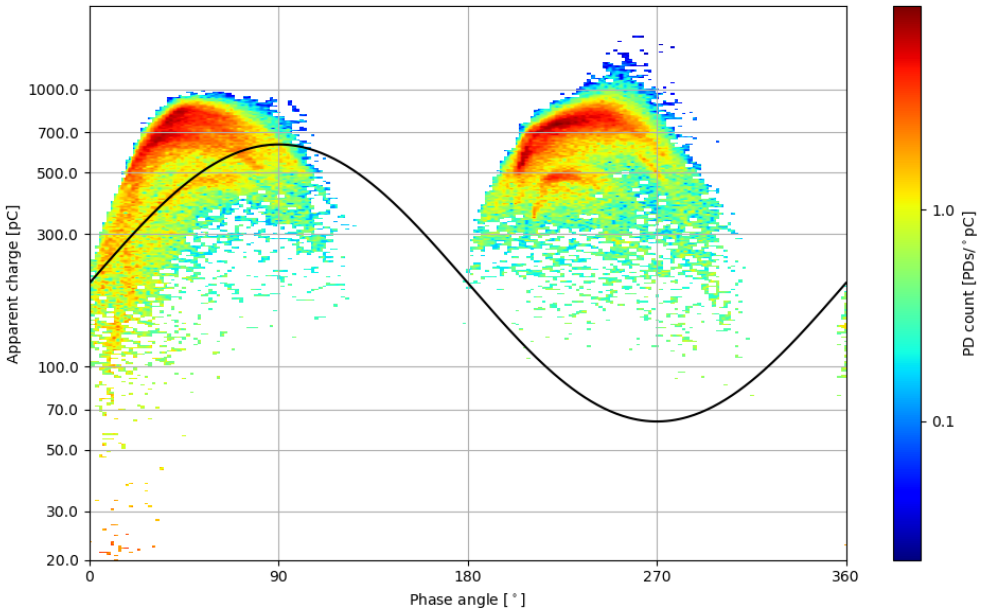


*Figure 23: The phase resolved partial discharge analysis (PRPDA) plot from the test performed using the 2 mm thick pressboard impregnated in Nytro 10XN. A sharp-edged top-electrode was used, and the applied sinusoidal voltage had amplitudes varying from 21 $kV_{peak}$ to 40 $kV_{peak}$. The PRPDA plot is based on the PDs detected and measured by the Omicron MPD 600.*

As seen from Figure 23, the PD patterns in the positive and negative half period were very similar. Almost perfect shape, magnitude, and phase symmetries can be observed. In both half periods, the majority of the PDs occurred at the rising edge (absolute value) of the

voltage. The middle of the rising edge (absolute value), i.e. at about 45° and 225°, was the phase angle at which the PD count was highest. There were also a significant amount of PDs occurring at the voltage peaks.

The apparent charge of the discharges ranged from 20 pC to about 1500 pC. The majority of the PDs, in both half periods, had an apparent charge somewhere between 300 pC and 1000 pC. There were, however, some differences between the two half periods with regard to the apparent charge. The positive half period had more PDs with apparent charge below 300 pC than the negative half period. The smallest apparent charge in the positive half period was significantly smaller than the smallest apparent charge in the negative half period, with an apparent charge of about 20 pC compared to an apparent charge of about 100 pC. The largest apparent charge in the positive half period was also significantly smaller than the largest apparent charge in the negative half period, with an apparent charge of almost 1000 pC in the positive half period, compared to an apparent charge of around 1500 in the negative half period.

Despite the almost eyebrow-shaped PD pattern in the two half periods being similar, they also had some distinctive differences. As already mentioned, the size of the apparent charge of the PDs occurring in the two half periods differed slightly. Where on the voltage edge, i.e. at what phase angle, the lowest and highest apparent charge occurred also differed between the two half periods. This resulted in the shape of the patterns differing as well.

In the positive half period, the PDs occurring at the beginning of the rising edge, i.e. right after the zero crossing, were many and ranging from about 20 pC to 300 pC. This created an almost tail-like start to the eyebrow-shaped main part of the pattern in this half period, almost as if the "eyebrow" was raised. The results from the pulse count clearly show how the majority of the PDs occurred around 45°. These were, coincidentally, the PDs in the positive half period with the largest apparent charges. When the voltage reached its peak, at 90°, both the size and the occurrence of the PDs in this half period were slightly reduced compared to the PD-peak at 45°. This gave the top of the pattern an arc-like quality. Shortly after the voltage peak in the positive half period, the PDs stopped.

Interestingly, the pattern in the positive half period seemed to start right before the zero crossing of the increasing edge, i.e. right before the phase angle reached 360°. This was, however, not the case for the pattern in the negative half period.

In the negative half period, the PDs started to occur after the zero crossing of the voltage at 180°. The first PDs in this half period had an apparent charge of 200 to 300 pC. The apparent charge of the PDs increased with the increasing phase angle. Simultaneously, PDs with apparent charges down to about 100 pC, with the majority having an apparent charge of 300 pC or more, occurred. Together, these PDs created a pattern that looked like a small hill. The PDs with the largest apparent charge in the negative half period, occurred near and at the peak of the voltage at 270°. This disturbed the otherwise smooth arc-shaped top of the pattern by creating a little cluster above the otherwise regular shape. The largest apparent discharge was about 1500 pC. After the voltage peak, both the apparent charge and amount of PDs decreased before stopping right before 315°.

#### 4.1.2.2 PDs detected by the current transformer

The PDs detected by the current transformer when the measurements on the Nytro 10XN impregnated system stressed by a sinusoidal voltage were performed will be presented in this section. The signal from the current transformer was filtered using a spectrum analyzer, see section 3.3. The resulting current transformer signal was then shifted 4 µs to the left during the post processing in order to compensate for the signal delay, as explained in section 4.1.1.

The plots where the sinusoidal voltage have amplitudes at 33, 36, and 40 $kV_{peak}$ applied voltage are included in this section. The plots where the sinusoidal voltage have amplitudes at 30 - 32 $kV_{peak}$, 34 - 35 $kV_{peak}$, and 37 - 39 $kV_{peak}$ can be found in appendix A.

**33 $kV_{peak}$ - the current transformer started to detect PDs:**
Figure 24 shows the signal from the current transformer when the insulation system was stressed by a 33 $kV_{peak}$ sinusoidal voltage. The current transformer started to detect some PDs at this applied voltage, as seen from the figure. Most of these pulses had amplitudes of between 0.75 and 1 mV.

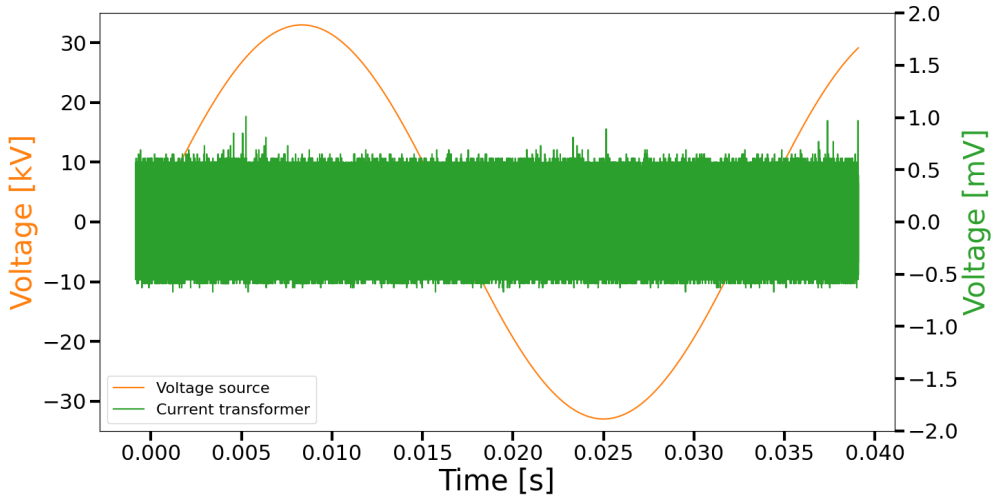


*Figure 24: The signal from the current transformer when a 33 $kV_{peak}$ sinusoidal voltage was applied to the Nytro 10XN impregnated system. The signal was collected using the envelope function on the oscilloscope for 1 minute.*

By looking at the first positive half period of the voltage, it can be observed that all of the pulses occurred on the rising edge of the voltage. The detected PDs in this half period seem to increase in size with the increasing voltage until the largest PD in this half period occurred right after the middle of the rising voltage edge. This PD had an amplitude of 1 mV. The second positive half period looked similar, see Figure 24. The main difference was more 1 mV pulses than in the first positive half period. These 1 mV pulses also seem to have occurred earlier on the voltage edge here compared to the first positive half period in Figure 24.

In the negative half period, the PDs were centered around the peak of the voltage, see Figure 24. In this half period, there were mainly two PDs detected by the current transformer. The first of these had an amplitude of approximately 0.75 mV and occurred right before the voltage peak. The second pulse occurred right after the peak of the voltage and had an amplitude of 1 mV, as seen from Figure 24.

**36 $kV_{peak}$ - the current transformer stopped detecting PDs:**
After the current transformer started to detect PDs at 33 $kV_{peak}$ applied voltage, the number and size of the PDs increased with increasing voltage, see appendix A. However, when the voltage amplitude was increased to 36 $kV_{peak}$, the current transformer did not detect any PDs. This can be seen from Figure 25. At 37 $kV_{peak}$ the current transformer started detecting PDs again, see appendix A.

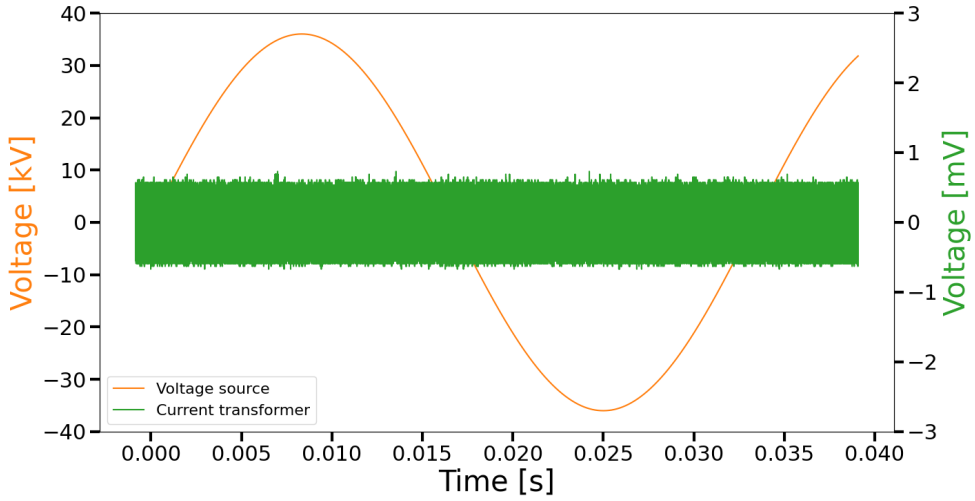


*Figure 25: The signal from the current transformer when a 36 $kV_{peak}$ sinusoidal voltage was applied to the Nytro 10XN impregnated system. The signal was collected using the envelope function on the oscilloscope for 1 minute.*

**40 $kV_{peak}$ - the PDs that occurred at the highest applied voltage:**
Figure 26 shows the signal from the current transformer when the insulation system was stressed by a 40 $kV_{peak}$ sinusoidal voltage. The current transformer detected several pulses, with amplitudes ranging from 1 to 3.5 mV.

In the positive half period, the majority of the pulses occurred on the rising edge of the voltage. The amplitudes of these pulses started at 1 mV, and increased with increasing voltage. When an amplitude of 3 mV was reached, a little after the middle of the rising edge of the voltage, the amplitudes of the pulses decreased until the peak of the voltage was reached. There were only a few 1 mV PDs in the positive half period after the voltage peak, see Figure 26. Some negative pulses were detected as well. These coincided with the positive pulses on the rising edge of the voltage, and had amplitudes ranging from -0.75 mV to -1 mV.

The majority of the pulses detected by the current transformer in the negative half period occurred at the rising edge (absolute value) and around the peak of the voltage. The amplitudes of these pulses started at approximately 1 mV, and increased with the increasing voltage (absolute value). When an amplitude of 3.5 mV was reached the amplitudes of the pulses started to decrease with the increase in voltage (absolute value). The 3.5 mV pulse occurred shortly before the peak of the voltage, see Figure 26.

After the voltage peak in the negative half period, the amplitudes of the PD pulses continued to decrease until the PDs stopped approximately half-way down the falling edge (absolute value) of the voltage. Some negative pulses were also detected by the current transformer. These coincided with the positive pulses in the negative half period, and had amplitudes ranging from -0.75 mV to -1 mV.

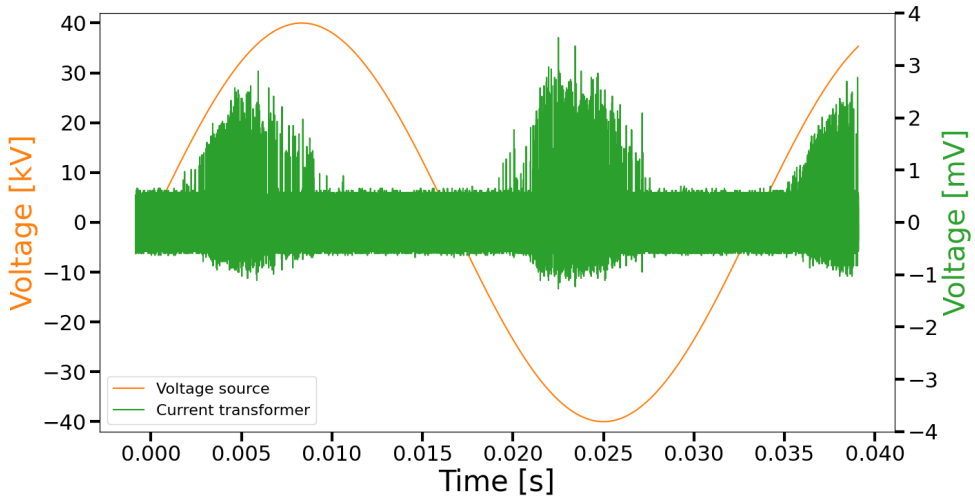


*Figure 26: The signal from the current transformer when a 40 $kV_{peak}$ sinusoidal voltage was applied to the Nytro 10XN impregnated system. The signal was collected using the envelope function on the oscilloscope for 1 minute.*

#### 4.1.2.3 Partial discharge inception voltage (PDIV)

The partial discharge inception voltage (PDIV) for the Nytro 10XN impregnated system stressed by a sinusoidal voltage was found using three different measuring devices: PMT, current transformer, and Omicron MPD 600. The voltage amplitude in kV of these PDIVs are listed in Table 3. All three measuring devices measured the PDIV to be 33 $kV_{peak}$, as seen from the table.

*Table 3: Voltage amplitude in kV of the partial discharge inception voltage (PDIV) for Nytro 10XN impregnated pressboard, stressed by a sinusoidal voltage.*

| **Measuring device** | **PDIV [kV]** |
|---|---|
| PMT | 33 |
| Current transformer | 33 |
| Omicron MPD 600 | 33 |

#### 4.1.2.4 Visible ageing of the pressboard

After the measurements, a black ring of soot was visible on the pressboard sample, see Figure 27. The ring of soot had its center in the middle of the pressboard sample, as seen from Figure 27i. The ring had the same diameter, i.e. 30 mm, as the sharp edged top electrode used during the measurements, see section 3.2.3 for more on the sharp edged electrode.

The soot-ring was approximately 1-2 mm thick. There were some short branches of soot going out from the ring, see Figure 27ii. Most of them went toward the inside of the circle, i.e. under the top electrode. The length of these branches varied from about 1 mm to about 4 mm.

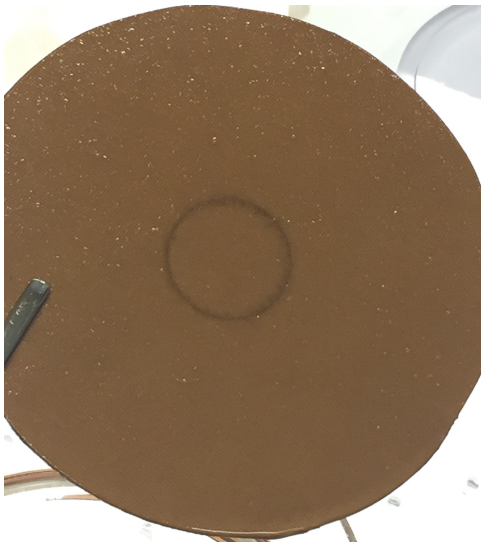

*(i) The circle of soot and the pressboard sample are concentric.*

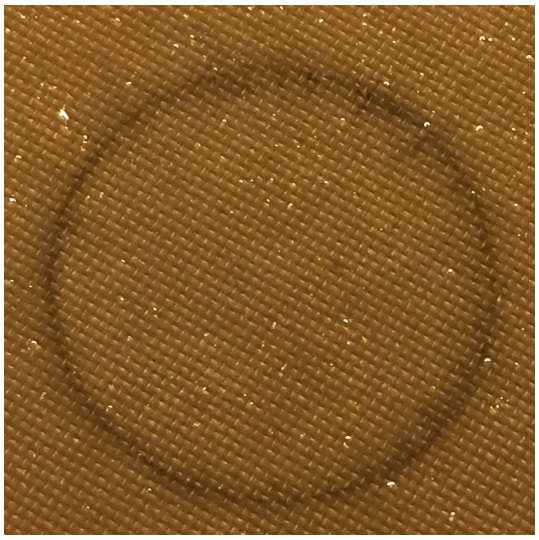

*(ii) The soot circle had the same diameter, i.e. 30 mm, as the sharp edged top electrode.*

*Figure 27: The circle of soot on the Nytro 10XN impregnated pressboard sample after the pressboard sample had been used in the measurements with the sinusoidal voltage.*

#### 4.1.2.5 PDs photographed by a high speed camera

A high speed camera was used to take pictures of streamers in the Nytro 10XN impregnated system, when the system was stressed by a sinusoidal voltage, as explained in section 3.1.1. Since the current transformer slightly obstructed the camera's view, this was done as a separate measurement from the rest of the measurements and results described in the previous sections.

A picture series was taken when the applied voltage had an amplitude of 35.4 $kV_{peak}$. Several frames in the series contained PDs, and a Python program was used to find the frames with the PDs. Photo-editing software was then used to layer frames on top of each other, in order to form one picture in which several different PDs could be observed at once. Adding more than two PDs did, however, make the picture a bit crowded and confusing. Thus, only two of the frames were used to create the picture in Figure 28i.

Another picture was also made. This one had a picture of the test object as a base layer, making it possible to see where on the electrode the PDs started, see Figure 28ii. The streamer discharges started on the edge of the electrode and moved towards the end of the pressboard sample, creating branches along the way, as seen from Figure 28. Neither of the two streamers reached the edge of the pressboard sample. This, i.e. the streamers stopping before the edge, is the desired result in this study. Had they reached over the insulation, i.e. from conductor to conductor, they would no longer have been partial discharges, but breakdowns in the insulation.

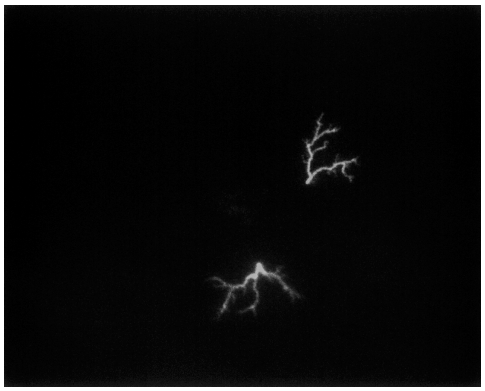

*(i) This is the same picture as Figure 28ii, minus the image of the test object. The streamers can start anywhere on the edge of the electrode.*

*(ii) A picture of the test object makes up the bottom layer. The light from the right was used to make the test object visible in order to take the picture.*

*Figure 28: PDs occurring at 35.4 $kV_{peak}$ for Nytro 10XN with the sharp-edged electrode. Two of the frames captured by the camera during this measuring series have been placed on top of each other, making it possible to see two different PDs at once.*

### 4.1.3 Midel 7131

In this section the results and observations from the measurements performed on the Midel 7131 impregnated insulation system stressed by a sinusoidal voltage will be presented. First, the phase resolved partial discharge analysis (PRPDA) plot based on results from the Omicron MPD 600 will be presented. This is followed by the PDs detected by the current transformer, and the partial discharge inception voltage (PDIV). Lastly, the visible ageing of the pressboard is presented.

Note that since the signal from the current transformer was collected from an oscilloscope using the envelope-function on the oscilloscope (the envelope function holds the highest pulses at each point on the voltage shape), it is not possible to tell how many pulses the current transformer detected at a given point on the voltage shape. It is only possible to determine the size of the largest pulse at each point and where on the voltage curve the pulses occurred.

The moisture content in the pressboard sample used in the measurements was below 0.6% the entire time. The insulation system is therefore considered to be dry to middle dry, see section 2.1.2.

#### 4.1.3.1 Phase resolved partial discharge analysis (PRPDA)

Figure 29 is the phase resolved partial dicharge analysis (PRPDA) plot from the test performed using the 2 mm thick pressboard impregnated in Midel in order to find the partial discharge inception voltage (PDIV). The PRPDA plot in Figure 29 is based on the PDs detected and measured by the Omicron MPD 600. A sharp-edged top-electrode was used, see section 3.2.3. The applied sinusoidal voltage had amplitudes varying from 15 $kV_{peak}$ to 36 $kV_{peak}$.

The y-axis in the plot in Figure 29 represents the apparent charge of the partial discharges in pC, and the scale of this axis is logarithmic. The x-axis in the same figure represents the phase angle of the applied voltage in degrees. The shape of the applied voltage itself is shown as a black curve (a sinusoidal wave) in Figure 29. The color map represents the pulse count, i.e. the number of PDs that occurred per phase angle and apparent charge, starting at dark blue (few pulses) and ending at dark red (many pulses).

There were some similarities between the PD patterns in the positive and negative half period in the plot in Figure 29. In both half periods the apparent charge of the PDs ranged from 20 pC to almost 10 000 pC. Another similarity was that the PDs with the largest apparent charges, 700 pC to 10 000 pC, occurred at the increasing edge (absolute value) near the peak of the voltage in both half periods. Lastly the PDs in both half periods could be divided into three different clusters/levels based on their apparent charge: the first ranging from 20 pC to about 70 pC, the second starting at 100 pC and ending around 2000 pC, and the third starting right below 3000 pC and ending at almost 10 000 pC, as can be seen from Figure 29.

In the positive half period, the majority of the PDs had an apparent charge between 20 pC and 70 pC. These discharges mainly occurred between 0° and 45°, and between 135° and

180°, i.e. around the zero crossings of the voltage.

A significant amount of the PDs in the positive half period occurred on the rising edge of the voltage, with apparent charge increasing with the increasing phase angle. The apparent charge of these PDs ranged from 100 pC to almost 2000 pC. Together, these PDs created a pattern that looked a bit like a triangle, with one corner at 100 pC at 0°, another at about 2000 pC somewhere around 70°, and the last corner at approximately 1000 pC and 100°. The majority of the PDs in this cluster occurred near 45°, but there were a couple near the peak of the voltage as well.

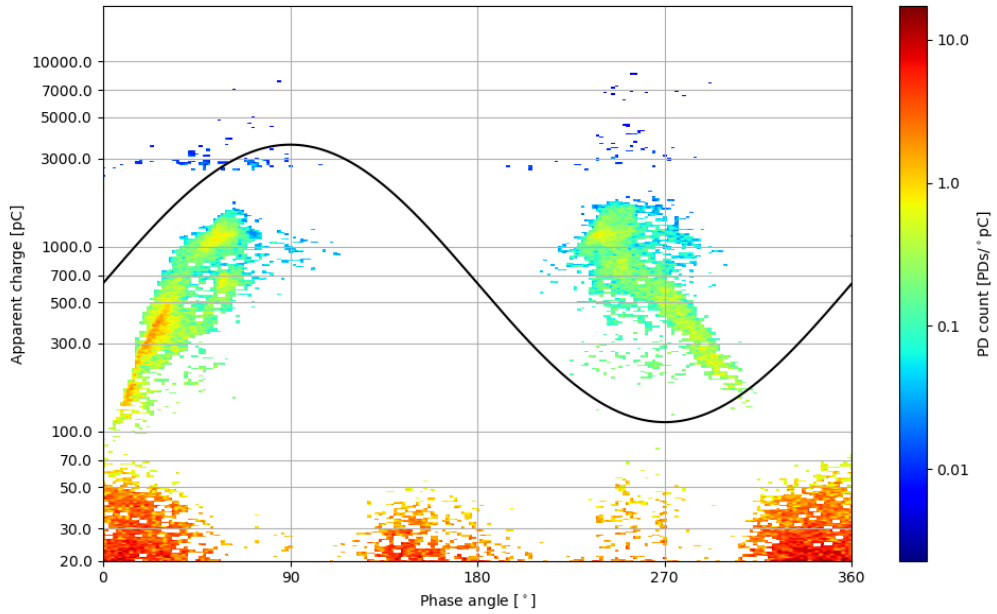


*Figure 29: The phase resolved partial discharge analysis (PRPDA) plot from the test performed using the 2 mm thick pressboard impregnated in Midel 7131. A sharp-edged top-electrode was used, and the applied sinusoidal voltage had amplitudes varying from 15 $kV_{peak}$ to 36 $kV_{peak}$. The PRPDA plot is based on the PDs detected and measured by the Omicron MPD 600.*

Lastly, some PDs with large apparent charges, ranging from right below 3000 pC to almost 10 000 pC, also occurred in the first half of the positive half period. The majority of these PDs occurred at about 45°. The PDs with the largest apparent charges occurred at about 90°, i.e. at the peak of the voltage.

In the negative half period, most of the PDs had an apparent charge between 20 pC and 70 pC. The majority of these PDs occurred between 315° and 360°. These, together with the PDs occuring right after the zero crossing at 0° in the positive half period, created a bush shape starting approximately 45° before the zero crossing of the voltage and ending at about 45° after the zero crossing. There were also some PDs with apparent discharges within the aforementioned range that occurred on the rising edge of the voltage (absolute value) in the negative half period, as seen from Figure 29. These mainly occurred at the start of the rising edge (absolute value) and right before the peak of the voltage.

The "cluster" with the second largest amount of PDs in the negative half period was situated around the peak of the voltage, from approximately 225° to 315°. The apparent charge of these PDs ranged from 100 pC to about 2000 pC. The PDs with the largest apparent charges in this cluster occurred between 225° and 270 °, i.e. on the second half of the rising edge (absolute value) of the voltage. After the voltage peak, the apparent charge of the PDs decreased with the increasing phase angle.

The largest PDs in the negative half period had an apparent charge between slightly less than 3000 pC and up to almost 10 000 pC. These PDs mainly occurred on the rising edge of the voltage (absolute value), with the majority occurring on the second half of this edge. The PDs with the largest apparent charge occurred right before the voltage peak, see Figure 29.

#### 4.1.3.2 PDs detected by the current transformer

The PDs detected by the current transformer when the measurements on the Midel 7131 impregnated system stressed by a sinusoidal voltage were performed will be presented in this section. The signal from the current transformer was filtered using a spectrum analyzer, see section 3.3. The resulting current transformer signal was then shifted 4 µs to the left during the post processing in order to compensate for the signal delay, as explained in section 4.1.1.

The plots where the sinusoidal voltage have amplitudes at 31, 32, and 36 $kV_{peak}$ applied voltage are included in this section. The plots where the sinusoidal voltage have amplitudes at 30 $kV_{peak}$, and 33 - 35 $kV_{peak}$ can be found in appendix B.

**31 $kV_{peak}$ - the current transformer started to detect PDs:**
Figure 30 shows the signal from the current transformer when the insulation system was stressed by a 31 $kV_{peak}$ sinusoidal voltage. The current transformer detected its first PD at this applied voltage for the Midel impregnated insulation system, as seen from the figure.

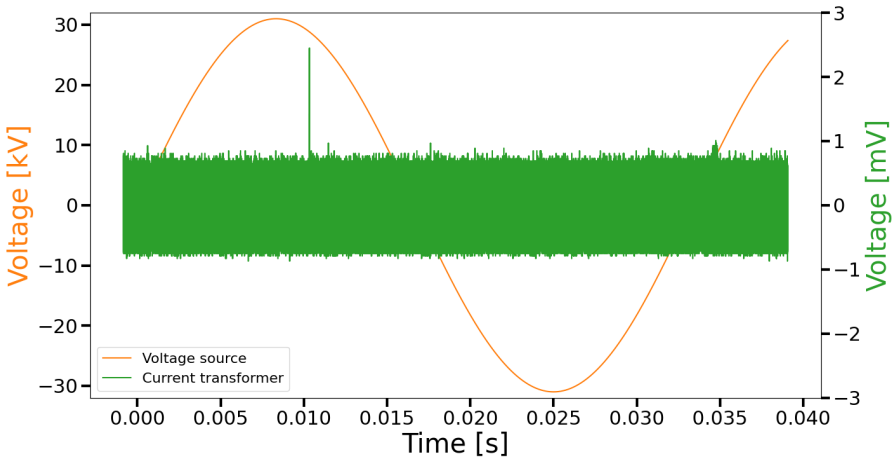


*Figure 30: The signal from the current transformer when a 31 $kV_{peak}$ sinusoidal voltage was applied to the Midel 7131 impregnated system. The signal was collected using the envelope function on the oscilloscope for 1 minute.*

The PD pulse occurred in the positive half period of the voltage, shortly after the voltage peak. The amplitude of this pulse was approximately 2.5 mV. Since only one single PD occurred, this pulse might be caused by noise. The Omicron system did, however, start to detect PDs at 30 $kV_{peak}$. This means that there probably were PDs occurring at 31 $kV_{peak}$ as well. Based on this, the pulse observed in Figure 30 was probably a PD.

**32 $kV_{peak}$ - the current transformer stopped detecting PDs:**
The current transformer started to detect PDs at 31 $kV_{peak}$ applied voltage, as already mentioned. However, when the voltage amplitude was increased to 32 $kV_{peak}$, the current transformer did not detect any PDs. This can be seen from Figure 31. At 34 $kV_{peak}$ the current transformer started detecting PDs again, see appendix B.

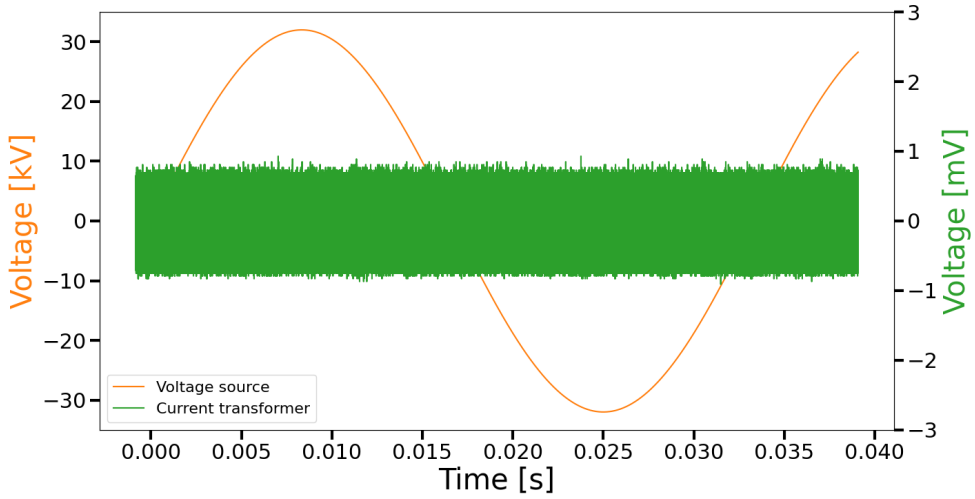


*Figure 31: The signal from the current transformer when a 32 $kV_{peak}$ sinusoidal voltage was applied to the Midel 7131 impregnated system. The signal was collected using the envelope function on the oscilloscope for 1 minute.*

**36 $kV_{peak}$ - the PDs that occurred at the highest applied voltage:**
Figure 32 shows the signal from the current transformer when the insulation system was stressed by a 36 $kV_{peak}$ sinusoidal voltage. The current transformer detected several pulses, as seen from the figure, with amplitudes ranging from 1 to almost 43 mV.

In the positive half period, the majority of the pulses occurred at the rising edge and around the peak of the voltage. The largest of these pulses had an amplitude of approximately 15 mV and occurred right before the voltage peak. The other pulses were a bit smaller, with amplitudes ranging from 1 to almost 10 mV. These pulses occurred around the 15 mV pulse, starting at the middle of the rising edge of the voltage and ending shortly after the voltage peak, as seen from Figure 32. Some tiny negative pulses were detected as well. These coincided with the positive pulses, and had amplitudes ranging from -0.75 mV to -1 mV, see Figure 32.

In the negative half period, the majority of the pulses detected by the current transformer

occurred around the peak of the voltage. The majority of these pulses had amplitudes ranging from 1 to 3 mV, and created a small belt of pulses starting shortly before the voltage peak and ending shortly after, as seen from Figure 32. Three larger pulses were also detected in the negative half period. Two of these three pulses occurred shortly after each other at the beginning of the "belt of pulses". They had amplitudes at approximately 29 and 43 mV. Two negative pulses coincided with these large pulses. They had amplitudes of approximately -5 mV, as seen from Figure 32. The third large pulse occurred at the end of the "belt of pulses", and had an amplitude of 15 mV. This pulse had a coinciding negative pulse as well, just like the other two large pulses. This negative pulse had an amplitude of approximately -2 mV.

From Figure 32 it can be seen that there occurred two pulses, one positive and one negative, at the zero crossing of the voltage after the negative half period. The amplitude of the positive pulse was approximately 3 mV, and the amplitude of the negative pulse was approximately -5 mV.

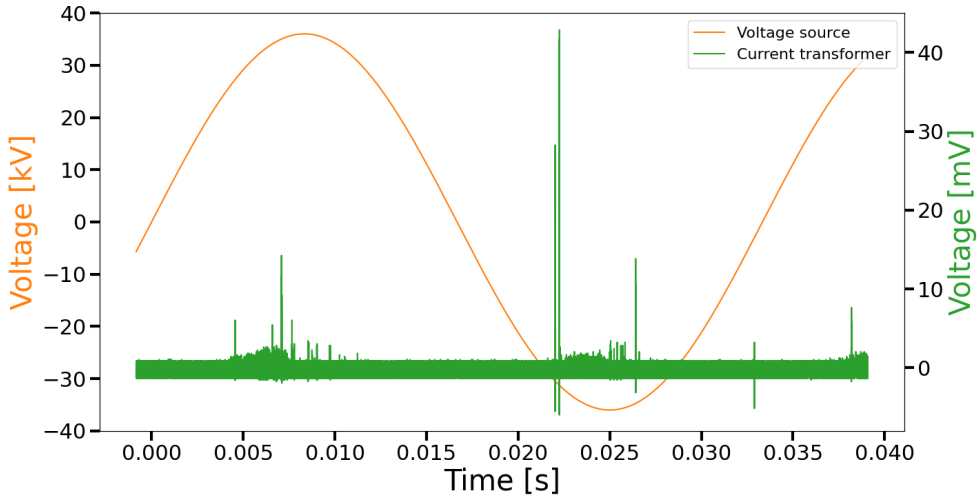


*Figure 32: The signal from the current transformer when a 36 $kV_{peak}$ sinusoidal voltage was applied to the Midel 7131 impregnated system. The signal was collected using the envelope function on the oscilloscope for 1 minute.*

#### 4.1.3.3 Partial discharge inception voltage (PDIV)

Three different measuring devices (PMT, current transformer and Omicron MPD 600) were used to find the partial discharge inception voltage (PDIV) for the Midel 7131 impregnated system stressed by a sinusoidal voltage. These three voltage amplitudes in kV are listed in Table 4.

The three measuring devices did not find the same PDIV, as seen from Table 4. The PDIVs found ranges from 30 $kV_{peak}$ to 35 $kV_{peak}$. The PDIV found by the PMT was the largest

of the three, with an amplitude of 35 kV. The current transformer and Omicron MPD 600 found the PDIV to be 31 and 30 $kV_{peak}$, respectively.

*Table 4: Voltage amplitude in kV of the partial discharge inception voltage (PDIV) for Midel 7131 impregnated pressboard, stressed by a sinusoidal shaped voltage.*

| **Measuring device** | **PDIV [kV]** |
|---|---|
| PMT | 35 |
| Current transformer | 31 |
| Omicron MPD 600 | 30 |

#### 4.1.3.4 Visible ageing of the pressboard

There were no visible signs of ageing, e.g. a ring of soot, on the pressboard sample after the measurements.

## 4.2 Bipolar pulse voltage

This section consists of the results and observations from the measurements performed on the two different insulation systems stressed by a bipolar voltage pulse. A brief discussion of the switching transient, signal delay of the current transformer signal, and the noise from the PMT, all of which affect the results in this section, are presented first. The results for the Nytro 10XN impregnated insulation system are presented next, followed by the results for the Midel 7131 impregnated insulation system.

### 4.2.1 Switching transients, signal delay, and PMT noise

#### 4.2.1.1 Switching transient

The switching of the voltage caused capacitive currents in the system. Every time the voltage switched polarity, a capacitive switching transient occurred. This transient was then registered by the current transformer, just like the current transformer registered pulses caused by PDs, as discussed in section 2.3.2. A spectrum analyzer was therefore used to filter the signal from the current transformer in order to reduce the capacitive switching transient in the signal, as described in section 3.1.2.

Despite using the spectrum analyzer as a filter, the switching transient was not fully removed, see Figure 33. This figure shows the switching transient when the Nytro 10XN impregnated insulation system was stressed by a 5 $kV_{peak}$ voltage. The Midel 7131 impregnated system resulted in a similar figure when a similar test was performed, see appendix D.1. There were no PDs at that applied voltage, i.e. the switching transient is the only pulse in the output signal.

Subtracting the current transformer signal with only the switching transient from the current transformer signals that contained both PDs and switching transients was therefore considered. This would, however, not give a "correct" result either, since PDs are likely to occur on the voltage edge, just like the switching transient. The part of the switching pulse that got past the filter is therefore kept in the plots, as a known limitation to the measuring system and the results.

#### 4.2.1.2 Signal delay

The switching transient occurs when the voltage switches polarity, i.e. on the edge of the voltage. This is, however, not the case in Figure 33. This is because the signal from the current transformer went through the spectrum analyzer, i.e. the bandpass filter, before it was sent to the oscilloscope. The digital processing in the spectrum analyzer caused a slight delay in the signal from the current transformer compared to the signals from the applied voltage and the PMT, both of which went directly to the oscilloscope. From Figure 33, the delay was found to be approximately 4 µs. In order to compensate for this, the signal from the current transformer was shifted 4 µs to the left in the post-processing of the data, see Figure 34.

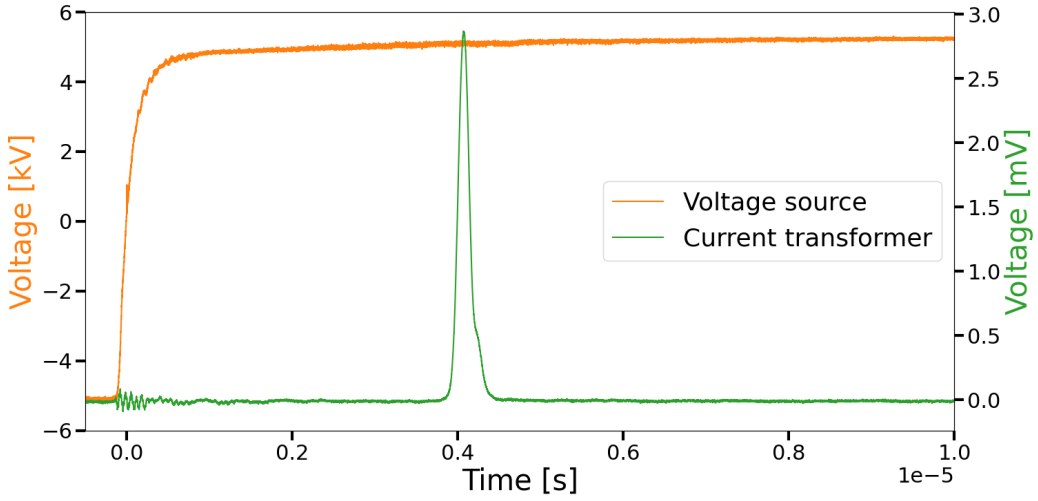


*Figure 33: The capacitive switching transient registered by the current transformer (green curve). The applied voltage is represented by the orange curve. There is a 4 µs delay in the signal from the current transformer. The test was performed on a Nytro 10XN impregnated pressboard sample.*

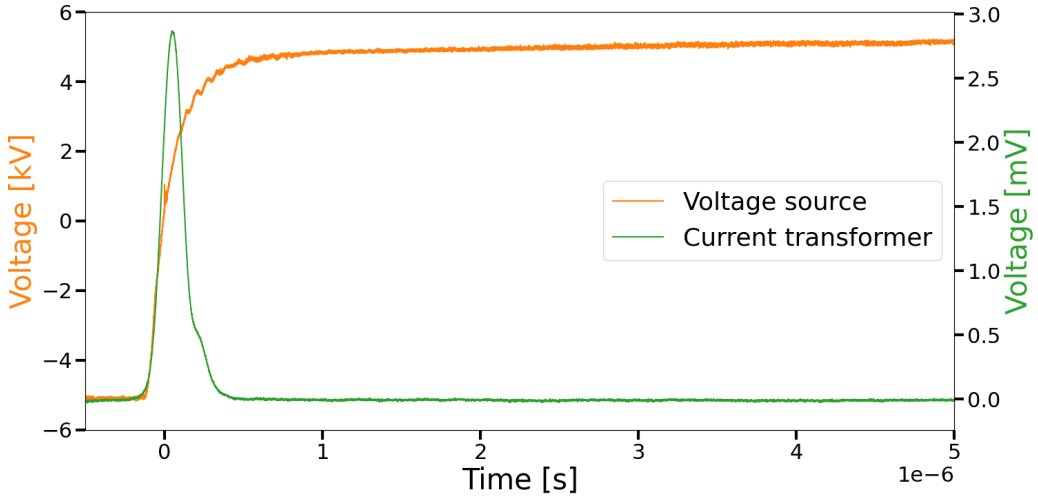


*Figure 34: The capacitive switching transient registered by the current transformer (green curve). The applied voltage is represented by the orange curve. The test was performed on a Nytro 10XN impregnated pressboard sample.*

Since the 4 µs delay was caused by the signal going through the bandpass filter, i.e. by the filter itself, this delay was considered to be the same for both the Nytro 10 XN and the Midel 7131 impregnated systems, and for both the sinusoidal voltage set-up and the bipolar voltage pulse set-up. It was the same for both lab set-ups because the same spectrum analyzer, current transformer and oscilloscope were used in both set-ups.

#### 4.2.1.3 Noise on the PMT signal

Figure 35 shows the signal from the PMT when no voltage was applied to the test object. The test was performed on a Midel 7131 impregnated pressboard sample. As seen from the figure, this signal had quite a lot of noise. The same was, unsurprisingly, the case when a Nytro 10XN impregnated sample was placed in the test cabinet, see appendix C.1. Any pulses detected by the PMT when the voltage is applied have to be larger than the noise in order to be considered a PD. From Figure 35 it can be seen that the pulses have to have amplitudes larger than 4 V (absolute value) in order to be considered a partial discharge.

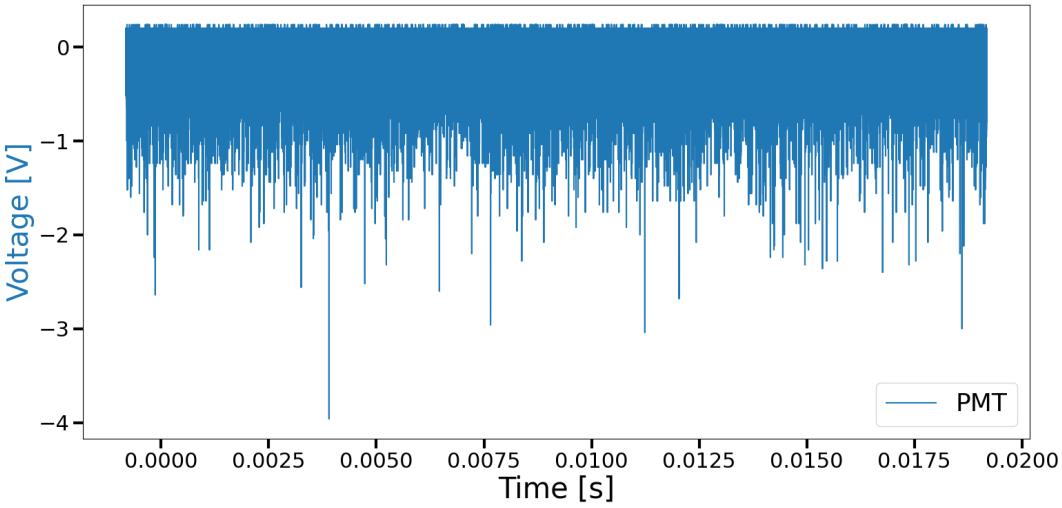


*Figure 35: The noise from the PMT when there were no applied voltage. The test was performed on a Midel 7131 impregnated pressboard sample.*

The resolution of the PMT signal was somewhat limited. This meant that the PMT signal detected by the oscilloscope could only reach a certain maximum value (absolute value). From the plots that will be discussed later, this limit seems to be -7.5 V, see for instance Figure 40.

### 4.2.2 Nytro 10XN

In this section the results and observations from the measurements performed on the Nytro 10XN impregnated insulation system stressed by a bipolar voltage pulse will be presented. First, the PDs detected by the current transformer will be presented. This is followed by the partial discharge inception voltage (PDIV), before ending with the visible ageing of the pressboard.

Note that since the signal from the current transformer was collected from an oscilloscope using the envelope-function on the oscilloscope (the envelope function holds the highest pulses at each point on the voltage shape), it is not possible to tell how many pulses the current transformer detected at a given point on the voltage shape. It is only possible to determine the size of the largest pulse at each point and where on the voltage curve the pulses occurred.

The moisture content in the pressboard sample used in the measurements was below 1.6% the entire time. Since 1.6% is between the defined limits of dry and middle dry, see section 2.1.2, the insulation system is considered to be dry to middle dry.

#### 4.2.2.1 PDs detected by the current transformer and the PMT

The figures in this section contain the applied voltage, the signal from the current transformer, and the signal from the PMT. The measurements were performed as described in section 3.3. A sharp-edged top-electrode was used, see section 3.2.3. The applied bipolar voltage pulse had amplitudes varying from 8 $kV_{peak}$ to 20 $kV_{peak}$. The signal from the current transformer in all of the figures in this section is shifted to the left in order to compensate for the delay, as explained in section 4.2.1.2.

The plots with a positive voltage pulse and the plots with a negative voltage pulse at 10, 16, and 20 $kV_{peak}$ applied voltage are included in this section. The plots, with both positive and negative voltage pulses, of the remaining voltage amplitudes can be found in appendix C.2.

**10 $kV_{peak}$ - the current transformer started to detect PDs:**
Figure 36 includes the plotted signals from the PMT and the current transformer when the applied voltage had an amplitude of 10 kV, and the voltage switches polarity from negative to positive. At this applied voltage, the PMT does not detect any PDs, as seen from Figure 36. The current transformer, on the other hand, does detect two small pulses.

The PDs occurred on the rising edge of the voltage, as seen from Figure 36, and overlapped slightly with each other. The first pulse was caused by the switching of the voltage, though PDs might also occur at this part of the voltage curve and hence contribute to the pulse that the current transformer detected, as discussed in section 4.2.1.1. The second pulse, however, was most likely caused by a partial discharge. Both of the pulses detected by the current transformer have an amplitude of approximately 1.5 mV.

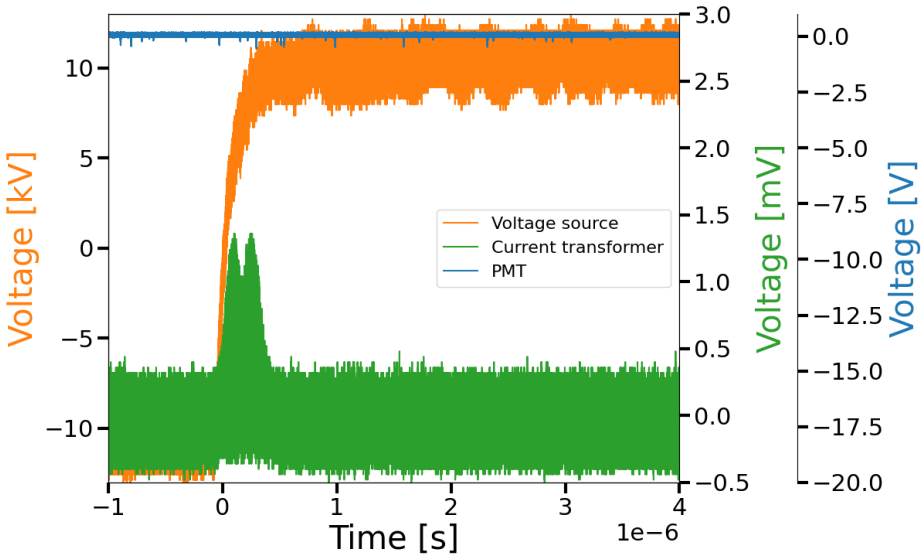


*Figure 36: Nytro 10XN impregnated insulation system. 10 $kV_{peak}$ applied voltage, positive voltage pulse. The signals were collected using the envelope function on the oscilloscope for 1 minute.*

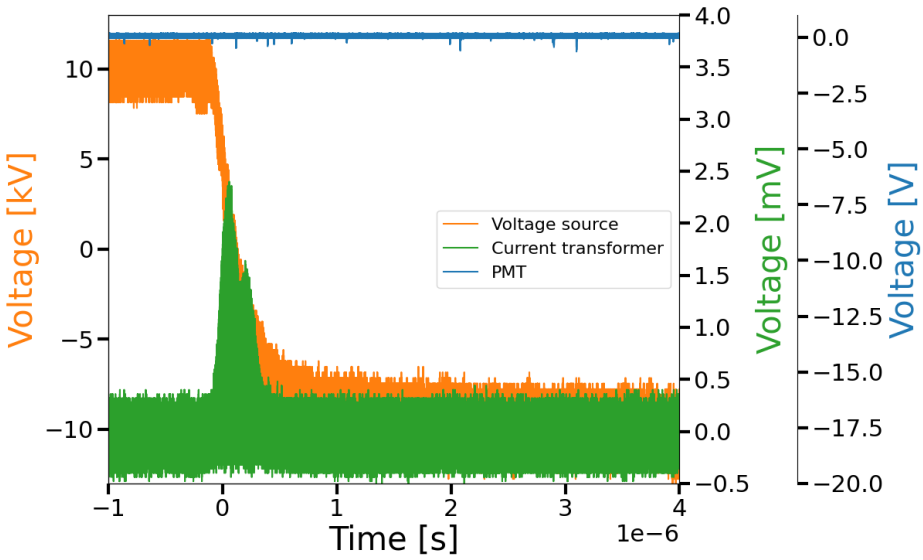


*Figure 37: Nytro 10XN impregnated insulation system. 10 $kV_{peak}$ applied voltage, negative voltage pulse. The signals were collected using the envelope function on the oscilloscope for 1 minute.*

The consequences of the negative voltage pulse at 10 $kV_{peak}$ applied voltage can be seen from Figure 37. The PMT did not detect any PDs here either. However, the current transformer did detect two PDs, just like it did at this applied voltage when the voltage switched from negative to positive. The pulses detected by the current transformer occurred on the falling edge of the voltage, see Figure 37. The amplitude of the first pulse was 2.5 mV. This pulse might have been a result of a combination of the switching transient and PDs, or just the switching transient, as discussed in section 4.2.1.1. The second pulse occurred right after, overlapping slightly with the first pulse. The second pulse had an amplitude of approximately 1.5 mV.

**16 $kV_{peak}$ - the PMT started to detect PDs:**
When the voltage switched polarity from negative to positive at 16 $kV_{peak}$ applied voltage, the PMT started to detect PDs, as seen from Figure 38. From Figure 38, it can be observed that the PMT detected some pulses with amplitudes around -3 V. These might have been caused by PDs, since they were significantly larger than the noise floor in this figure. They might, however, also have been caused by noise since there was a lot of noise on the signal from the PMT, as discussed in section 4.2.1.3.

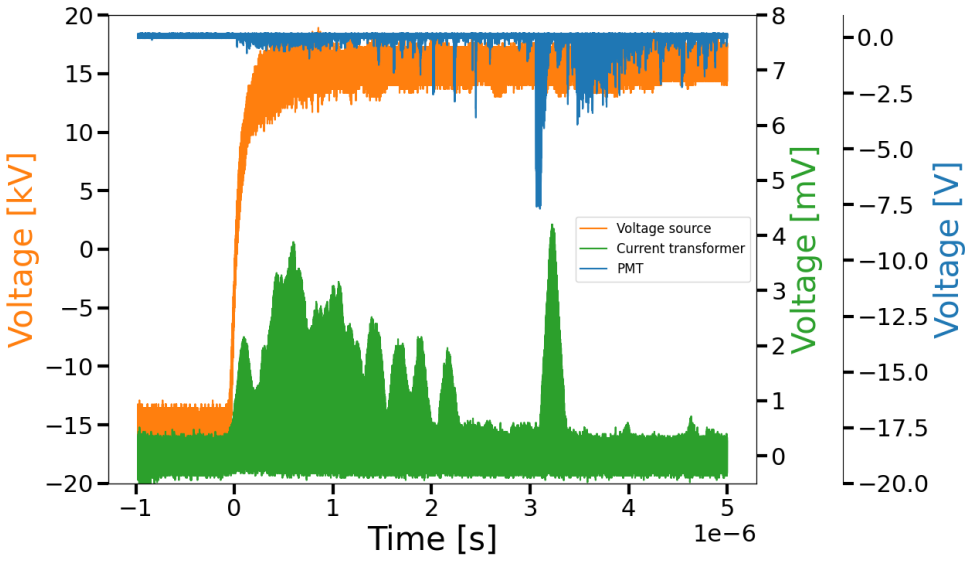


*Figure 38: Nytro 10XN impregnated insulation system. 16 $kV_{peak}$ applied voltage, positive voltage pulse. The signals were collected using the envelope function on the oscilloscope for 1 minute.*

All of these medium sized pulses measured by the PMT occurred after the voltage had switched polarity. The first pulse occurred at 1.5 µs, whilst the majority of these medium sized pulses occurred around 3.5 µs. The pulses at 3.5 µs formed a small cluster. Since so many of the pulses occurred at the same part of the applied voltage, i.e. at 3.5 µs, these pulses are less likely to have been caused by noise than the other pulses. These are, in other words, more likely to have been PDs compared to the other pulses with the same

amplitude that the PMT detected. The largest PD detected by the PMT had an amplitude of approximately -7.5 mV and occurred at approximately 3.1 µs. This was approximately 3 µs after the voltage switched polarity, right before the cluster of pulses with -3 V amplitudes. The large pulse is drawn by a thick line in the plot, indicating that there were several pulses with similar amplitudes detected around 3.1 µs.

At 16 $kV_{peak}$ applied voltage, the current transformer detected a lot of PDs, as seen from Figure 38. Almost all of these occurred after the switching transient, i.e. almost all of the PDs occurred after the voltage had changed polarity. The only pulse to occur on the edge of the voltage had an amplitude of approximately 2 mV. This pulse might have been a result of a combination of the switching transient and PDs, or just the switching transient, as discussed in section 4.2.1.1.

The majority of the PDs detected by the current transformer occurred between 0.25 µs and 2.25 µs. These PDs had amplitudes varying from approximately 2 mV to about 3.8 mV. Some of these pulses, especially the pulses occurring between 0.5 µs and 1.5 µs, overlapped slightly. Combined with the other PDs detected by the current transformer between 0.25 µs and 2.25 µs, these PDs created a pattern that resembles a mountain range, see Figure 38. The largest PD detected by the current transformer at 16 $kV_{peak}$ applied voltage, had an amplitude of approximately 4.2 mV. From Figure 38 it can be seen that this PD occurred as an isolated peak at about 3.2 µs, i.e. almost simultaneously with the largest PD detected by the PMT, and about 3 µs after the voltage switched polarity.

Figure 39 depicts the signals from the current transformer and the PMT when the applied voltage with an amplitude of 16 $kV_{peak}$ switched from positive to negative polarity. From this figure, it can be observed that the PMT detected pulses with amplitudes ranging from approximately -1 V to almost -6 V. The smaller pulses, those with amplitudes below 4 V (absolute value), were probably noise and not PDs. The larger pulses might, on the other hand, have been caused by PDs.

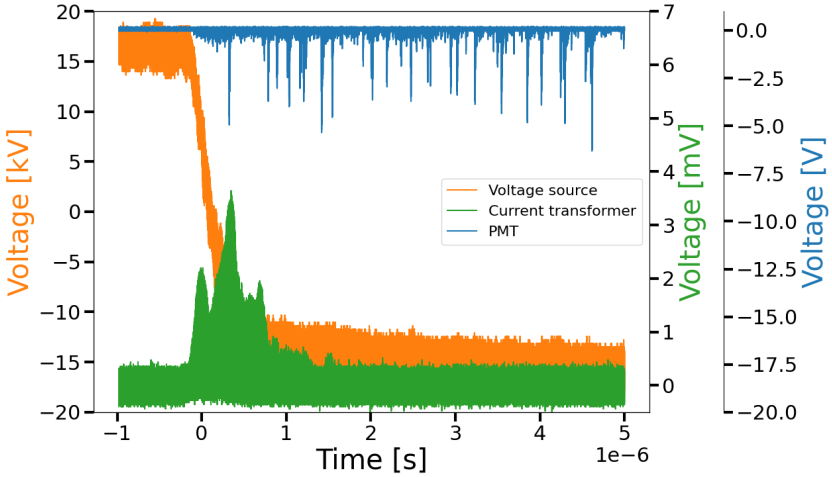


*Figure 39: Nytro 10XN impregnated insulation system. 16 $kV_{peak}$ applied voltage, negative voltage pulse. The signals were collected using the envelope function on the oscilloscope for 1 minute.*

The first PD detected by the PMT occurred at approximately 0.4 µs, i.e. at the moment where the applied voltage reached -16 $kV_{peak}$, and had an amplitude of -5 V. The other PDs detected by the PMT occurred after this, i.e. after the voltage had switched polarity. These PDs occurred "on their own", without forming any clusters of pulses. The largest PD detected by the PMT had an amplitude of approximately -6 V, and occurred at about 4.8 µs. The two second largest PDs both had amplitudes of around -5 V, and occurred at approximately 0.4 and 1.4 µs, respectively.

The PD pulses detected by the current transformer all occurred between approximately 0 µs and 1.5 µs, as seen from Figure 39. The first of these pulses had an amplitude of approximately 2 mV. This pulse might have been a result of a combination of the switching transient and PDs, or just the switching transient, as discussed in section 4.2.1.1. After the voltage reached -16 $kV_{peak}$, at approximately 0.8 µs, and until the PDs detected by the current transformer stopped at around 1.5 µs, the amplitudes of the PD pulses were all 1 mV and lower. They were, in other words, so small that they could almost be considered as part of the noise floor. However, they were probably caused by PDs since the noise floor of the current transformer signal had a near constant amplitude of 0.5 mV, and these pulses are easily distinguishable from the noise, see Figure 39.

The PDs occurring at the falling edge of the voltage all had amplitudes above 1.5 mV. They all occurred close together, and consequently overlapped slightly. The largest of the PDs detected by the current transformer had an amplitude of almost 4 mV, and was the first PD to occur after the switching transient, at approximately 0.2 µs. The second largest PD had an amplitude of approximately 2 mV. This pulse was, at 0.8 µs, the last PD the current transformer detected before the aforementioned tiny pulses with amplitudes below 1 mV.

**20 $kV_{peak}$ - the PDs that occurred at the highest applied voltage:**
Figure 40 includes the plotted signals from the PMT and the current transformer when the applied voltage had an amplitude of 20 kV, and the voltage switched polarity from negative to positive. Under this voltage stress, the PMT detected PDs almost continuously starting from when the applied voltage reached its new positive amplitude at 20 kV. The PDs detected by the PMT all had an amplitude of approximately -7.5 V. Despite the PMT detecting PDs at almost every part of the voltage after the voltage pulse, there were some instances around 4 µs where the PMT did not detect any PDs. This is particularly visible at about 3.6 and 4.2 µs. The near continuous curtain of PD-pulses created by the PMT in Figure 40 makes it difficult to study the results from the current transformer properly. The PMT signal has therefore been removed from the plot in Figure 41, making it significantly easier to study the signal from the current transformer.

From Figure 41 it can be seen that the first pulse detected by the current transformer had an amplitude of approximately 3 mV. This pulse might have been a result of a combination of the switching transient and PDs, or just the switching transient, as discussed in section 4.2.1.1. The second pulse occurred near 0.5 µs. The current transformer then detected PDs continuously, just like the PMT except that the PDs detected by the current transformer had varying amplitudes. The PDs after the switching transient, starting at around 0.5 µs and ending at 1 µs, overlapped slightly. This created a small mountain range pattern. The largest pulses in this cluster had amplitudes of almost 6 mV. After these pulses, between 1 and 1.7 µs, some smaller PDs followed. These had amplitudes up to 2 mV. Almost all of the PDs detected by the current transformer after 1.7 µs had amplitudes below 2 mV. These small pulses might be a result of noise. They might, however, also be caused by PDs. Since

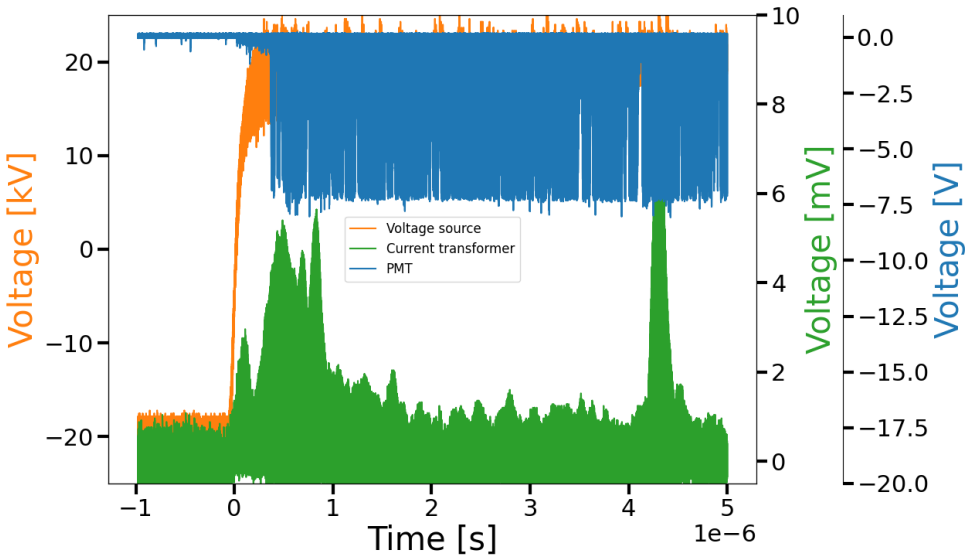


*Figure 40: Nytro 10XN impregnated insulation system. 20 $kV_{peak}$ applied voltage, positive voltage pulse. The signals were collected using the envelope function on the oscilloscope for 1 minute.*

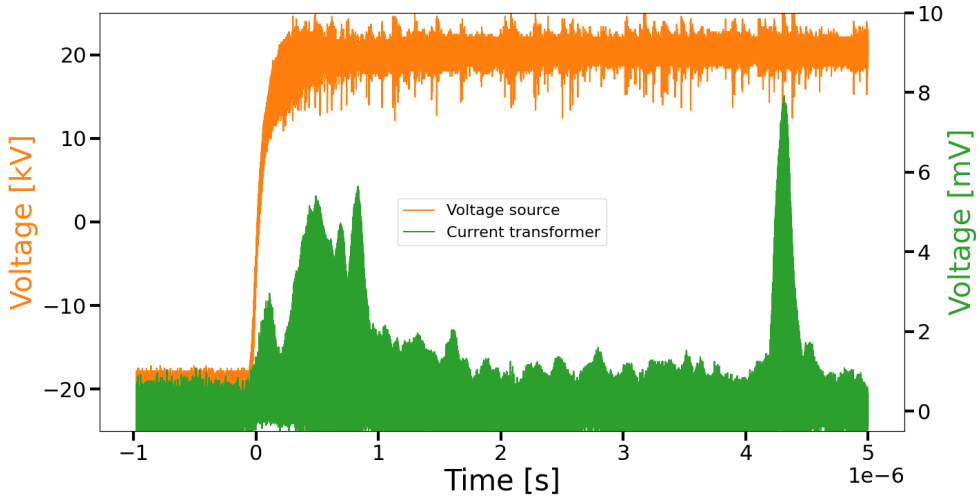


*Figure 41: Nytro 10XN impregnated insulation system. 20 $kV_{peak}$ applied voltage, positive voltage pulse. The signal from the PMT is not included. The signals were collected using the envelope function on the oscilloscope for 1 minute.*

they are easily distinguishable and different to the noise floor, see Figure 41, they were most likely caused by PDs. The largest PD detected by the current transformer had an amplitude of almost 8 mV. It occurred at approximately 4.4 µs, i.e. some microseconds after both the switching of the voltage and the PDs with 6 mV amplitudes.

Figure 42 depicts the results from the PMT and the current transformer when the applied voltage switched polarity from positive to negative, at 20 $kV_{peak}$. The PMT registered pulses almost continuously after the voltage had switched polarity. These pulses all had amplitudes of about -7.5 V. The PMT detected some PDs at the edge of the voltage as well, see Figure 42. These two PDs occurred at approximately 0.2 and 0.4 µs respectively, i.e. on the second half of the falling edge of the voltage. Both of these PDs had amplitudes of approximately -5 V.

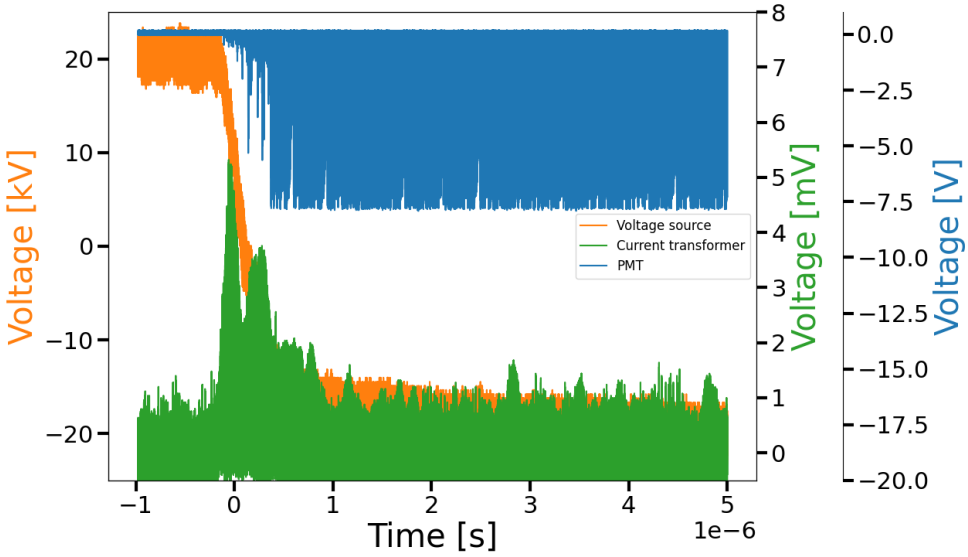


*Figure 42: Nytro 10XN impregnated insulation system. 20 $kV_{peak}$ applied voltage, negative voltage pulse. The signals were collected using the envelope function on the oscilloscope for 1 minute.*

The current transformer registered pulses almost continuously as well. The majority of these pulses had amplitudes of 1.5 mV or less. Some larger pulses were also detected by the current transformer. These occurred at the edge of the voltage, see Figure 42. The largest PDs detected by the current transformer occurred between 0 and 0.9 µs, i.e. on the falling edge of the voltage. The largest pulse had an amplitude of about 5.5 mV. This pulse might have been a result of a combination of the switching transient and PDs, or just the switching transient, as discussed in section 4.2.1.1. The second largest pulse had an amplitude of approximately 4 mV. This pulse occurred at the second half of the voltage edge, around 0.3 µs. The other "large" PDs had amplitudes ranging from 2 to 3 mV, see Figure 42. These pulses occurred between 0.3 and 0.9 µs.

#### 4.2.2.2 Partial discharge inception voltage (PDIV)

Both a PMT and a current transformer were used to find the partial discharge inception voltage (PDIV) for the Nytro 10XN impregnated insulation system stressed by a bipolar voltage pulse. The voltage amplitude in kV of the PDIVs found by the two measuring devices are listed in Table 5. The PDIV found by the PMT was 16 $kV_{peak}$. This is significantly higher than the PDIV found by the current transformer, which was found to be 10 $kV_{peak}$. This is only about 2/3 of the PDIV found by the PMT.

*Table 5: Voltage amplitude in kV of the partial discharge inception voltage (PDIV) for Nytro 10XN impregnated pressboard, stressed by a bipolar voltage pulse.*

| **Measuring device** | **PDIV [kV]** |
|---|---|
| PMT | 16 |
| Current transformer | 10 |

#### 4.2.2.3 Visible ageing of the pressboard

A thin circle of soot could be observed on the pressboard sample after the measurements had been performed, see Figure 43. The center of the ring coincided with the center of the pressboard sample, as seen from Figure 43i.

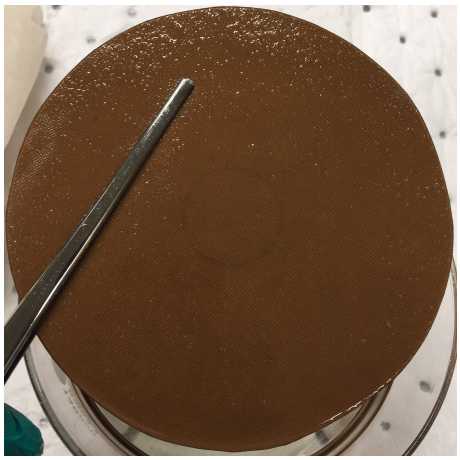

*(i) The thin circle of soot and the pressboard sample are concentric.*

*(ii) The soot circle had the same diameter, i.e. 30 mm, as the sharp edged top electrode.*

*Figure 43: The thin circle of soot on the Nytro 10XN impregnated pressboard sample after the pressboard sample had been used in the measurements with the bipolar voltage pulse. Note that the quality of these pictures might make it difficult to observe the soot circle if they are printed.*

The soot-circle had the same diameter, i.e. 30 mm, as the sharp edged top electrode that was used for the measurements, see section 3.2.3 for more on the sharp edged electrode. The circle of soot was more of a dark grey shadow than a thick black line, see Figure 43ii. The thickness of the soot-circle was measured to approximately 1 mm. There were no easily distinguishable branches going out from the circle.

### 4.2.3 Midel 7131

In this section the results and observations from the measurements performed on the Midel 7131 impregnated insulation system stressed by a bipolar voltage pulse will be presented. First, the PDs detected by the current transformer will be presented. This is followed by the partial discharge inception voltage (PDIV), before ending with the visible ageing of the pressboard.

Note that since the signal from the current transformer was collected from an oscilloscope using the envelope-function on the oscilloscope (the envelope function holds the highest pulses at each point on the voltage shape), it is not possible to tell how many pulses the current transformer detected at a given point on the voltage shape. It is only possible to determine the size of the largest pulse at each point and where on the voltage curve the pulses occurred.

The moisture content in the pressboard sample used in the measurements was below 0.9% the whole time. Since 0.9% is between the defined limits of dry and middle dry, see section 2.1.2, the insulation system is considered to be dry to middle dry.

#### 4.2.3.1 PDs detected by the current transformer and the PMT

The figures in this section contain the applied voltage, the signal from the current transformer, and the signal from the PMT. The measurement series was performed as described in section 3.3. A sharp-edged top-electrode was used, see section 3.2.3. The applied bipolar voltage pulse had amplitudes varying from 8 $kV_{peak}$ to 20 $kV_{peak}$. The signal from the current transformer in all of the figures in this section is shifted to the left in order to compensate for the delay, as explained in section 4.2.1.2.

In this section, the plots with a positive voltage pulse and the plots with a negative voltage pulse at 10, 16, and 20 $kV_{peak}$ applied voltage will be described. The plots, with both positive and negative voltage pulses, of the remaining voltage amplitudes can be found in appendix D.2.

**10 $kV_{peak}$ - the current transformer started to detect PDs:**
The pulses detected by the PMT and the current transformer when the applied voltage switched polarity from negative to postive with an amplitude of 10 $kV_{peak}$ is plotted in Figure 44. From this figure it can be seen that the PMT did not detect any PDs at this voltage. The current transformer did, however, detect some pulses.

The largest pulse detected by the current transformer had an amplitude of approximately 5 mV and occurred at the edge of the voltage. This pulse might have been a result of a combination of the switching transient and PDs, or just the switching transient, as discussed in section 4.2.1.1. The current transformer also detected some smaller pulses, starting at about 0.25 µs, when the applied voltage had just reached its new positive amplitude. These pulses are difficult to study properly in Figure 44, since their amplitudes are small compared to the scale of the plot. An up-scaled version can therefore be found in Figure 45.

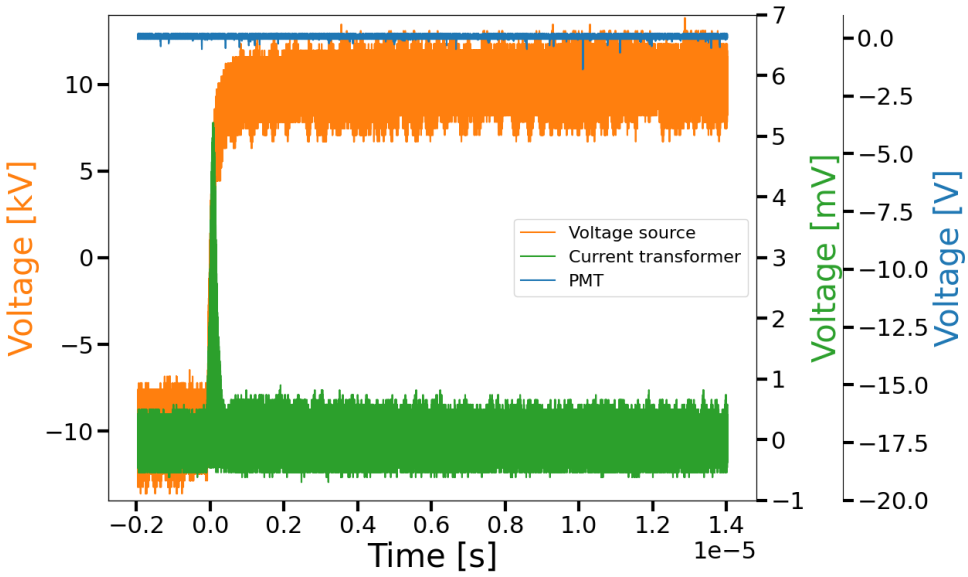


*Figure 44: Midel 7131 impregnated insulation system. 10 $kV_{peak}$ applied voltage, positive voltage pulse. The signals were collected using the envelope function on the oscilloscope for 1 minute.*

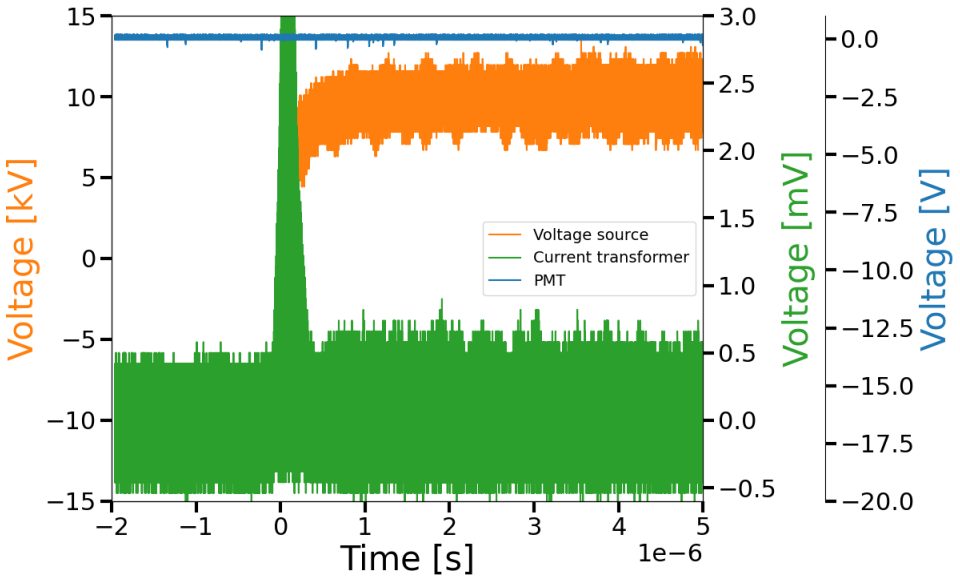


*Figure 45: Midel 7131 impregnated insulation system. 10 $kV_{peak}$ applied voltage, positive voltage pulse. This is a part of the main plot found in Figure 44. The signals were collected using the envelope function on the oscilloscope for 1 minute.*

From Figure 45 it can bee seen that the smaller pulses detected by the current transformer had amplitudes ranging from 0.5 to 0.9 mV, i.e. right above the noise floor. These pulses were very small, and might therefore be noise. However, they were distinguishable as small pulses rather than noise when compared to the noise floor that can be observed before 0 µs. 10 $kV_{peak}$ is therefore considered the inception voltage found by the current transformer for the PDs in the Midel 7131 impregnated system.

Figure 46 includes the plots of the pulses detected by the current transformer and the PMT when the voltage switched polarity from positive to negative at 10 $kV_{peak}$ applied voltage. The PMT did not detect any discharges at this voltage.

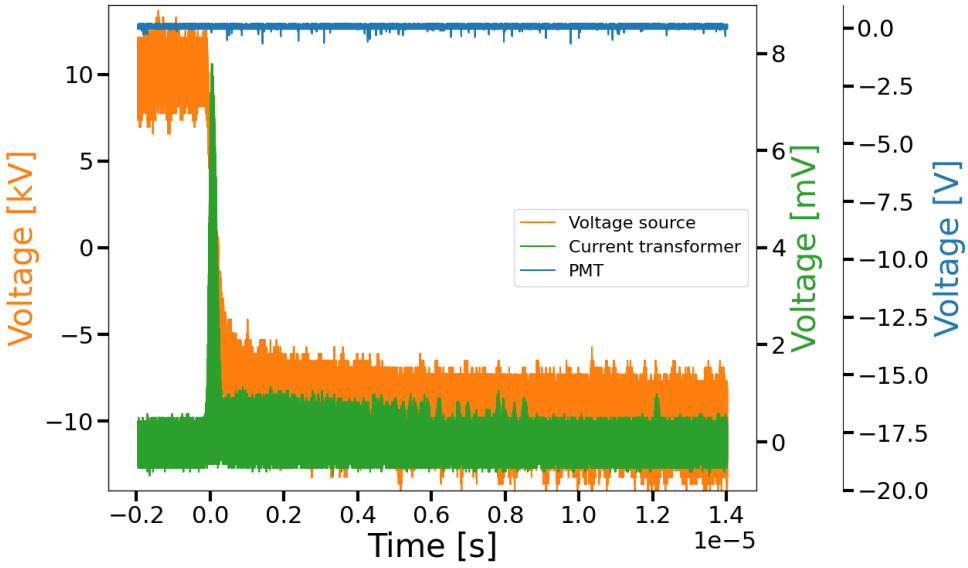


*Figure 46: Midel 7131 impregnated insulation system. 10 $kV_{peak}$ applied voltage, negative voltage pulse. The signals were collected using the envelope function on the oscilloscope for 1 minute.*

The current transformer detected a large pulse with an amplitude of almost 8 mV at the edge of the voltage. This pulse might have been a result of a combination of the switching transient and PDs, or just the switching transient, as discussed in section 4.2.1.1. A lot of smaller pulses were also detected by the current transformer. These had amplitudes ranging from 0.75 to 1.25 mV, as seen from Figure 46. The majority of these PDs occurred between 0.25 and 6 µs, creating a continuous band. The PDs continued between 6 and 8.5 µs, but here they had some space between them. Finally, a pulse with an amplitude of approximately 1.25 mV was detected by the current transformer at 12 µs.

**16 $kV_{peak}$:**
The signals from the PMT and the current transformer when the voltage switched polarity from negative to positive at 16 $kV_{peak}$ applied voltage are plotted in Figure 47. The PMT did not detect any pulses at this applied voltage. The current transformer, on the other hand, detected many pulses. Since the majority of these pulses occurred between 0 and 3 µs, see Figure 47, an up-scaled version of this part of the plot has been made, see Figure 48.

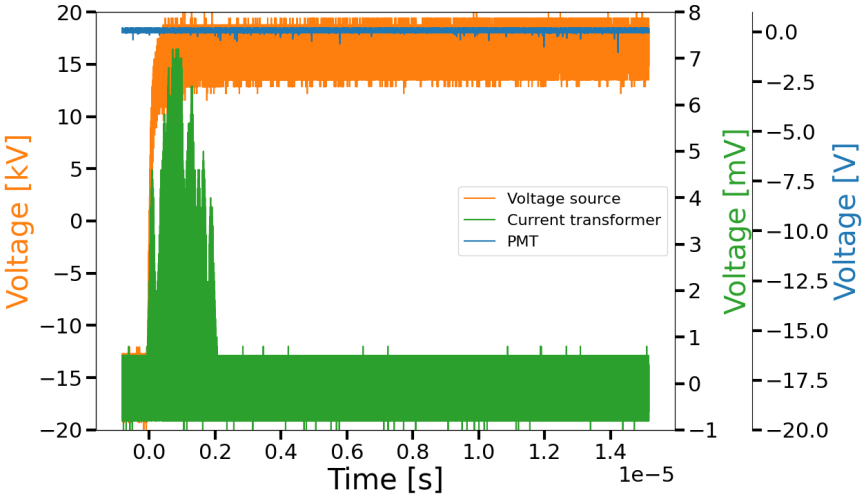


*Figure 47: Midel 7131 impregnated insulation system. 16 $kV_{peak}$ applied voltage, positive voltage pulse. The signals were collected using the envelope function on the oscilloscope for 1 minute.*

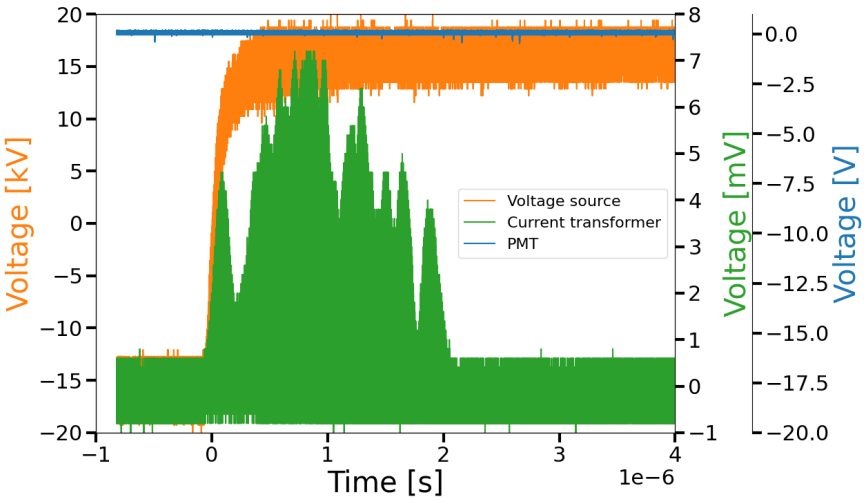


*Figure 48: Midel 7131 impregnated insulation system. 16 $kV_{peak}$ applied voltage, positive voltage pulse. This is a part of the main plot found in Figure 47. The signals were collected using the envelope function on the oscilloscope for 1 minute.*

From Figure 48 it can be seen that the current transformer detected many large pulses between 0 and 2 µs. The first pulse occurred on the edge of the voltage, and had an amplitude of almost 5 mV. It might have been a result of a combination of the switching transient and PDs, or just the switching transient, as discussed in section 4.2.1.1. After this first pulse followed many pulses that overlapped each other slightly, creating a mountain range shaped pattern. The "mountain range" started at approximately 0.25 µs, and ended with a "lone mountain" at almost 2 µs, see Figure 48. The amplitudes of these PD pulses ranged from 4 mV to 7.2 mV. The largest pulses occurred right after the voltage had changed polarity, at approximately 0.5 µs. The amplitudes of these pulses were all above 6 mV. The largest pulse occurred at about 0.8 µs, and had, as mentioned, an amplitude of approximately 7.2 mV.

Figure 49 includes the signals from the current transformer and the PMT when the voltage switched polarity from positive to negative at 16 $kV_{peak}$ applied voltage. The PMT did not detect any PDs at this voltage, as seen from the figure. The current transformer detected some smaller pulses between 1 and 8 µs, i.e. after the voltage had switched polarity. These pulses had amplitudes ranging from 1 to 1.5 mV, as seen from Figure 49. The current transformer detected som larger PDs as well. These occurred at the edge of the voltage. In order to study these properly, an up-scaled version of the plot is depicted in Figure 50.

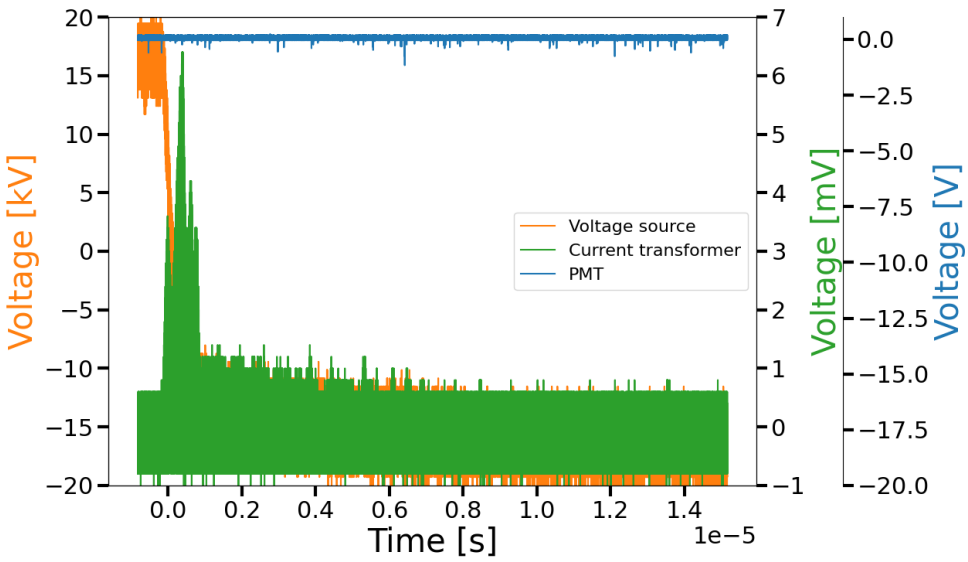


*Figure 49: Midel 7131 impregnated insulation system. 16 $kV_{peak}$ applied voltage, negative voltage pulse. The signals were collected using the envelope function on the oscilloscope for 1 minute.*

The current transformer detected four large pulses at the edge of the voltage, see Figure 50. These pulses overlap slightly, as seen from the figure. The first pulse had a 3.5 mV amplitude. This pulse might have been a result of a combination of the switching transient and PDs, or just the switching transient, as discussed in section 4.2.1.1. At approximately 0.5 µs,

i.e. when the voltage had just reached -16 $kV_{peak}$, the largest pulse detected by the current transformer occurred. This pulse had an amplitude of almost 6.5 mV. This large pulse was followed by two pulses with amplitudes of about 4.5 and 3.5 mV, respectively.

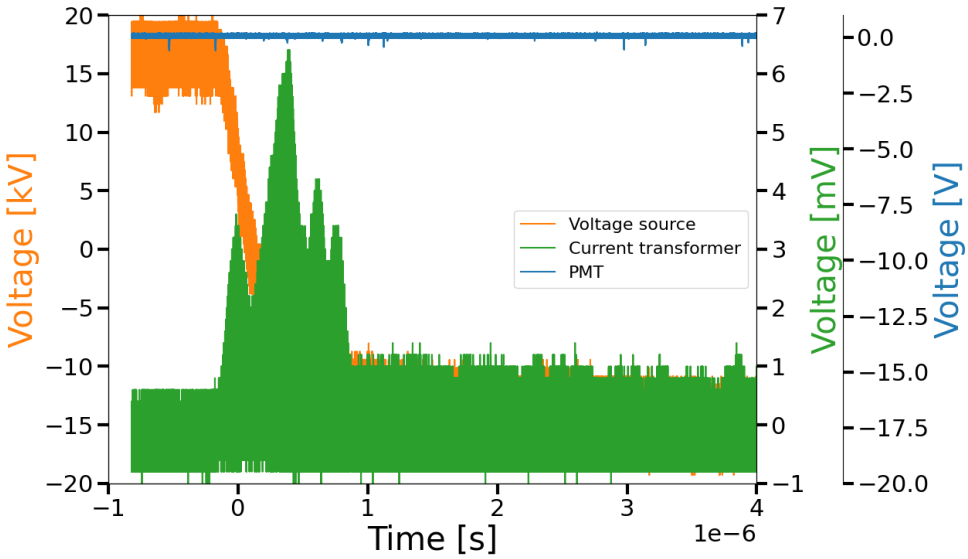


*Figure 50: Midel 7131 impregnated insulation system. 16 $kV_{peak}$ applied voltage, negative voltage pulse. This is a part of the main plot found in Figure 49. The signals were collected using the envelope function on the oscilloscope for 1 minute.*

**20 $kV_{peak}$ - the PMT started to detect PDs:**
Figure 51 includes the results from both the PMT and the current transformer when the voltage switched polarity from negative to positive at 20 $kV_{peak}$ applied voltage. At this voltage, the PMT started to detect PDs. The first pulse detected by the PMT occurred when the voltage had just reached 20 $kV_{peak}$. This pulse had an amplitude of approximately -7.5 V. The PMT continued to detect pulses after this. The majority of these pulses had the same amplitude, -7.5 V, see Figure 51. Around 14 µs, the PMT detected a lot of pulses. This coincided with the largest pulse detected by the current transformer. In order to study this pulse detected by the current transformer properly, a plot without the signal from the PMT is depicted in Figure 52.

From Figure 52 it can be seen that the large pulse detected by the current transformer at 14 µs had an amplitude of approximately 32 mV. The current transformer also detected some smaller pulses with amplitudes around 4 mV at 8 and 10 µs. The majority of the pulses detected by the current transformer occurred at and right after the voltage edge. In order to study this properly, an up-scaled version of this has been plotted in Figure 53.

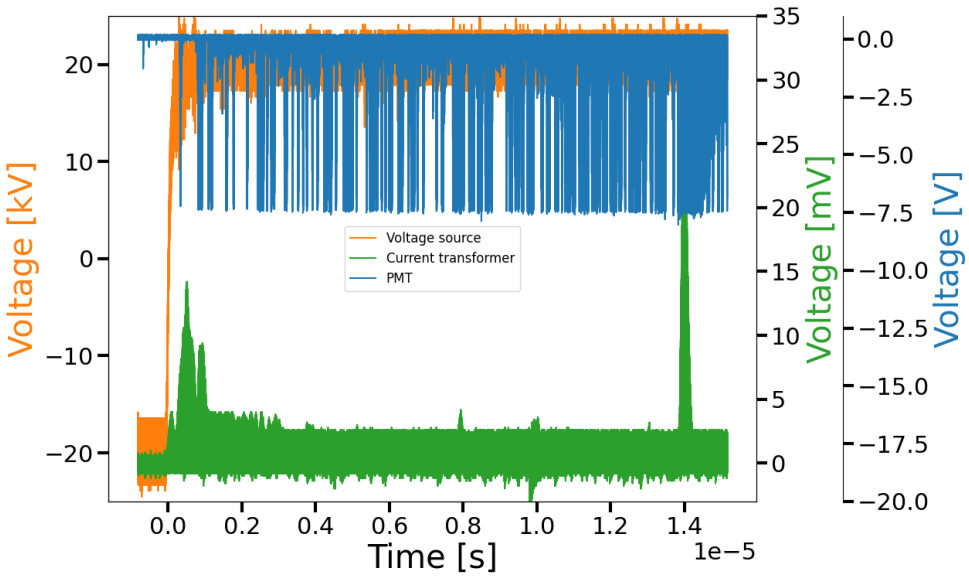


*Figure 51: Midel 7131 impregnated insulation system. 20 $kV_{peak}$ applied voltage, positive voltage pulse. The signals were collected using the envelope function on the oscilloscope for 1 minute.*

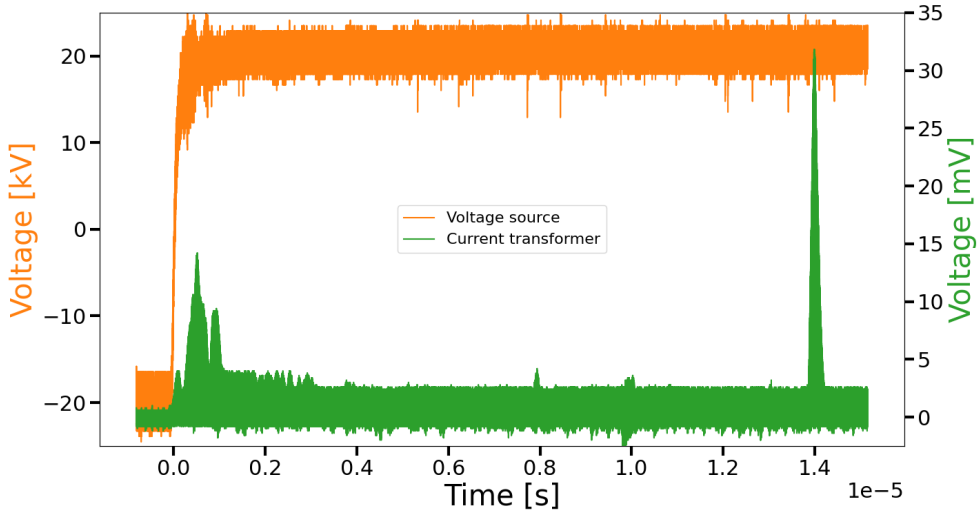


*Figure 52: Midel 7131 impregnated insulation system. 20 $kV_{peak}$ applied voltage, positive voltage pulse. The signal from the PMT is not included. The signals were collected using the envelope function on the oscilloscope for 1 minute.*

From Figure 53 it can be seen that only one of the pulses occurred on the edge of the voltage. This pulse had an amplitude of 4 mV, and might have been a result of a combination of the switching transient and PDs, or just the switching transient, as discussed in section 4.2.1.1. The current transformer detected many other pulses with amplitudes of 4 mV as well, these were situated between 1 and 3µs. The largest pulses detected by the current transformer, apart from the pulse at 14 µs, occurred right after the voltage had reached 20 $kV_{peak}$. These pulses overlapped slightly with each other, but still managed to create two distinct peaks. The first peak was situated at approximately 0.6 µs, and had an amplitude of 14 mV. The second pulse followed at 1 µs, with an amplitude of almost 10 mV.

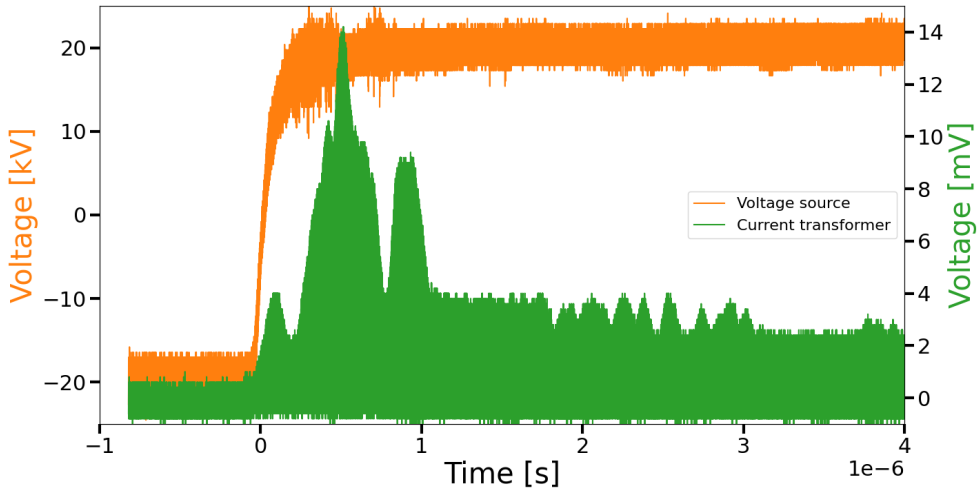


*Figure 53: Midel 7131 impregnated insulation system. 20 $kV_{peak}$ applied voltage, positive voltage pulse. The signal from the PMT is not included. This is a part of the main plot found in Figure 52. The signals were collected using the envelope function on the oscilloscope for 1 minute.*

The signals from the PMT and the current transformer when the voltage switched polarity from positive to negative at 20 $kV_{peak}$ are plotted in Figure 54. From this figure it can be seen that the PMT started to detect PD pulses right after the polarity switch, i.e. at approximately 0.5 µs. These pulses all had an amplitude of -7.5 V, and created a curtain of pulses starting at 0.5 µs and ending at 7.5 µs. The next PDs the PMT detected occurred right after 8 µs, both with an amplitude of -7.5 V, see Figure 54.

The PMT detected another pulse with amplitude -7.5 V right before 10 µs. A pulse was detected simultaneously by the current transformer. After this the PMT detected pulses continuously between 10 and 12 µs. The first of these pulses had an amplitude of -7.5 V, the following pulses had smaller and smaller amplitudes until a pulse with amplitude -2 V was detected right before 12 µs. The pulses that had amplitudes below 4 V (absolute value) are likely to have been caused by noise. At 12 µs, another -7.5 V sized pulse occurred. The PMT detected some other smaller pulses as well, for instance one at 13 µs, see Figure 54. These smaller pulses were probably caused by noise. The pulses detected by the current

transformer are difficult to study properly due to the PMT signal. A plot without the signal from the PMT has therefore been included as Figure 55.

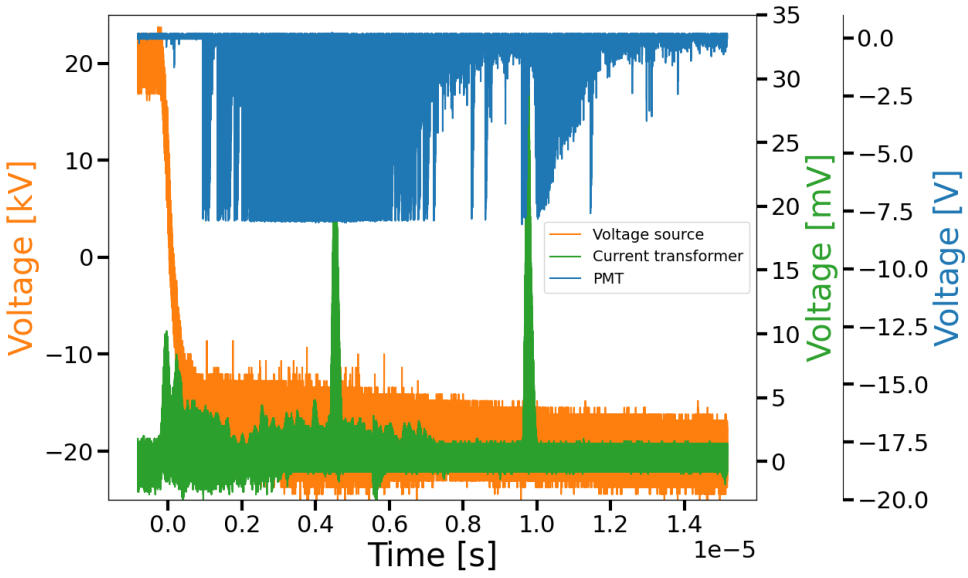


*Figure 54: Midel 7131 impregnated insulation system. 20 $kV_{peak}$ applied voltage, negative voltage pulse. The signals were collected using the envelope function on the oscilloscope for 1 minute.*

The two largest pulses detected by the current transformer occurred right before 5 µs and before 10 µs, as seen from Figure 55. These pulses had amplitudes of 27 mV and 30 mV, respectively. The current transformer detected a belt of smaller pulses between 0.25 µs and 7 µs. These pulses had amplitudes ranging from 1 to 5 mV, as seen from Figure 55. Some medium sized pulses were also detected by the current transformer. These occurred at the edge of the voltage. In order to study these properly, an up-scaled version of this part of the plot has been plotted in Figure 56.

From Figure 56 it can be seen that several pulses occurred on the voltage edge. These pulses overlapped slightly with each other, resulting in two main peaks. The first peak occurred at 0 µs, and had an amplitude of 10 mV. This pulse might have been a result of a combination of the switching transient and PDs, or just the switching transient, as discussed in section 4.2.1.1. The second pulse occurred at 0.25 µs, i.e. when the voltage reached -20 $kV_{peak}$, and had an amplitude of approximately 9 mV. This pulse was followed by a "forest" of pulses with amplitudes ranging from 1 to 5 mV. This "forest" was the "belt of pulses" seen in Figure 55, and continued until almost 7 µs.

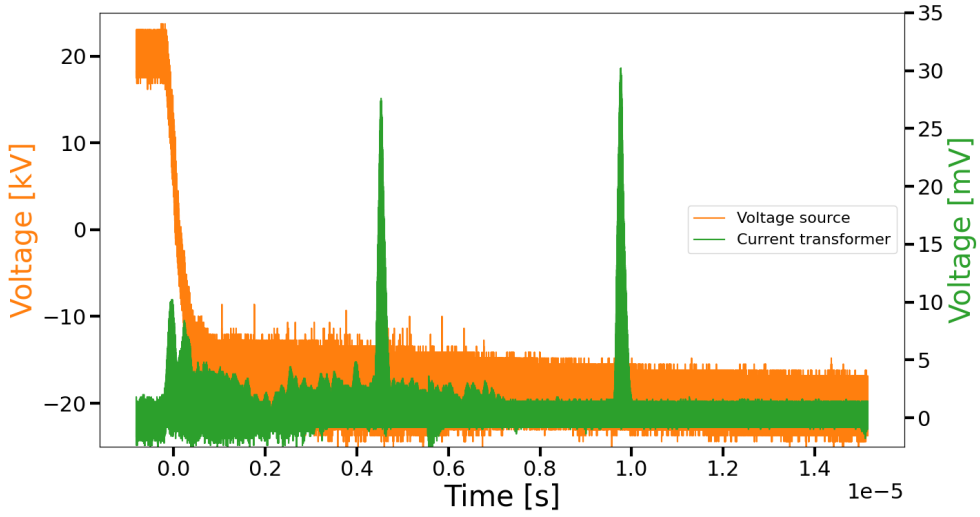


*Figure 55: Midel 7131 impregnated insulation system. 20 $kV_{peak}$ applied voltage, negative voltage pulse. The signal from the PMT is not included. The signals were collected using the envelope function on the oscilloscope for 1 minute.*

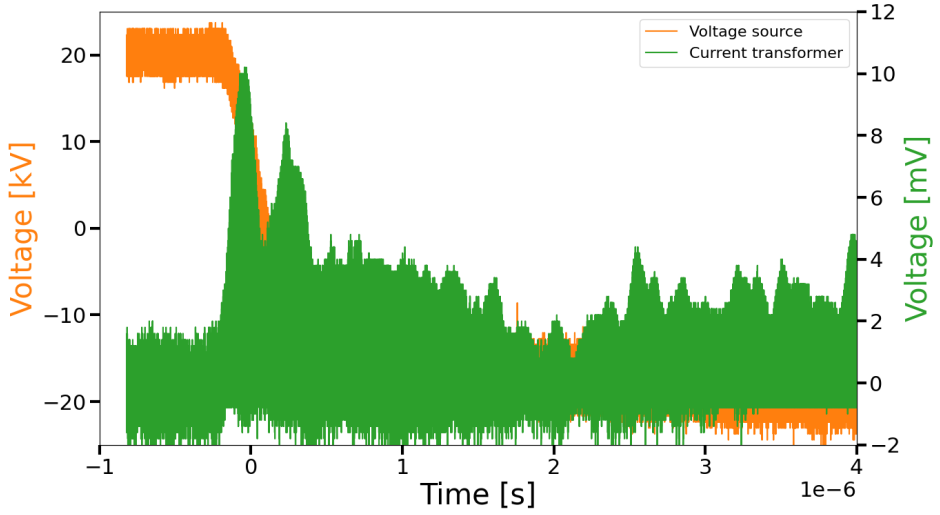


*Figure 56: Midel 7131 impregnated insulation system. 20 $kV_{peak}$ applied voltage, negative voltage pulse. The signal from the PMT is not included. This is a part of the main plot found in Figure 55. The signals were collected using the envelope function on the oscilloscope for 1 minute.*

#### 4.2.3.2 Partial discharge inception voltage (PDIV)

The partial discharge inception voltage (PDIV) found for the sample impregnated in Midel 7131 and stressed by a bipolar voltage pulse is listed in Table 6. The voltage amplitudes of the PDIVs listed in Table 6 are measured in kV.

Two different measuring devices, a PMT and a current transformer, were used to find the PDIV. The PDIV found by these two devices were very different, as seen from Table 6. The PMT found the PDIV to be 20 $kV_{peak}$, whilst the current transformer found the PDIV to be 10 $kV_{peak}$. The amplitude of the PDIV found by the PMT was, in other words, twice as large as the amplitude of the PDIV found by the current transformer.

*Table 6: Voltage amplitude in kV of the partial discharge inception voltage (PDIV) for Midel 7131 impregnated pressboard, stressed by a bipolar voltage pulse.*

| **Measuring device** | **PDIV [kV]** |
|---|---|
| PMT | 20 |
| Current transformer | 10 |

#### 4.2.3.3 Visible ageing of the pressboard

There were no visible signs of ageing, e.g. a ring of soot, on the pressboard sample after the measurements.

# 5 Discussion

## 5.1 The partial discharge inception voltage (PDIV)

The measured partial discharge inception voltages (PDIV) for both insulation systems and both voltage stresses are plotted in Figure 57. These results have been presented briefly in sections 4.1.2.3, 4.1.3.3, 4.2.2.2, and 4.2.3.2. In this section, the measured PDIVs will be discussed more thoroughly.

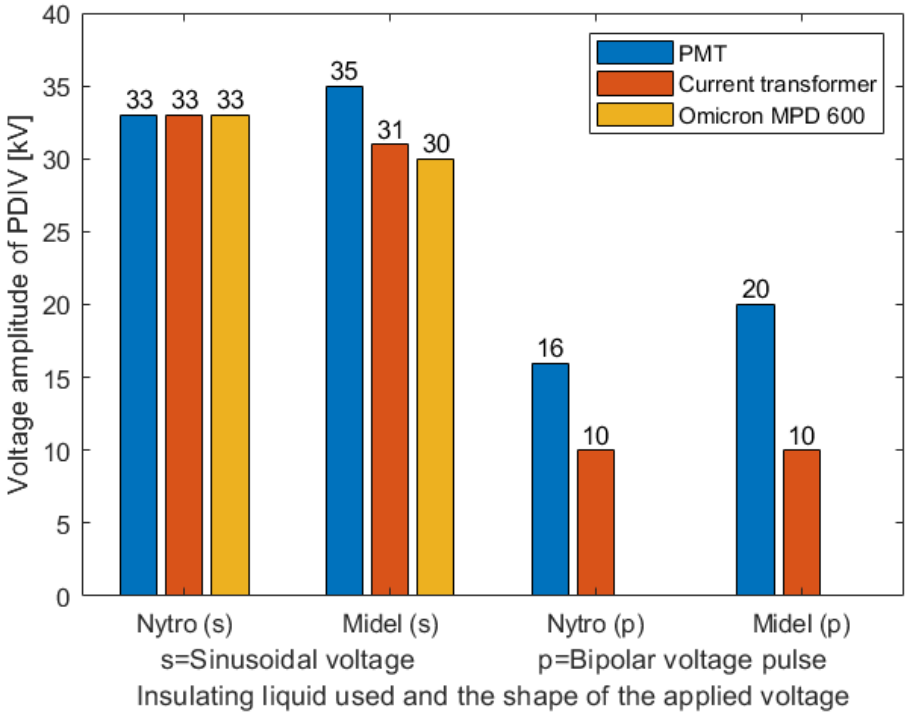


*Figure 57: The measured partial discharge inception voltage (PDIV).*

**PDIVs when the systems were stressed by a sinusoidal voltage:**
When the insulation systems were stressed by a sinusoidal voltage, the PDIV results from the Nytro 10XN impregnated system differed slightly from the PDIV results from the Midel 7131 impregnated system, as seen from Figure 57. For the Nytro 10XN impregnated system, the PDIV was found to be 33 $kV_{peak}$ by both the PMT, the current transformer, and the Omicron MPD 600. For the Midel 7131 impregnated system, however, the PMT found the PDIV to be 35 $kV_{peak}$, the current transformer found it to be 31 $kV_{peak}$, and the Omicron MPD 600 found the PDIV to be 30 $kV_{peak}$. Thus, there are two main differences between the results for the Nytro 10XN and Midel 7131 impregnated systems. Firstly, the measured PDIVs are not the same for the two systems. Secondly, all three measuring devices found different PDIVs for the Midel 7131 impregnated system, but the same PDIV for the Nytro

10XN impregnated system, see Figure 57.

The two types of PD that are likely to occur in the liquid-paper insulation systems during the measurements performed in this project are void discharges and surface discharges, as discussed in section 2.2.1. Void discharges can occur both in cavities in the pressboard and in gas-filled bubbles in the liquid. Since the PMT detects photons, i.e. light, only void discharges in the liquid and surface discharges can be detected by the PMT. Because the current transformer and Omicron started to detect PDs at a lower voltage than the PMT for the Midel 7131 impregnated system, the discharges that occurred before the PMT started to register them were probably void discharges in cavities in the pressboard. This also matches the theory, as surface discharges tend to require stronger electric fields than void discharges in order to occur, see section 2.2.

If the type of PD is the main factor that determines when the different measuring devices start to detect PDs, which it probably is, then the PDs in the Nytro 10XN impregnated system were probably either surface discharges or void discharges inside bubbles in the liquid, or both. Void discharges in cavities in the pressboard sample might have been present as well, though not before at least one of the other PD types started to occur since the PMT started to detect PDs at the same time as the other two measuring devices.

This leads to the question: why did void discharges in cavities in the pressboard sample start to occur before the PMT-visible discharges in the Midel 7131 impregnated system and not in the Nytro 10XN impregnated insulation system? One possibility is, of course, that something went wrong with one of the measurements, and that this difference between the two insulation systems does not really exist. There are, however, other possible answers to the question.

Two different types of high density 2 mm thick pressboard were used, one with a smooth surface for the Midel 7131 impregnated system and one with a slightly uneven surface for the Nytro 10XN impregnated insulation system, as explained in section 3.2.1.2. Maybe "loose" electrons were more prone to either stick to or appear near the slightly uneven pressboard-surface? If this is the case, then there would be more potential start electrons at a lower voltage on the surface between the liquid and the pressboard in the insulation system with the slightly uneven pressboard-surface (Nytro 10XN) compared to the system with the completely smooth pressboard-surface (Midel 7131). More free charges increases the probability that a PD will occur, see section 2.2. The different pressboard-surfaces might therefore be the answer, or a part of the answer, to the question stated in the previous paragraph.

Another possible explanation is that the two insulation liquids caused the difference in the results. Midel and Nytro have, as discussed in section 2.1.1, different properties. If more free charges in a Nytro 10XN impregnated system compared to a Midel 7131 impregnated system tend to end up on the pressboard, then this is a likely explanation to why PMT-visible PDs occurred earlier in the Nytro 10 XN impregnated system. It does not, however, explain why the void discharges in cavities in the pressboard started to occur before the PMT-visible discharges in the Midel 7131 impregnated system and not in the Nytro 10XN impregnated insulation system. Another problem with this explanation is that Midel was found to generate more charges than Nytro when circulated in a transformer, see section 2.1.1. Midel was, in other words, found to have a higher charge density. How many of these charges that tend to end up on the pressboard is, however, unknown. The Nytro 10XN

impregnated system could therefore still have more charges on the pressboard-surface than the Midel 7131 impregnated system.

High density pressboard was used in both insulation systems, and the pressboard samples were impregnated using the same method for both systems, see section 3.2.1.3. The inside of the pressboard samples in the two systems should therefore be very similar. It is therefore unlikely that the pressboard samples themselves are to blame for the void discharges (or lack thereof). It is therefore more probable that the stochastic nature of the PDs, see section 2.2, is to blame. Had the experiment been performed again, then there might have been void discharges in cavities inside the pressboard in the Nytro 10XN impregnated system before the PMT-visible discharges started to occur. This is the easiest, and most likely, explanation as to why void discharges in cavities in the pressboard sample started to occur before the PMT-visible discharges in the Midel 7131 impregnated system and not in the Nytro 10XN impregnated insulation system.

The next question that needs to be addressed is why the Omicron MPD 600 started to detect PDs before the current transformer for the Midel 7131 impregnated insulation system. The Omicron system detects current pulses caused by PDs, and the current transformer detects the change in magnetic field caused by the current pulse that is caused by PD. These two measuring devices should therefore detect the same pulses. How is it possible that the PDIV for the Midel 7131 impregnated system was found to be 30 $kV_{peak}$ by the Omicron MPD 600 and 31 $kV_{peak}$ by the current transformer?

This difference might be caused by noise on the signal from either the current transformer or the Omicron MPD 600. The signal measured by the Omicron at 30 $kV_{peak}$ might have been caused by noise, and therefore have been an invalid measurement. Another possibility is that the current transformer detected a PD pulse at 30 $kV_{peak}$ with an amplitude that made it indistinguishable from the noise on the current transformer signal. This is made more probable by the fact that the PDIVs only had 1 $kV_{peak}$ between them, making it perfectly possible for the current transformer to have detected a tiny PD that got lost in the noise. It is also possible that the spectrum analyzer used to filter the signal from the current transformer filtered out the PD pulse at 30 $kV_{peak}$, since the center frequency used to filter the signal was based on the frequency of streamer discharges found in the system (as explained in section 3.3). It might also be explained by the different frequency range and sensitivity of the two measuring devices.

**PDIVs when the systems were stressed by a bipolar voltage pulse:**
When the insulation systems were stressed by a bipolar voltage pulse, the PDIV results for the two insulation systems were rather similar, as seen from Figure 57. The PMT found the PDIV to be 16 $kV_{peak}$ and 20 $kV_{peak}$ in the Nytro 10XN and Midel 7131 impregnated systems, respectively. The PDIV was found to be 10 $kV_{peak}$ by the current transformer for both systems. Hence, only the PDIV found by the PMT differs between the two insulation systems.

The PDs that started at 10 $kV_{peak}$ were probably void discharges inside cavities in the pressboard, since the PMT did not detect them. This matches the theory, as surface discharges tend to require stronger electric fields than void discharges in order to occur, see section 2.2. It seams unlikely that the void discharges inside bubbles in the liquid should have a significantly larger PDIV than the void discharges inside cavities in the pressboard within the same small insulation system. Thus, the PMT probably detected streamer discharges

and not void discharges inside bubbles in the liquid, since the PDIV found by the PMT was significantly higher than the PDIV found by the current transformer. This will be discussed in greater detail in section 5.2.

Why the PMT-visible PDs, i.e. void discharges inside bubbles in the liquid and streamers on the pressboard surface, occurred at a lower voltage in the Nytro 10XN impregnated system than in the Midel 7131 impregnated system is difficult to say for certain. One possible explanation is that this is not always the case, but merely the case in the test performed during this project. If the same measurements were to be performed again, the PDIV found by the PMT might differ slightly from the one in Figure 57, due to the stochastic nature of the PDs, see section 2.2. Other possible explanations are the difference in pressboard-surface or the different properties of the insulation liquids, as discussed above for the PDIVs when the systems were stressed by a sinusoidal voltage.

**PDIV - sinusoidal voltage vs bipolar voltage pulse:**
The PDIVs found for the two insulation systems stressed by a sinusoidal voltage were significantly larger than the PDIVs found for the systems stressed by a bipolar voltage pulse, as seen from Figure 57. There might, as discussed earlier, have been made errors during the measurements, noise might have affected the results, and the stochastic nature of the PDs will also have affected the measured PDIVs. All three of these uncertainty factors are reduced if more measurements are performed. That being said, the difference between the results for the two voltage stresses is so large that it can not have been caused by noise, measuring errors, and the stochastic nature of the PDs. This is further backed up by the two insulation systems behaving similarly when put under the same type of voltage stress.

The PDIVs being larger when the insulation systems were being stressed by a sinusoidal voltage compared to a bipolar voltage pulse leads to the question: what is causing this difference? This difference can not be credited to measuring errors, noise on the signals, or the PDs' stochastic behaviour, as already discussed. Since the same types of insulation systems and test objects were used for both voltage stresses, the only difference between the tests performed under the different voltage stresses is the voltage stress itself. The only sound explanation for why the PDs start at a lower voltage is therefore that the rapid changes in the electric field caused by the voltage pulse causes PDs to occur at a lower voltage. PDs are known to lead to deterioration and ageing of the insulation over time, as discussed in section 2.2. A lower PDIV will lead to more PDs since the PDs will start to occur earlier. Consequently, insulation stressed by rapid voltage pulses is likely to deteriorate and age faster than insulation stressed by a sinusoidal voltage.

Another difference between the PDIV results for the two voltage stresses is the PDIV found by the PMT compared to the PDIV found by the current transformer. When the systems were stressed by a bipolar voltage pulse, the PDIVs found by the current transformer was only about 60% and 50% of the PDIVs found by the PMT in the Nytro 10XN and Midel 7131 impregnated systems, respectively. The PDIVs for the systems stressed by the sinusoidal voltage hardly differed depending on the measuring device.

This difference indicates that there were more void discharges in cavities in the pressboard, i.e. PMT-invisible PDs, when the systems were stressed by the bipolar voltage pulse compared to when they were stressed by the sinusoidal voltage. Void discharges starting at a lower voltage than surface discharges matches the theory, see section 2.2, as mentioned earlier. This in itself does not, however, explain why the difference between the PDIV for

PMT-visible and PMT-invisible PDs was greater under the bipolar voltage pulse stress than under the sinusoidal voltage stress. What might explain the difference in PDIV is where on the voltage the different PD types tend to occur. Surface discharges usually occur near the peak of the voltage, see section 2.2.1. Void discharges, on the other hand, tend to occur on the rising edge of the voltage (absolute value), see section 2.2.1. The edge of the voltage pulse was steeper than the edge of the sinusoidal voltage. This can explain why the void discharges started a lot earlier than the surface discharges when the systems were stressed by a bipolar voltage pulse compared to when they were stressed by a sinusoidal voltage.

## 5.2 Partial discharge patterns and types of PD

In order to try and determine the type of PDs that occurred during the measurements, the PRPDA plots and the plots of the data collected by the oscilloscope will be studied more closely. This will be done by comparing the size and number of PDs, as well as where on the voltage the PDs occurred.

**Sinusoidal voltage stress:**
The PRPDA plots for the Nytro 10XN and Midel 7131 impregnated systems stressed by a sinusoidal voltage were shown and described in sections 4.1.2.1 and 4.1.3.1. From these plots it can be observed that the majority of the PDs, for both insulation systems, occurred on the rising edge (absolute value) and around the peak of the voltage. PDs on the edge of the voltage indicate void discharges, and PDs around the peak of the voltage indicate surface discharges, as discussed in section 2.2.1. Thus, both streamers on the surface of the pressboard and void discharges are likely to have been present in both insulation systems when stressed by a sinusoidal voltage.

Despite the voltage only being increased to 36 $kV_{peak}$, the largest apparent charge of the PDs in the Midel 7131 impregnated system reached almost 10 000 pC, as seen from the PRPDA plot in Figure 29. The apparent charge of the PDs in the Nytro 10XN impregnated system barely passed 1000 pC, despite the voltage amplitude being increased to 40 $kV_{peak}$, as seen from the PRPDA plot in Figure 23. PDs with large apparent charge appearing near the peak of the voltage is typical for surface discharges, see section 2.2.1. This might therefore indicate that there are more, or larger, streamer discharges in the Midel 7131 impregnated system than in the Nytro 10XN impregnated system. This matches the results found in [11].

Another difference between the two PRPDA plots is the different symmetries in the plots. The plot for the Nytro 10XN impregnated system has phase position, magnitude, and shape symmetry between the two half periods, apart from some "stray" PDs with low apparent charge at the start of the rising edge in the positive half period. The plot for the Midel 7131 impregnated system only has magnitude, and partial shape and phase symmetry between the two half periods. The lack of phase position symmetry indicates that the conditions for PDs differ for positive and negative polarity, see section 2.2.1. In order to see if this is the case for Midel 7131 impregnated insulation systems in general, or just caused by some kind of measuring error, more tests have to be performed. The lack of complete shape symmetry indicates that some of the places where the PDs occurred were physically unsymmetrical.

When studying the PRPDA plots, there seem to be more PDs in the Nytro 10XN impregnated system than in the Midel 7131 impregnated system. It is, however, difficult to say this

for certain by just studying the plot, and practically impossible to quantify the potential difference. Partial discharges occurring consistently over time are considered to be more harmful to the insulation than PDs occurring irregularly, see section 2.2.1. If there really are more PDs in the Nytro 10XN impregnated system than in the Midel 7131 impregnated system, the degradation of the Nytro 10XN impregnated system is likely to be more severe than the degradation of the Midel 7131 impregnated system. The voltage was increased to 40 $kV_{peak}$ for the Nytro 10XN impregnated system, and to 36 $kV_{peak}$ for the Midel 7131 impregnated system. This resulted in the Nytro 10XN impregnated system being both subjected to higher voltages and subjected to voltage stress for a longer period of time than the Midel 7131 impregnated system. This might explain why there were more PDs in the Nytro 10XN impregnated insulation system. Another possible explanation is that there usually are more PDs in Nytro than in Midel.

The PDs in the Nytro 10XN impregnated system were found to start at 33 $kV_{peak}$ by the current transformer. The signal from the current transformer at this voltage is presented in Figure 24 in section 4.1.2.2, and described in the same section. The PDs detected by the current transformer occurred on the rising edge of the voltage in the positive half period, indicating void discharges, and at the peak of the voltage in the negative half period, indicating a surface discharge. The fact that the PMT also detected PDs at this voltage further supports the claim that a surface discharge was present, or at least a void discharge inside a bubble in the liquid. The latter is the least likely option of the two, since the test objects were degassed before the measurement were performed, see section 3.2.1.3. This was done to remove any air from the insulation liquid. There is, of course, a possibility that this air-removal was unsuccessful. In that case, the PDs might have occurred inside air-bubbles in the liquid. However, since the test objects were degassed for at least 15 minutes before they were used, the majority, if not all, of the air bubbles are likely to have left the insulation liquid. From the pictures in section 4.1.2.5, surface discharges were known to occur in the Nytro 10XN impregnated system at voltages with similar magnitudes. This makes it even more likely that the PDs detected by the PMT were streamers.

In the Midel 7131 impregnated system, the PDs were found to start at 31 $kV_{peak}$ by the current transformer. The signal from the current transformer at this voltage is presented in Figure 30 in section 4.1.3.2, and described in the same section. The current transformer detected a pulse shortly after the voltage peak in the positive half period. Whether this was a surface discharge or a void discharge is therefore hard to tell. However, the PMT did not detect any PDs at this voltage for the Midel 7131 impregnated system, so it was probably a void discharge. This is quite different from the signal detected for the Nytro 10XN impregnated system.

The current transformer stopped detecting PDs for both insulation systems for a short period when stressed by a sinusoidal voltage. For the Nytro 10XN impregnated system this happened at 36 $kV_{peak}$, 3 $kV_{peak}$ higher than the PDIV. For the Midel 7131 impregnated system this happened at 32 $kV_{peak}$, just 1 $kV_{peak}$ higher than the PDIV. The current transformer started detecting PDs again after the voltage was increased by 1-2 $kV_{peak}$. One reason for the PDs to stop and then start again can be a sudden lack of start electrons, or some sort of saturation of the insulation system where the voltage stress at a certain level temporarily stops resulting in PDs.

At 36 $kV_{peak}$, the current transformer detected a lot of pulses around the peak of the voltage in both half periods, for the Midel 7131 impregnated system, as seen from Figure 32

in section 4.1.3.2. This is a clear indication that the PDs at this voltage predominantly were surface discharges. The amplitudes of the pulses detected by the current transformer are significantly larger than those found at 31 $kV_{peak}$, with the largest at 36 $kV_{peak}$ having an amplitude of about 43 mV compared to the 2.5 mV amplitude of the PD at 31 $kV_{peak}$. The increased size of the PD is probably caused by the increased voltage and the PDs being surface discharges instead of void discharges. There were some negative pulses at this voltage amplitude as well, as described in section 4.1.3.2. This indicates that the current flowing in the conductor going through the current transformer switched direction. These currents might have been noise caused by the large PD pulses.

40 $kV_{peak}$ was the largest voltage amplitude the Nytro 10XN impregnated system was subjected to. The signal detected by the current transformer at this voltage was quite different from the signal detected for the Midel 7131 impregnated system at 36 $kV_{peak}$, as seen from Figure 26 in section 4.1.2.2. The signal for the Nytro 10XN impregnated system consisted of pulses with amplitudes up to 4 mV, which is significantly lower than the 43 mV pulse in the Midel 7131 impregnated system. The number of pulses can not be counted from this plot, as explained in section 4.2.2, but there seem to be more PDs in the Nytro 10XN impregnated system compared to the Midel 7131 impregnated system. The PDs are at least covering a wider range of phase angles. The majority of the pulses were situated at the rising edge and around the peak of the voltage. This matches the pattern in the PRPDA plot. It also supports the claim that the Midel 7131 impregnated system had more and larger streamer discharges, and that the there were longer periods with continuous PD activity and more void discharges in the Nytro 10XN impregnated system.

**Bipolar voltage pulse stress:**
The signals from the PMT and the current transformer for the insulation systems stressed by a bipolar voltage pulse were shown and described in section 4.2.2.1 and 4.2.3.1. For both insulation systems the current transformer started to detect PDs at 10 $kV_{peak}$. The detected signals were, however, rather different from each other. In the Nytro 10XN impregnated system the pulses occurred at the edge of the voltage, for both the negative and the positive voltage pulse. For the Midel 7131 impregnated system, only one pulse was detected at the edge of the voltage. This was the switching transient (although PDs might have overlapped with it). The other PDs occurred after the voltage had switched polarity. These pulses were so small that they might be mistaken for noise. However, their amplitudes were a bit larger than the noise floor before the switching transient. The claim that these pulses were PD and not noise is further backed up by the current transformer detecting a similar pattern with slightly larger amplitudes at 11 $kV_{peak}$, as seen from Figure 102 in appendix D.2. The PDs in the Nytro 10XN impregnated system were, in other words, larger than the PDs occurring in the Midel 7131 impregnated system at 10 $kV_{peak}$ applied voltage. Since the PMT did not detect any PDs in either insulation systems at this voltage amplitude, the PDs that did occur were probably void discharges.

At 16 $kV_{peak}$, the PMT started to detect PDs in the Nytro 10XN impregnated system. The pulses detected by the PMT were larger and fewer at the positive voltage pulse than at the negative voltage pulse. This indicates that surface discharges are more likely to occur at a negative voltage pulse, but that they tend to be larger if they occur at the positive voltage pulse. This might be why they are rarer at the positive pulse. The pulses detected by the PMT at the negative voltage pulse might, however, have been caused by noise since their amplitudes were somewhere between the noise floor and the amplitude of the PD pulse from

the positive voltage pulse. This would indicate that surface discharges are more likely to occur when there is a positive voltage pulse compared to when a negative voltage pulse is applied. The PMT did not detect any pulses for the Midel 7131 impregnated system at this voltage.

The pattern detected by the current transformer at 16 $kV_{peak}$ for the positive voltage pulse was similar for the two insulation systems. In both cases, the switching transient was the first pulse to occur. This was followed by a "mountain range" of pulses starting right after the voltage switched polarity and lasting for a few microseconds. These pulses in the Nytro 10XN impregnated system had amplitudes up to almost 4 mV. This is a bit smaller than the pulses in the Midel 7131 impregnated system, which had amplitudes up to approximately 7.5 mV. This is different from 10 $kV_{peak}$, where Nytro 10XN had larger PD pulses than Midel 7131. After these pulses, the patterns start to differ as the current transformer did not detect any other pulses in the Midel 7131 impregnated system. In the Nytro 10XN impregnated system, one other PD was detected by the current transformer. This had, at 4.2 mV, the largest amplitude of the pulses detected by the current transformer in this insulation system, and occurred shortly after the "mountain range" of PDs. Since this pulse coincided with the pulse detected by the PMT, this PD was probably a surface discharge. Since the "mountain range" of PDs was similar for both insulation systems, and no PMT-visible discharges occurred in the Midel impregnated system, these discharges were probably void discharges. It makes sense that void discharges occur at (or at least near) the edge of the voltage since a rapid change in the electric field is a trigger for void discharges, see section 2.2.1.

The pulses detected by the current transformer at the negative voltage pulse at 16 $kV_{peak}$ forms a similar pattern to the one observed at the positive voltage pulse for both insulation systems. A "mountain range" pattern is started by the switching transient at the edge of the voltage, and continues for the remaining part of the voltage edge. The amplitudes of the pulses in Midel 7131 were larger than the ones in Nytro 10XN, with a maximum amplitude of about 6.5 mV for Midel 7131 and 4 mV for Nytro 10XN. This is similar to the results for the positive voltage pulse at 16 $kV_{peak}$. After the "mountain range" of pulses, there were pulses with lower amplitudes, below 2 mV for Midel 7131 and below 1 mV for Nytro 10XN. These occurred as a continuous belt for several microsecond in the Midel 7131 impregnated system and for about 1 µs in the Nytro 10XN impregnated system. Since the patterns are similar for the two insulation systems, and the PMT-visible discharges were yet to occur in the Midel 7131 impregnated system, the PDs were probably void discharges. The potential PDs detected by the PMT for the Nytro 10XN impregnated system would then have to be void discharges inside bubbles in the insulation liquid.

A key difference between the results from the negative and positive voltage pulse at 16 $kV_{peak}$ is therefore that the pulses, for both insulation systems, predominantly occurred at the edge of the voltage for the negative pulse compared to right after the voltage had reached its new peak at the positive voltage pulse.

The PMT started to detect PDs in the Midel 7131 impregnated insulation system at 20 $kV_{peak}$. For both insulation systems and both pulse polarities, the signal from the PMT created an almost continuous curtain-like pattern. This does not mean that there were pulses occurring at each part of the voltage. The signal from the PMT was, as explained in section 3.3, gathered by using the envelope function on the oscilloscope. Pulses overlapping slightly can therefore look like a continuous curtain-like signal in the resulting graph. Single

pulses covering larger areas than just a slim spike, were common for the PMT-signal, as seen from Figure 58. This also contributes to the curtain-pattern.

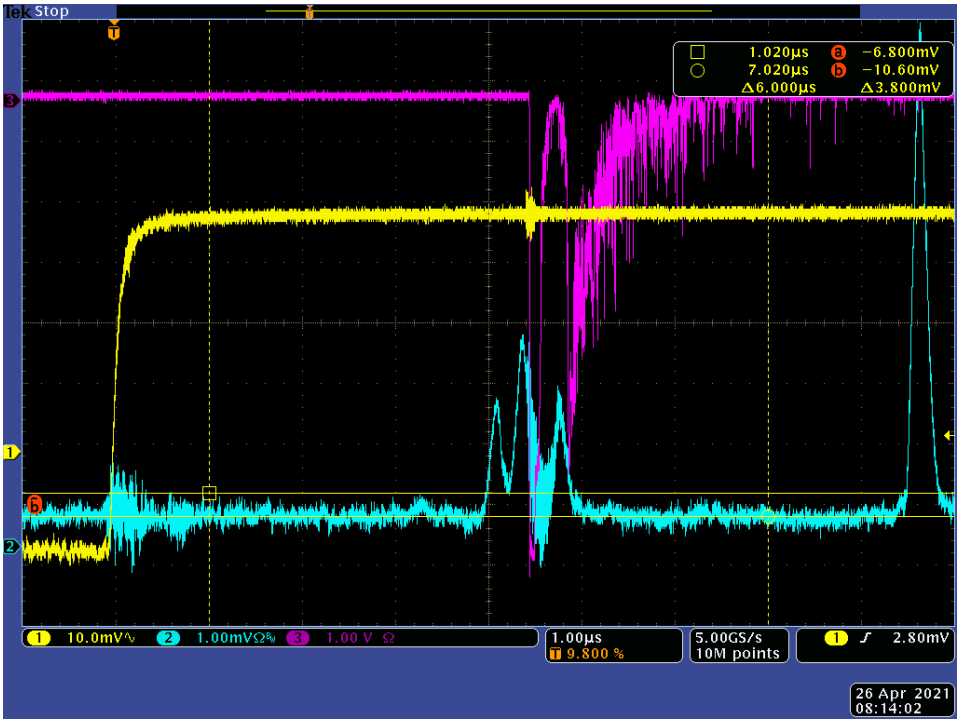


*Figure 58: A snapshot from the oscilloscope when the Nytro 10XN impregnated system was stressed by a bipolar voltage pulse with a 20 $kV_{peak}$ applied voltage. The yellow graph is the applied voltage, the turquoise one is the signal from the current transformer, and the purple graph is the signal from the PMT. Note that the current transformer signal is delayed by approximately 4 µs compared to the other two signals as explained in section 4.2.1.2.*

The pattern detected by the current transformer at 20 $kV_{peak}$, for both polarities and both insulation systems, resembles the pattern it detected at 16 $kV_{peak}$. The main similarity between the signals from the two voltage levels is that the pattern from the positive and negative pulse look very similar. They both started with a "mountain range" of pulses at and right after the edge of the voltage. The main difference between the two polarities is, just like at 16 $kV_{peak}$, that the amplitude of the pulses were slightly lower at the negative pulse compared to the positive pulse. The pattern at 20 $kV_{peak}$ is different from the one detected by the current transformer at 16 $kV_{peak}$ in that there are some large pulses standing by themselves after the "mountain range". These large pulses were probably surface discharges, whilst the "mountain range" pulses probably were void discharges. No isolated large pulses were detected by the current transformer at the negative voltage pulse for the Nytro 10XN impregnated system.

In the Midel 7131 impregnated system, the large isolated pulses were twice as large and three times as large as the largest pulse in the "mountain range" at the positive and negative voltage pulse, respectively. The difference in the Nytro 10XN impregnated system at the positive voltage pulse is not as severe, with the largest PD in the "mountain range" having

an amplitude of 6 mV compared to the 8 mV amplitude of the larger isolated pulse. Just like at 16 $kV_{peak}$, the PDs were significantly larger in the Midel 7131 impregnated sample, with amplitudes passing 30 mV, compared to the Nytro 10XN impregnated system where all of the PDs had amplitudes below 10 mV.

**Sinusoidal voltage vs bipolar voltage pulse:**
By comparing the results from the two different voltage stresses, the patterns detected by the current transformer have some similarities. For both voltage stresses, the Midel 7131 impregnated system seemed to have more surface discharges than the Nytro 10XN impregnated system, despite the PDIV for this type of PD being slightly lower for Nytro 10XN. The patterns also indicate a lot of void discharges, for both voltage stresses. Especially the Nytro 10XN impregnated system seemed to have a lot of void discharges. The Nytro 10XN impregnated system also seemed to have longer periods of sustained PD activity than Midel 7131.

For the sinusoidal voltage stress, the current transformer detected signals with a large degree of symmetry between the voltage polarities for both insulation systems. When a bipolar voltage pulse was applied, the pulses at the negative voltage pulse tended to be a bit smaller than those found at the positive voltage pulse, for both insulation systems. In the Nytro 10XN impregnated system there seemed to be more surface discharges at the positive voltage pulse compared to the negative voltage pulse. These slight differences in symmetry are the main difference between the results from the two voltage stresses, with regard to the pattern of the PDs.

## 5.3 Visible ageing of the pressboard samples

The visible ageing of the pressboard samples were described in sections 4.1.2.4, 4.1.3.4, 4.2.2.3, and 4.2.3.3. There were no visible signs of ageing on the Midel 7131 impregnated pressboard samples. There was a ring of soot where the top-electrode had been on the Nytro 10XN impregnated samples, as an easily distinguishable sign of ageing. The soot ring on the Nytro 10XN impregnated pressboard sample stressed by a sinusoidal voltage was darker and thicker than the circle of soot on the sample stressed by a bipolar voltage pulse. Why were there no visible signs of ageing on the Midel 7131 impregnated pressboard samples, when there were rings of soot on the Nytro 10XN impregnated samples? And why was the ring of soot darker and thicker when the Nytro 10XN was stressed by a sinusoidal voltage compared to a bipolar voltage stress?

There are several possible explanations as to why there were no ring of soot on the Midel 7131 impregnated samples, when this was present on the Nytro 10XN impregnated samples. The first factor that should be considered is the different surfaces of the pressboard samples used in the two insulation systems. The surface of the Nytro 10XN impregnated samples were slightly uneven, whilst the Midel 7131 impregnated samples had smooth surfaces, as previously mentioned. This was assumed to have little to no bearing on the results, but in order to eliminate this explanation, the measurements should be repeated using pressboard with an identical surface for the two insulation systems.

Periods of continuous PD activity are known to be more harmful than sporadic PD activity, see section 2.2.1. The Nytro 10XN impregnated systems seemed to have longer periods

of sustained activity than the Midel 7131 impregnated insulation systems, as discussed in section 5.2. The Nytro 10XN impregnated samples were also subjected to more PDs for longer than the Midel 7131 impregnated samples, because the PDIV for the PMT-visible PDs were lower for Nytro 10XN at both voltage stresses. For the systems stressed by a sinusoidal voltage, the Nytro 10XN impregnated sample had the added stress of being subjected to voltage amplitudes up to 40 $kV_{peak}$, whilst the Midel 7131 impregnated system only was subjected to voltages up to 36 $kV_{peak}$. These factors might explain why there was no ring of soot on the Midel 7131 impregnated samples, when this was present on the Nytro 10XN impregnated samples.

The amplitudes used for the sinusoidal voltage stress were up to twice as large (40 $kV_{peak}$) as the amplitude used for the bipolar voltage pulse (20 $kV_{peak}$). The insulation system stressed by a sinusoidal voltage was therefore stressed by a voltage for a longer period of time than the system stressed by a bipolar voltage pulse. This might be the reason why the ring of soot was darker and thicker when the Nytro 10XN was stressed by a sinusoidal voltage compared to a bipolar voltage stress. The large voltage amplitude of the sinusoidal voltage might also have lead to larger, and more harmful, PDs.

# 6 Conclusion

The consequences of fast repetitive voltage pulses on transformer insulation have been studied by studying the partial discharges in two different insulation systems, both under a sinusoidal voltage stress and under a bipolar voltage pulse stress. Nytro 10XN, a mineral oil that is commonly used in transformer insulation, was used as the insulation liquid in one of the systems. Midel 7131, a biodegradable synthetic ester that is becoming a popular alternative to Nytro for use in transformer insulation, was used as the insulation liquid in the other system. The insulation systems were stressed by a sinusoidal voltage in order to see how the systems behave under "normal" conditions, and by a bipolar voltage pulse in order to see how they behave when stressed by fast repetitive voltage pulses.

Due to time constraints, only four test series were performed, i.e. one for each combination of voltage stress and insulation system. This affects the accuracy of the results. Despite this, the results show some very clear trends, making it possible to conclude something from them.

The partial discharges (PDs), predominantly with regard to the partial discharge inception voltage (PDIV), but also with regard to the PD patterns and the visible ageing caused by the PDs, were studied. The PDIV was found to be much higher, for both insulation systems, when the systems were stressed by a sinusoidal voltage. When the systems were stressed by a sinusoidal voltage, their PDIVs were between 30 and 35 $kV_{peak}$ for both void discharges and surface discharges. This is approximately three times larger than the PDIV for void discharges when the systems were stressed by a bipolar voltage pulse, which was found to be 10 $kV_{peak}$. It is almost twice as large as the PDIV for surface discharges, which was found to be 16-20 $kV_{peak}$, depending on the insulation system. This difference in PDIV suggests that PDs, which might lead to deterioration and ageing of the insulation systems, occur at lower voltages if the insulation system is stressed by fast repetitive voltage pulses compared to if it is stressed by a sinusoidal voltage. The results have therefore reaffirmed the hypothesis that fast repeating voltage pulses are more harmful to transformer insulation than a sinusoidal voltage.

Some slight differences were observed between the behaviour of the two insulation systems. The results suggest that Midel tends to have a slightly higher PDIV than Nytro. Midel was also observed to have PDs with higher apparent charges than Nytro. More surface discharges were also observed in the Midel 7131 impregnated system, even though the PDIV for surface discharges was higher for Midel than for Nytro. Nytro, on the other hand, was considered to have more void discharges. Nytro was also found to have longer periods of sustained PD activity, which can be harmful to the insulation. The Nytro 10XN impregnated pressboard samples both got a ring of soot as a result of the measurements, as a visible sign of degradation. The Midel 7131 impregnated samples had no visible signs of ageing. This suggests that the Nytro 10XN impregnated samples were more damaged than the Midel 7131 impregnated samples. Due to the limited number of tests, these results can only be viewed as suggestions, and not definitive answers, to how the behaviour of the two insulation liquids compare to each other. More measurements should be performed in order to gain a better understanding of the two insulation systems. This has therefore been listed as a suggestion for further work.

# 7 Suggestions for further work

- Perform more measurements under similar conditions in order to gain a better understanding of the differences between Midel 7131 impregnated systems and Nytro 10XN impregnated systems. Particularly with regard to:
  - Different PD patterns.
  - Different PDIV, for both void discharges and surface discharges.
- Perform measurements using pressboard samples with the same surface for both insulation system, in order to see if this affects the results.
- Perform measurements to find the partial discharge extinction voltage (PDEV).
- Perform measurements with other electric fields, for instance by using a round edged electrode.
- The PD patterns development over time can be studied more properly by performing measurements for extended periods of time.
- Take pictures of streamers with a high-speed camera, for both insulation systems and both stresses, and use these pictures to study the streamers (their length, the branching, etc.).
- Different pressboard thicknesses can be used to see how this affects the results.
- Different moisture levels, i.e. performing measurements for middle dry and wet transformer insulation as well.
- Perform measurements with different switching frequencies.

# References


[1] NVE. Solkraft, 2020. Access date: January 27, 2021.

[2] Norway's Ministry of Petroleum and Energy. Meld. St. 28 (2019–2020): Vindkraft på land — Endringer i konsesjonsbehandlingen, 2020. Access date: January 27, 2021.

[3] REN21. Renewables 2020 - Global status report. Technical report, REN21, 2020.

[4] F. Skirbekk. Transformer insulation stressed by a sinusoidal voltage. Project report in TET4520, Department of Electric Power Engineering, NTNU – Norwegian University of Science and Technology, Dec. 2020.

[5] A. Nysveen. TET4195 High voltage equipment - Power transformers. Technical report, NTNU, Department of Electric Power Engineering, 2015.

[6] E. Ilstad. TET4160 Insulation Materials for High Voltage Applications. Technical report, NTNU, Department of Electric Power Engineering, 2018.

[7] CIGRE Working group A2-35. Experiences in service with new insulating liquids. Technical report, Cigré, 2010.

[8] The Editors of Encyclopaedia Britannica. Flash point, 2012. Access date: December 12, 2020.

[9] D.F. Binns and K.T. Yoon. Breakdown phenomena in midel 7131, silicone fluid 561 and transformer oil. *Journal of Electrostatics*, 12:593 – 600, 1982.

[10] C. Perrier and A. Beroual. Experimental investigations on insulating liquids for power transformers: Mineral, ester, and silicone oils. *IEEE Electrical Insulation Magazine*, 25(6):6–13, 2009.

[11] X. Wang. *Partial Discharge Behaviours and Breakdown Mechanisms of Ester Transformer Liquids under ac Stress*. PhD thesis, The University of Manchester, 2011.

[12] F. Vahidi, S. Tenbohlen, M. Rösner, C. Perrier, and T. Stirl. The influence of moisture during the electrical conductivity measurement on the high density impregnated pressboard. 08 2015.

[13] L. Lundgaard. Partielle utladninger - Begreper, måleteknikk og mulige anvendelser for tilstandskontroll. Technical report, SINTEF Energy Research, 1996.

[14] L. Lundgaard. Partial Discharges - General Description. Technical report, SINTEF Energy Research, 2008.

[15] H.K.H. Meyer. Characterization of partial discharge detection methods - Test on the FastTrans AC resonant setup. Technical report, SINTEF Energy Research, 2020. version 1.0.

[16] L. Kebbabi and A. Beroual. Fractal analysis of creeping discharge patterns propagating at solid/liquid interfaces-influence of the nature and geometry of solid insulators. In *CEIDP '05. 2005 Annual Report Conference on Electrical Insulation and Dielectric Phenomena, 2005.*, pages 132–135, 2005.

[17] S. Strachan et al. Knowledge-based diagnosis of partial discharges in power transformers. *Dielectrics and Electrical Insulation, IEEE Transactions on*, 15:259 – 268, 03 2008.

[18] RCA Corporation. *Photomultiplier manual*, 1970.

[19] Lambert. *Lambert HiCAM 500 user manual v1.3*.

[20] H.K.H. Meyer. AC resonant voltage source for PD-measurement. Technical report, SINTEF Energy Research, 2020. version 1.0.

[21] Omicron Energy. Partial discharge 101 series - How to Measure Partial Discharge. Technical report, Omicron Energy, 2020.

[22] D. Linhjell. High voltage pulse source 65 kV - Report and user manual. Technical report, SINTEF Energy Research, 2021. version 1.0.

[23] I. Atanasova-Höhlein et al. Moisture measurement and assessment in transformer insulation - evaluation of chemical methods and moisture capacitive sensors. Technical report, Cigré, 2017. WG D1.52.

# Appendices

# A Nytro 10XN impregnated system, sinusoidal voltage

The PDs detected by the current transformer when the applied voltage had amplitudes at 30 - 32 $kV_{peak}$, 34 - 35 $kV_{peak}$, and 37 - 39 $kV_{peak}$ are included in this appendix. These plots are from the measurements on the Midel 7131 impregnated system stressed by a sinusoidal voltage. The signal from the current transformer was filtered using a spectrum analyzer, see section 3.3. The resulting current transformer signal was then shifted 4 µs to the left during the post processing in order to compensate for the signal delay, as explained in section 4.1.1.

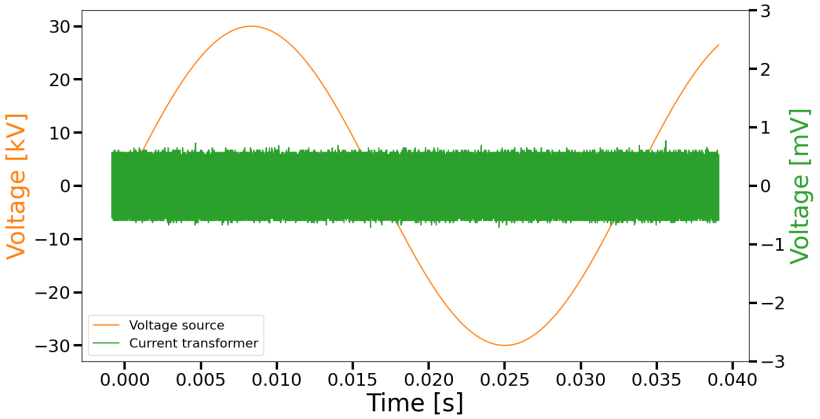


*Figure 59: The signal from the current transformer when a 30 $kV_{peak}$ sinusoidal voltage was applied to the Nytro 10XN impregnated system. The signal was collected using the envelope function on the oscilloscope for 1 minute.*

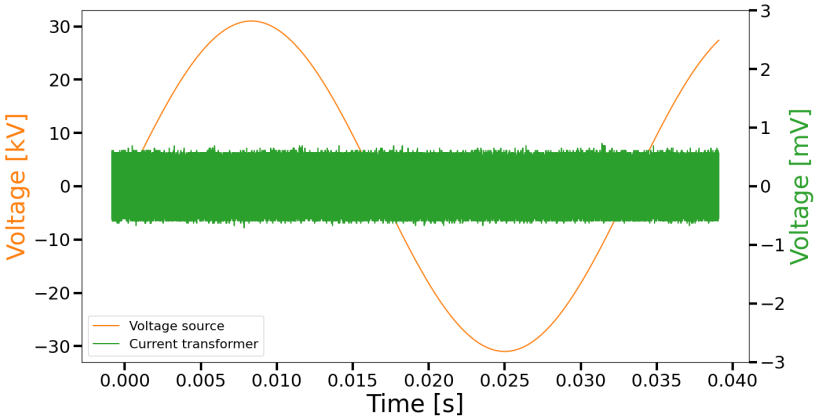


*Figure 60: The signal from the current transformer when a 31 $kV_{peak}$ sinusoidal voltage was applied to the Nytro 10XN impregnated system. The signal was collected using the envelope function on the oscilloscope for 1 minute.*

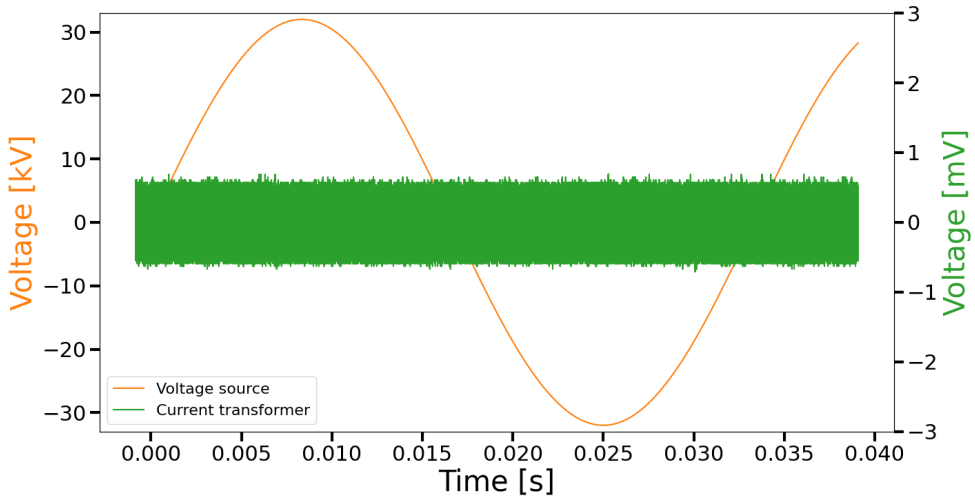


*Figure 61: The signal from the current transformer when a 32 $kV_{peak}$ sinusoidal voltage was applied to the Nytro 10XN impregnated system. The signal was collected using the envelope function on the oscilloscope for 1 minute.*

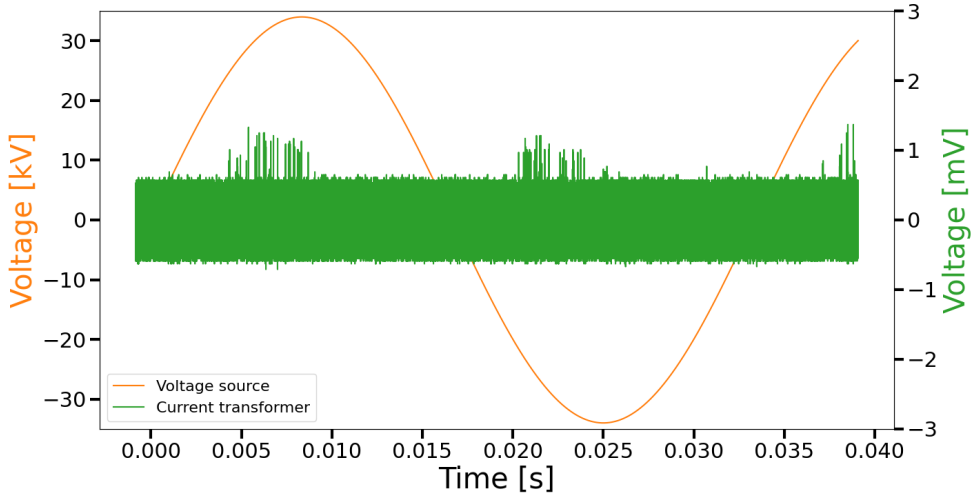


*Figure 62: The signal from the current transformer when a 34 $kV_{peak}$ sinusoidal voltage was applied to the Nytro 10XN impregnated system. The signal was collected using the envelope function on the oscilloscope for 1 minute.*

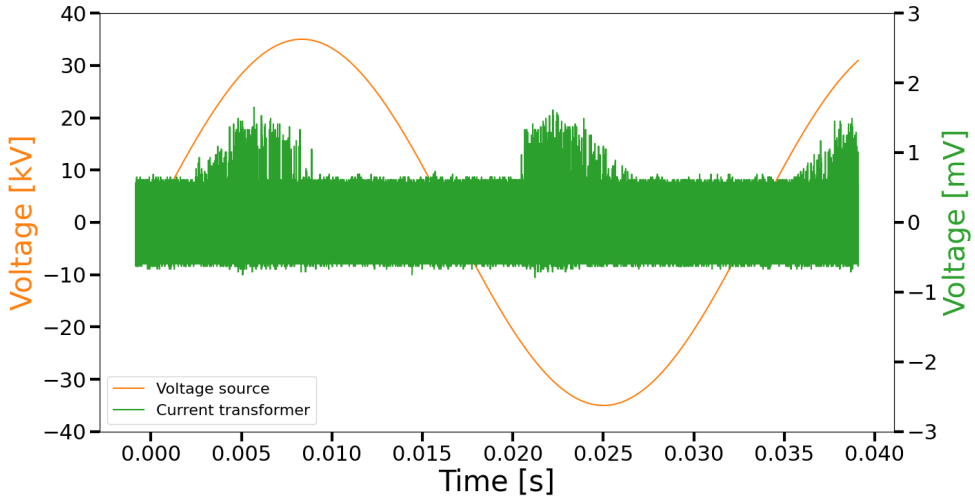


*Figure 63: The signal from the current transformer when a 35 $kV_{peak}$ sinusoidal voltage was applied to the Nytro 10XN impregnated system. The signal was collected using the envelope function on the oscilloscope for 1 minute.*

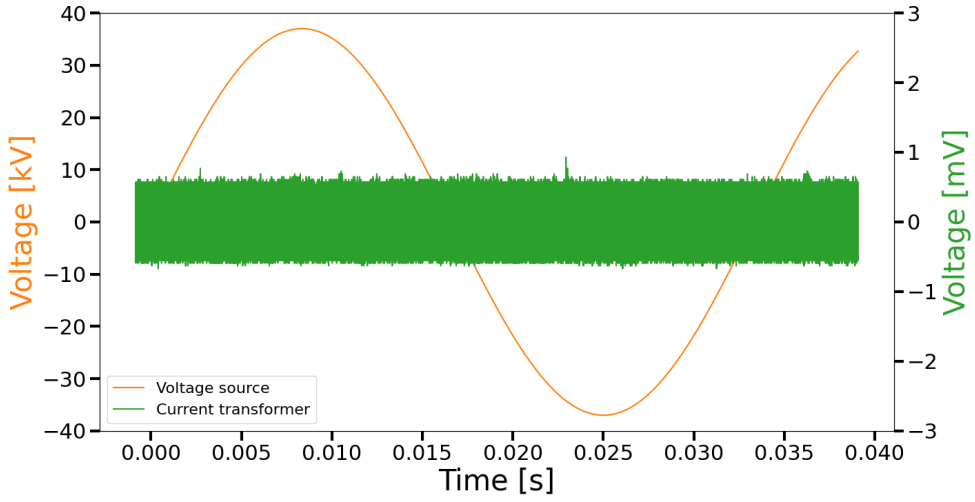


*Figure 64: The signal from the current transformer when a 37 $kV_{peak}$ sinusoidal voltage was applied to the Nytro 10XN impregnated system. The signal was collected using the envelope function on the oscilloscope for 1 minute.*

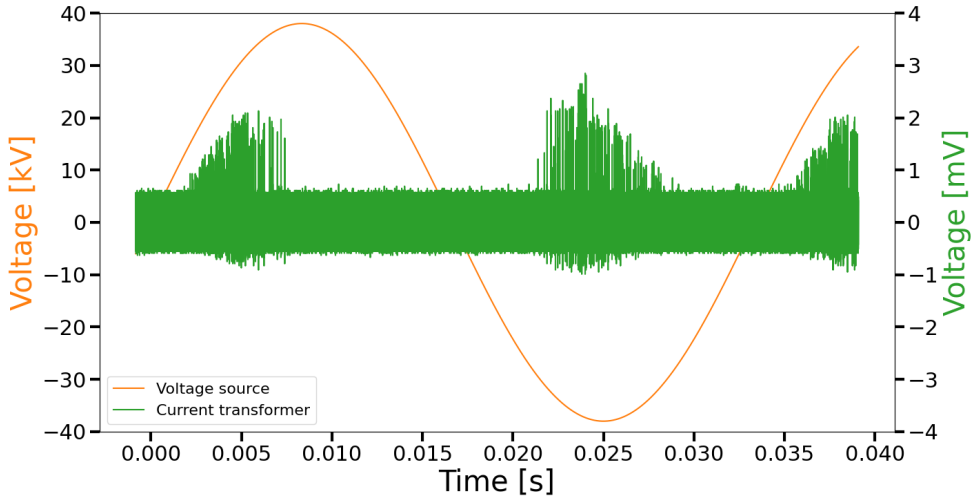


*Figure 65: The signal from the current transformer when a 38 $kV_{peak}$ sinusoidal voltage was applied to the Nytro 10XN impregnated system. The signal was collected using the envelope function on the oscilloscope for 1 minute.*

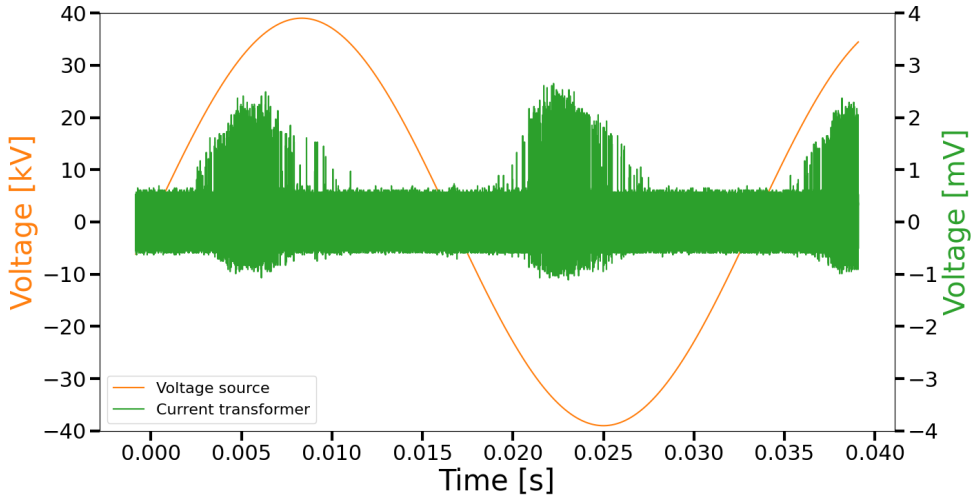


*Figure 66: The signal from the current transformer when a 39 $kV_{peak}$ sinusoidal voltage was applied to the Nytro 10XN impregnated system. The signal was collected using the envelope function on the oscilloscope for 1 minute.*

# B Midel 7131 impregnated system, sinusoidal voltage

The PDs detected by the current transformer when the applied voltage had amplitudes at 30 $kV_{peak}$, and 33 - 35 $kV_{peak}$ are included in this appendix. These plots are from the measurements on the Midel 7131 impregnated system stressed by a sinusoidal voltage. The signal from the current transformer was filtered using a spectrum analyzer, see section 3.3. The resulting current transformer signal was then shifted 4 µs to the left during the post processing in order to compensate for the signal delay, as explained in section 4.1.1.

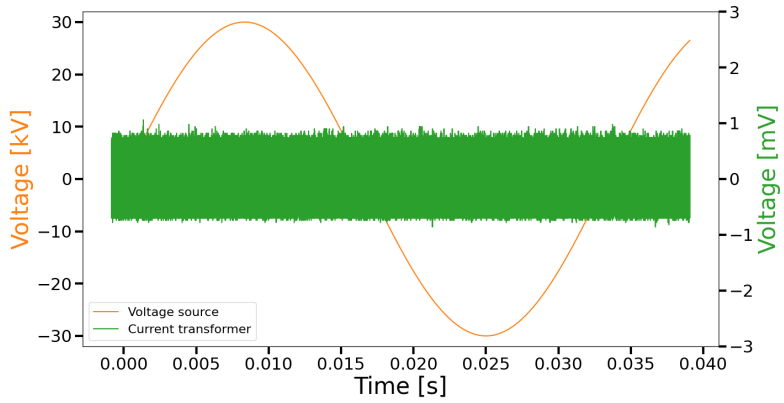


*Figure 67: The signal from the current transformer when a 30 $kV_{peak}$ sinusoidal voltage was applied to the Midel 7131 impregnated system. The signal was collected using the envelope function on the oscilloscope for 1 minute.*

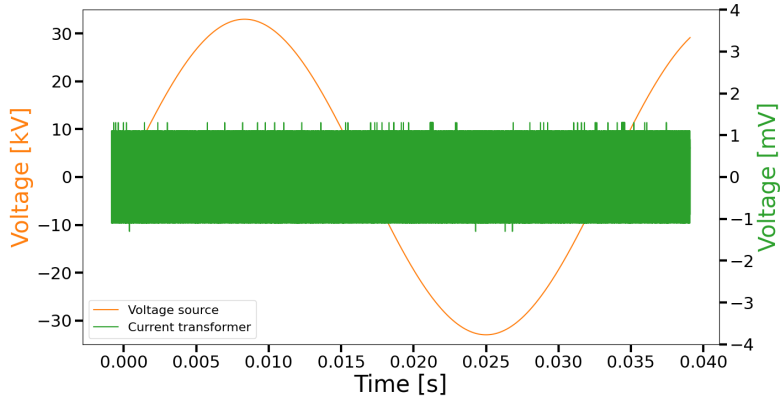


*Figure 68: The signal from the current transformer when a 33 $kV_{peak}$ sinusoidal voltage was applied to the Midel 7131 impregnated system. The signal was collected using the envelope function on the oscilloscope for 1 minute.*

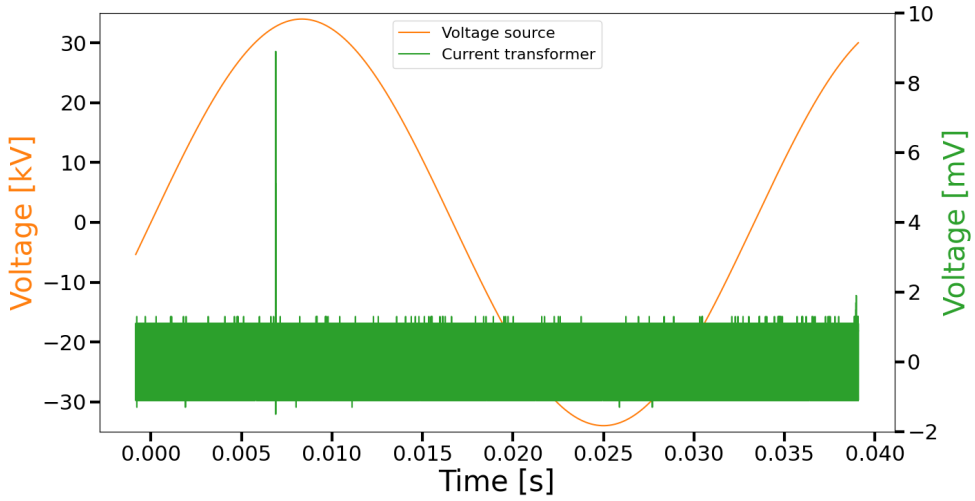


*Figure 69: The signal from the current transformer when a 34 $kV_{peak}$ sinusoidal voltage was applied to the Midel 7131 impregnated system. The signal was collected using the envelope function on the oscilloscope for 1 minute.*

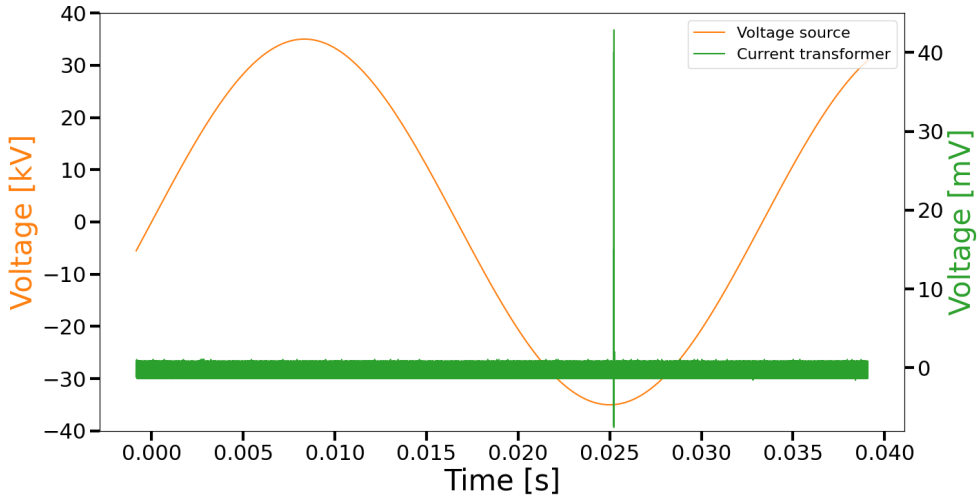


*Figure 70: The signal from the current transformer when a 35 $kV_{peak}$ sinusoidal voltage was applied to the Midel 7131 impregnated system. The signal was collected using the envelope function on the oscilloscope for 1 minute.*

# C Nytro 10XN impregnated system, bipolar voltage pulse

## C.1 Noise on the PMT signal

Figure 71 shows the signal from the PMT when no voltage was applied to the test object. The test was performed on a Nytro 10XN impregnated pressboard sample. As seen from the figure, this signal had quite a lot of noise.

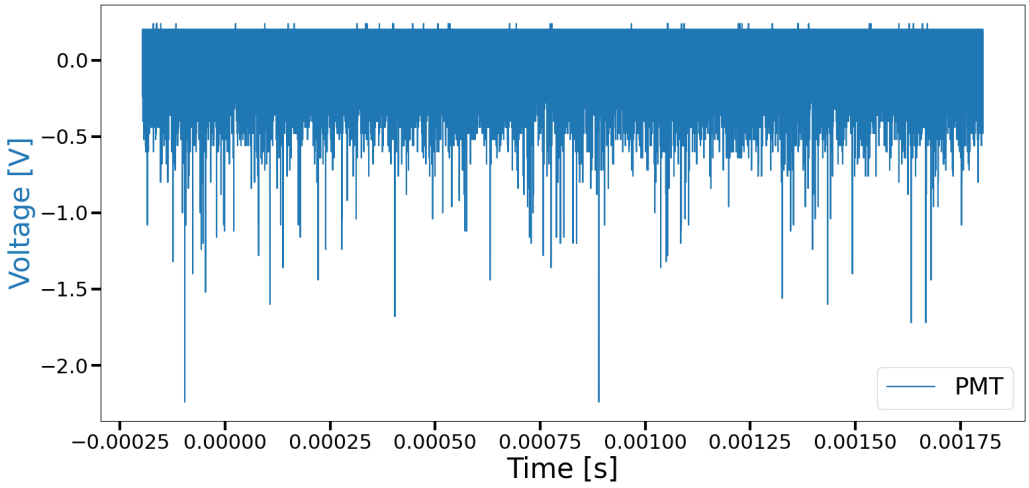


*Figure 71: The noise from the PMT when there was no applied voltage. The test was performed on a Nytro 10XN impregnated pressboard sample.*

## C.2 PDs detected by the current transformer and the PMT

The PDs detected by the current transformer and the PMT when the applied voltage had amplitudes at 8 - 9 $kV_{peak}$, 11 - 15 $kV_{peak}$, and 17 - 19 $kV_{peak}$, for both positive and negative voltage pulses, are included in this appendix. These plots are from the measurements on the Nytro 10XN impregnated system stressed by a bipolar voltage pulse. The signal from the current transformer was filtered using a spectrum analyzer, see section 3.3. The resulting current transformer signal was then shifted 4 µs to the left during the post processing in order to compensate for the signal delay, as explained in section 4.2.1.2.

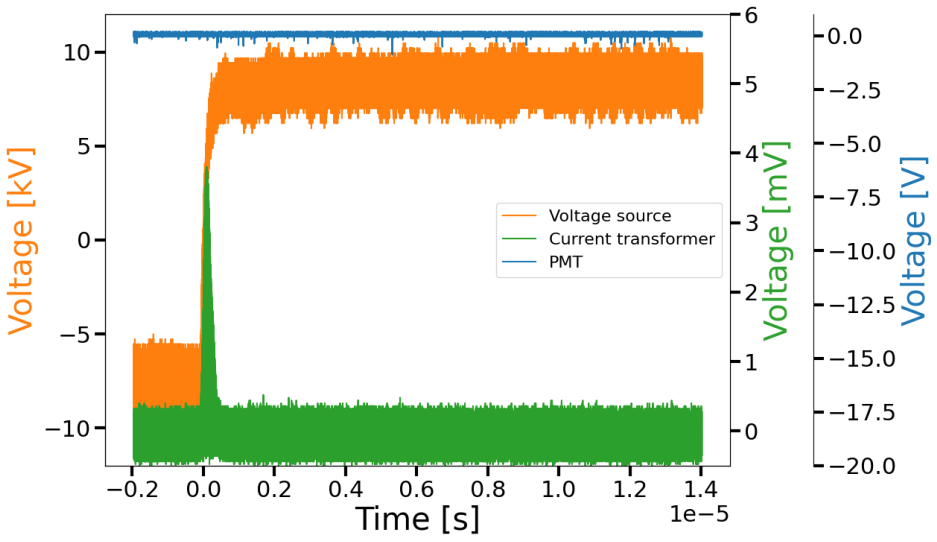


*Figure 72: Nytro 10XN impregnated insulation system. 8 $kV_{peak}$ applied voltage, positive voltage pulse. The signals were collected using the envelope function on the oscilloscope for 1 minute.*

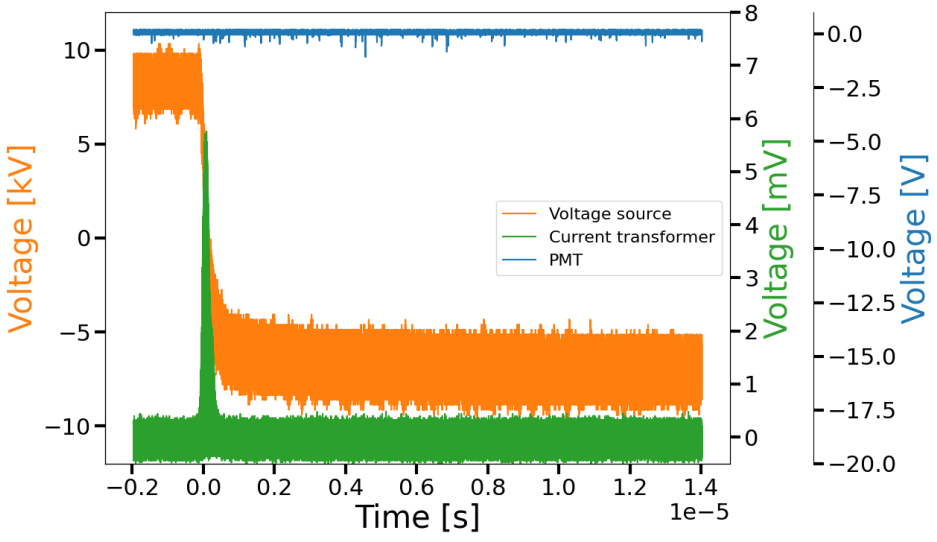


*Figure 73: Nytro 10XN impregnated insulation system. 8 $kV_{peak}$ applied voltage, negative voltage pulse. The signals were collected using the envelope function on the oscilloscope for 1 minute.*

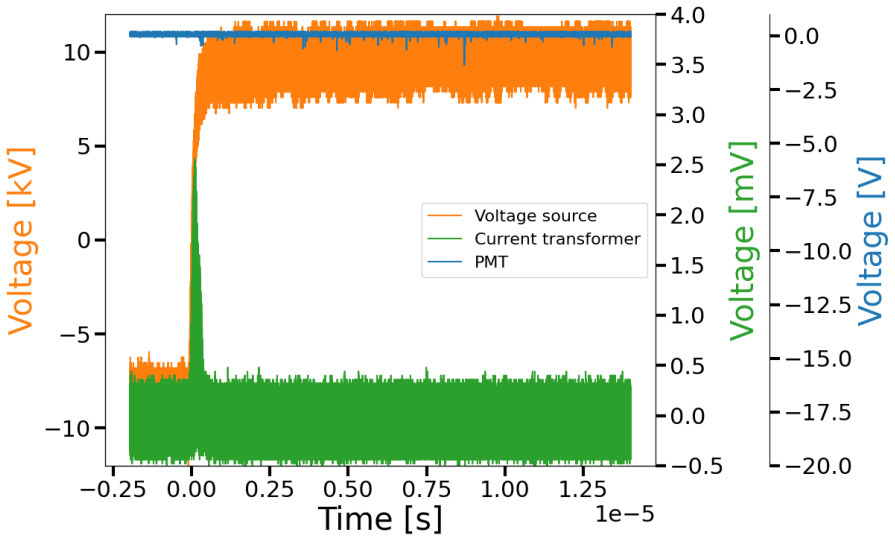


*Figure 74: Nytro 10XN impregnated insulation system. 9 $kV_{peak}$ applied voltage, positive voltage pulse. The signals were collected using the envelope function on the oscilloscope for 1 minute.*

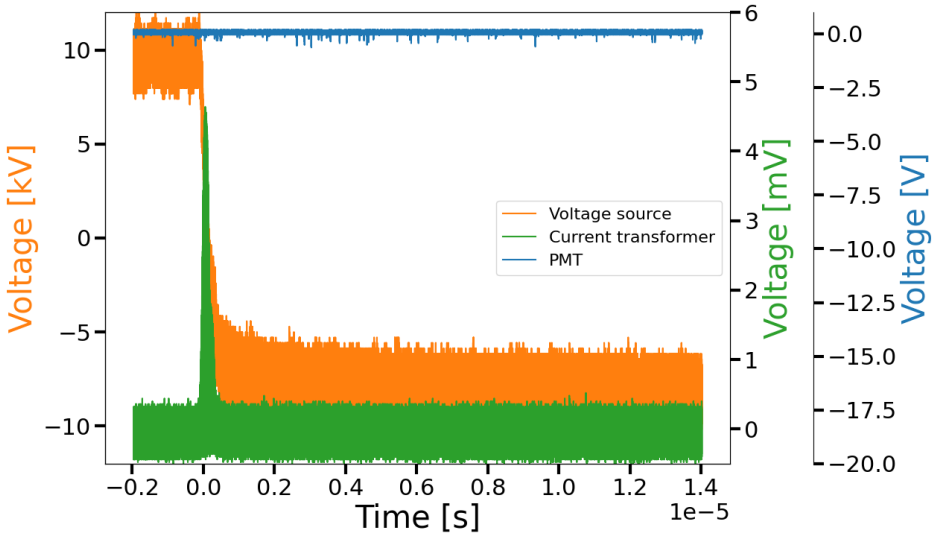


*Figure 75: Nytro 10XN impregnated insulation system. 9 $kV_{peak}$ applied voltage, negative voltage pulse. The signals were collected using the envelope function on the oscilloscope for 1 minute.*

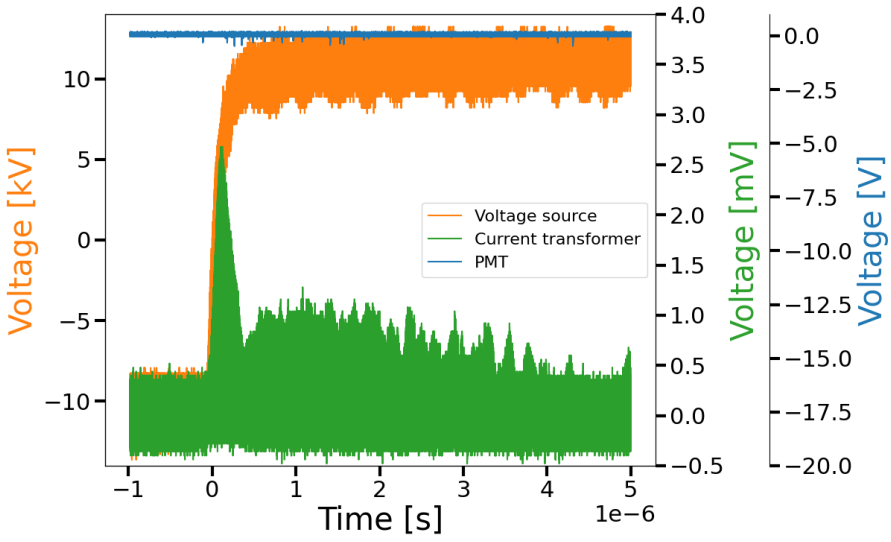


*Figure 76: Nytro 10XN impregnated insulation system. 11 $kV_{peak}$ applied voltage, positive voltage pulse. The signals were collected using the envelope function on the oscilloscope for 1 minute.*

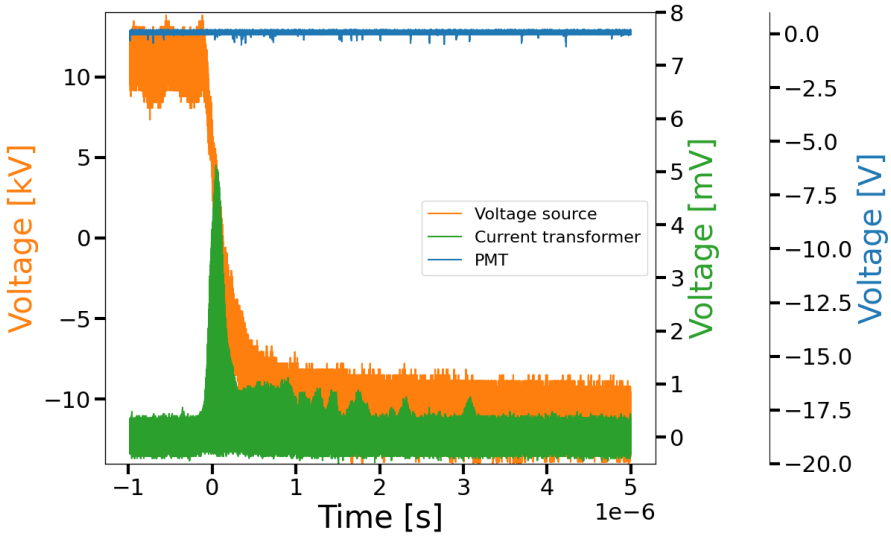


*Figure 77: Nytro 10XN impregnated insulation system. 11 $kV_{peak}$ applied voltage, negative voltage pulse. The signals were collected using the envelope function on the oscilloscope for 1 minute.*

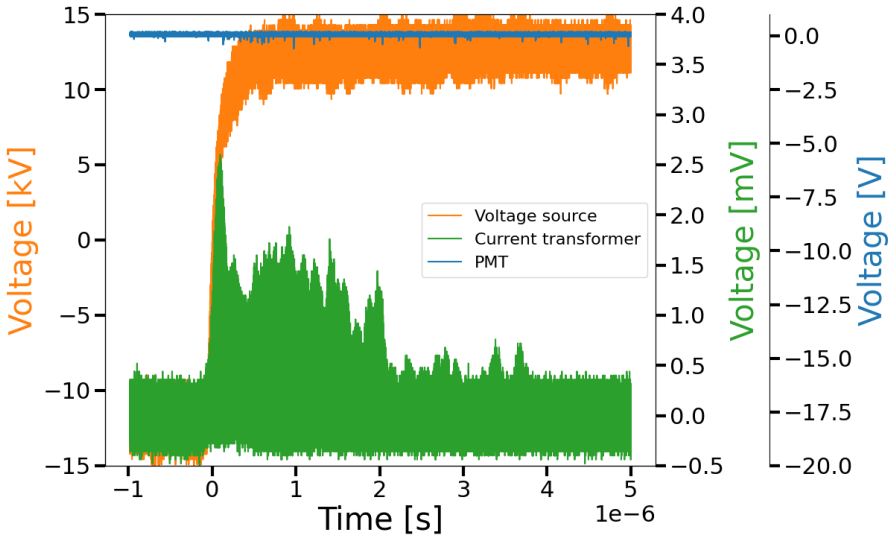


*Figure 78: Nytro 10XN impregnated insulation system. 12 $kV_{peak}$ applied voltage, positive voltage pulse. The signals were collected using the envelope function on the oscilloscope for 1 minute.*

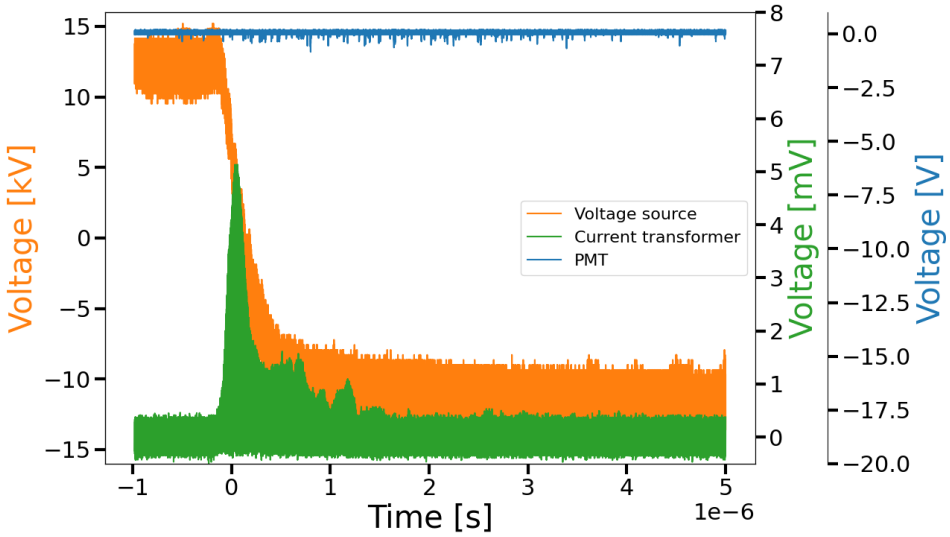


*Figure 79: Nytro 10XN impregnated insulation system. 12 $kV_{peak}$ applied voltage, negative voltage pulse. The signals were collected using the envelope function on the oscilloscope for 1 minute.*

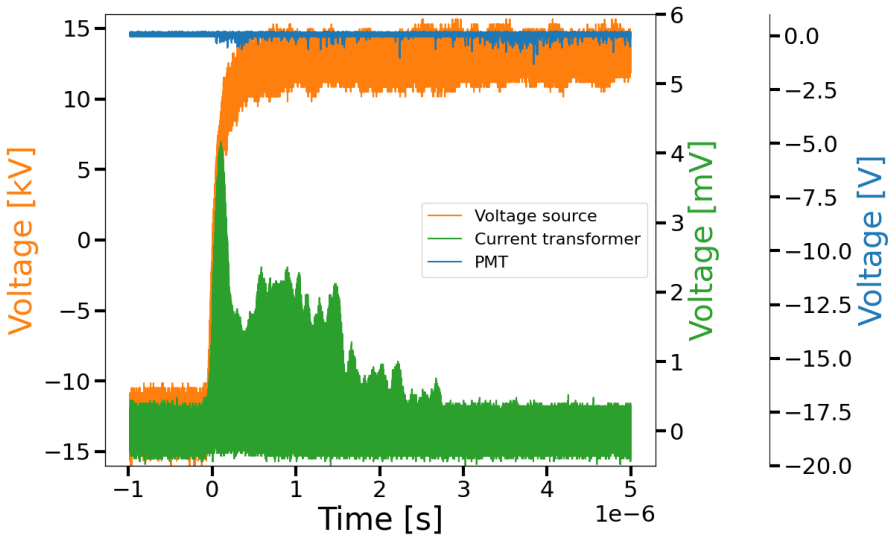


*Figure 80: Nytro 10XN impregnated insulation system. 13 $kV_{peak}$ applied voltage, positive voltage pulse. The signals were collected using the envelope function on the oscilloscope for 1 minute.*

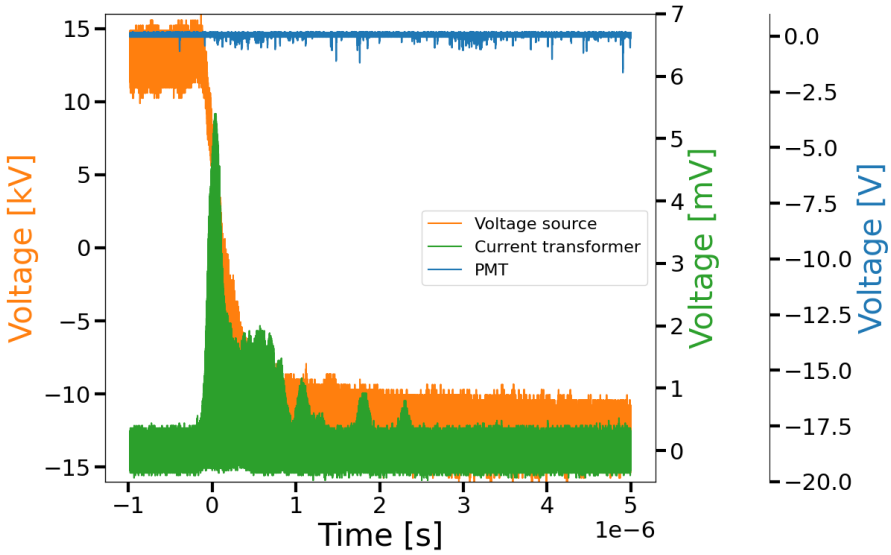


*Figure 81: Nytro 10XN impregnated insulation system. 13 $kV_{peak}$ applied voltage, negative voltage pulse. The signals were collected using the envelope function on the oscilloscope for 1 minute.*

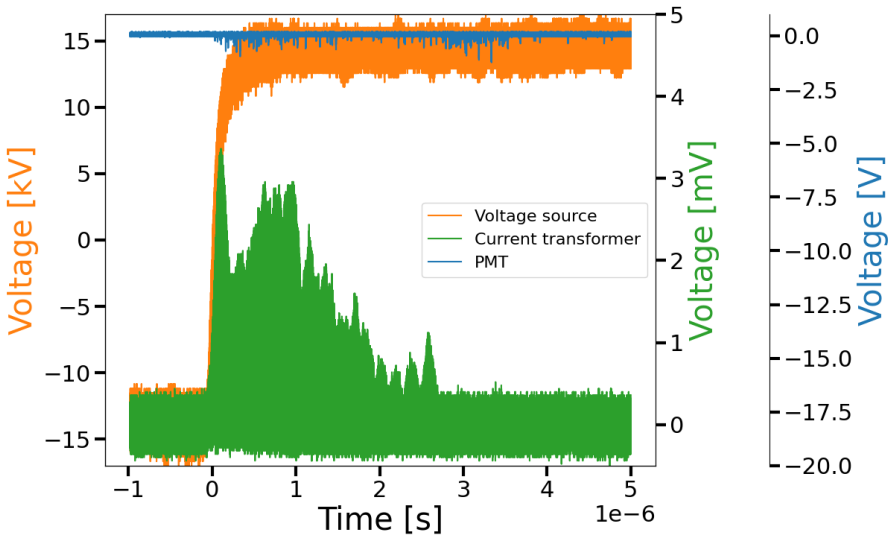


*Figure 82: Nytro 10XN impregnated insulation system. 14 $kV_{peak}$ applied voltage, positive voltage pulse. The signals were collected using the envelope function on the oscilloscope for 1 minute.*

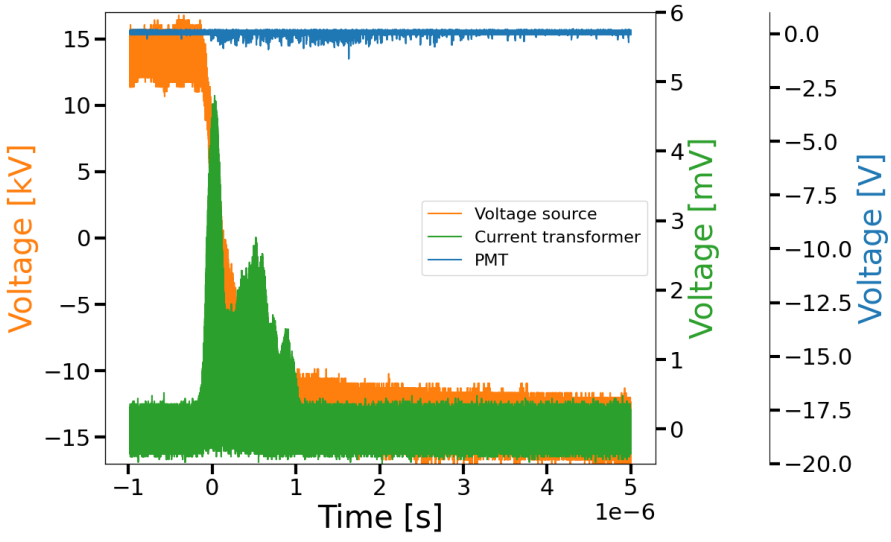


*Figure 83: Nytro 10XN impregnated insulation system. 14 $kV_{peak}$ applied voltage, negative voltage pulse. The signals were collected using the envelope function on the oscilloscope for 1 minute.*

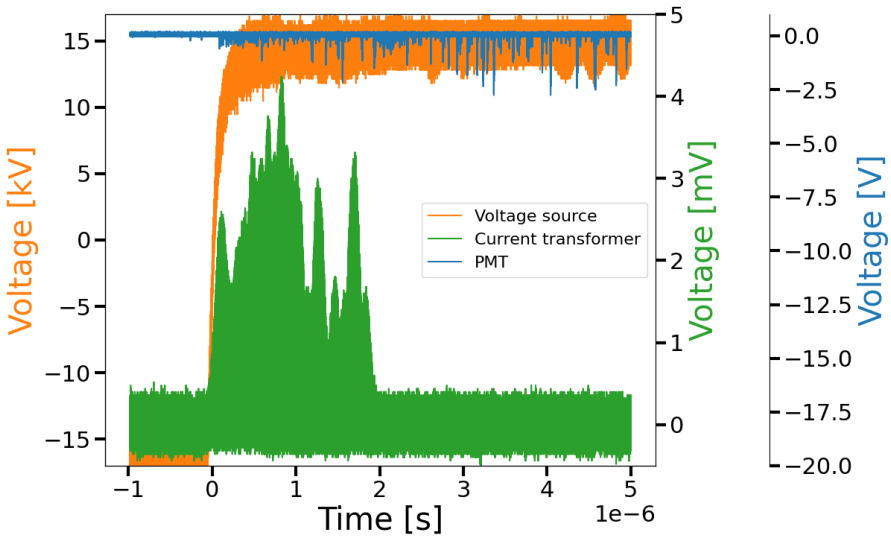


*Figure 84: Nytro 10XN impregnated insulation system. 15 $kV_{peak}$ applied voltage, positive voltage pulse. The signals were collected using the envelope function on the oscilloscope for 1 minute.*

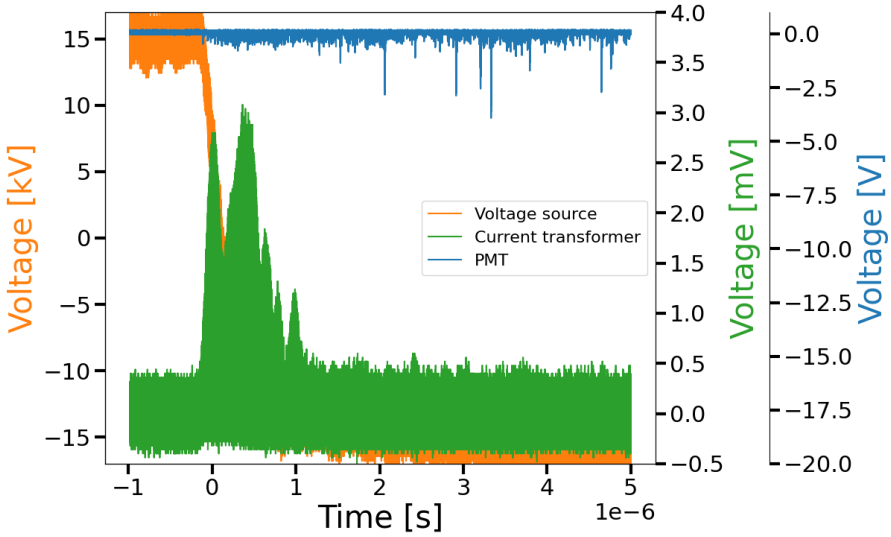


*Figure 85: Nytro 10XN impregnated insulation system. 15 $kV_{peak}$ applied voltage, negative voltage pulse. The signals were collected using the envelope function on the oscilloscope for 1 minute.*

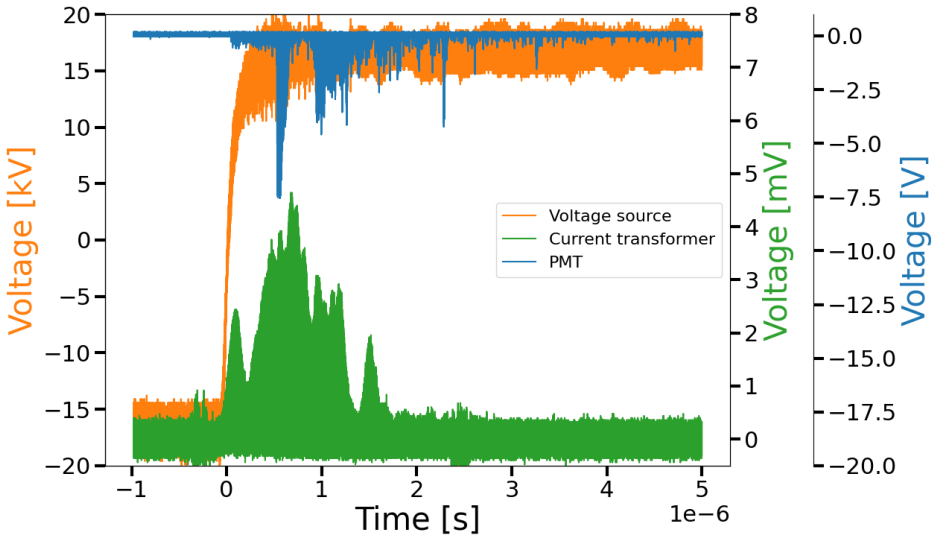


*Figure 86: Nytro 10XN impregnated insulation system. 17 $kV_{peak}$ applied voltage, positive voltage pulse. The signals were collected using the envelope function on the oscilloscope for 1 minute.*

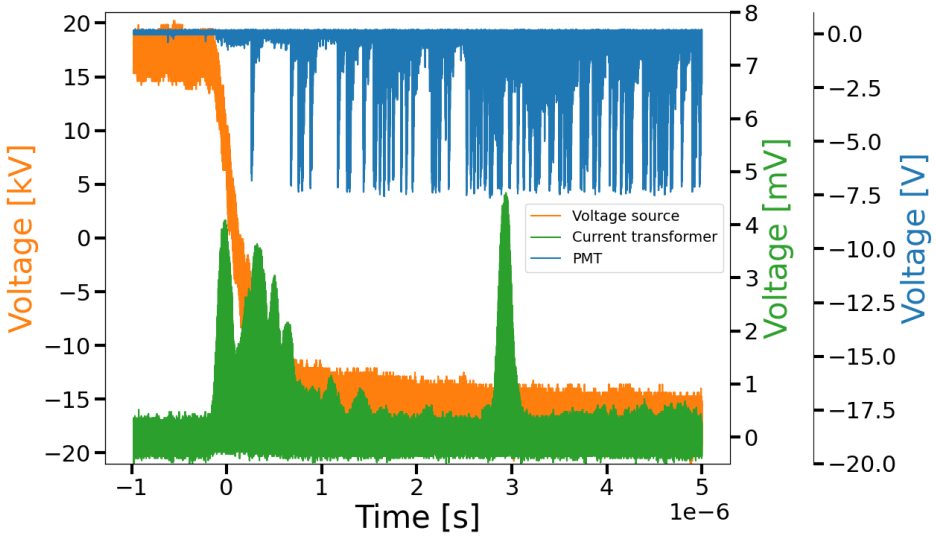


*Figure 87: Nytro 10XN impregnated insulation system. 17 $kV_{peak}$ applied voltage, negative voltage pulse. The signals were collected using the envelope function on the oscilloscope for 1 minute.*

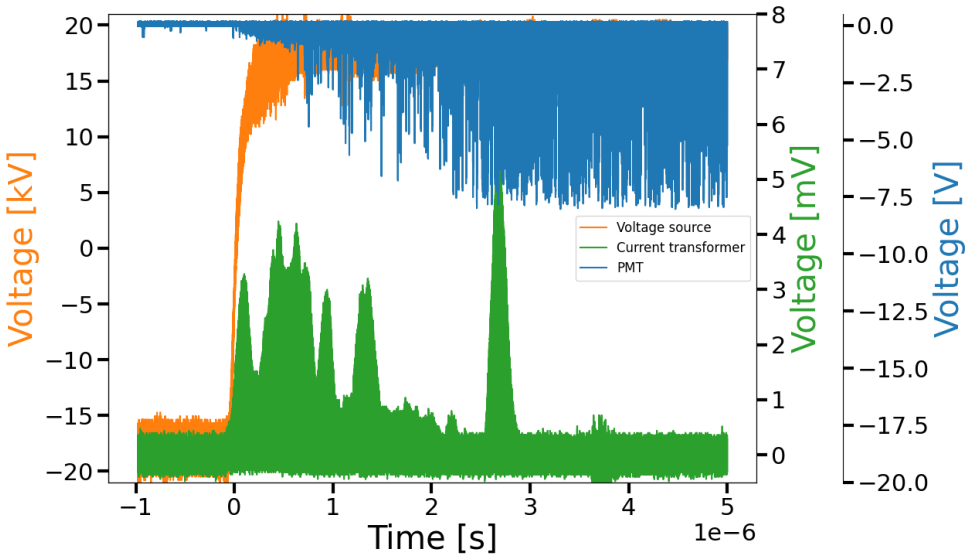


*Figure 88: Nytro 10XN impregnated insulation system. 18 $kV_{peak}$ applied voltage, positive voltage pulse. The signals were collected using the envelope function on the oscilloscope for 1 minute.*

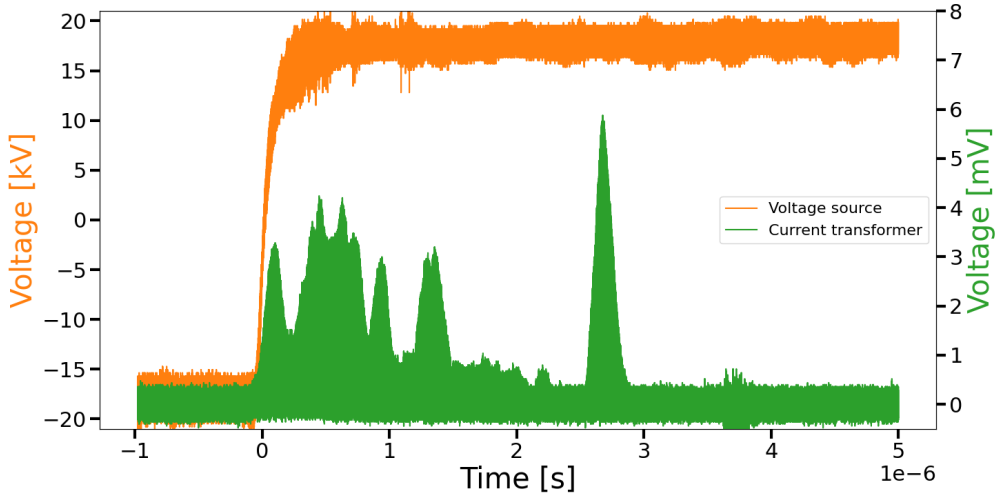


*Figure 89: Nytro 10XN impregnated insulation system. 18 $kV_{peak}$ applied voltage, positive voltage pulse. The signal from the PMT is not included. The signals were collected using the envelope function on the oscilloscope for 1 minute.*

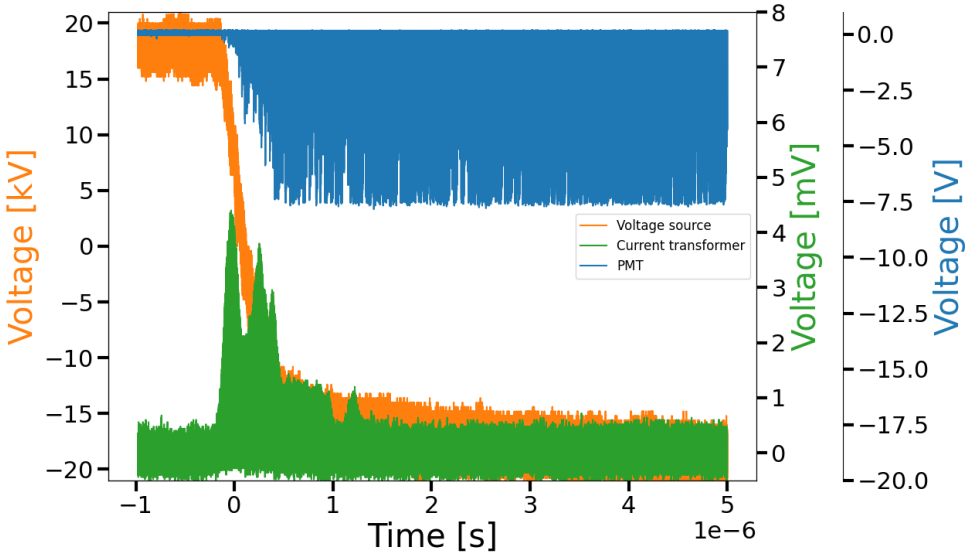


*Figure 90: Nytro 10XN impregnated insulation system. 18 $kV_{peak}$ applied voltage, negative voltage pulse. The signals were collected using the envelope function on the oscilloscope for 1 minute.*

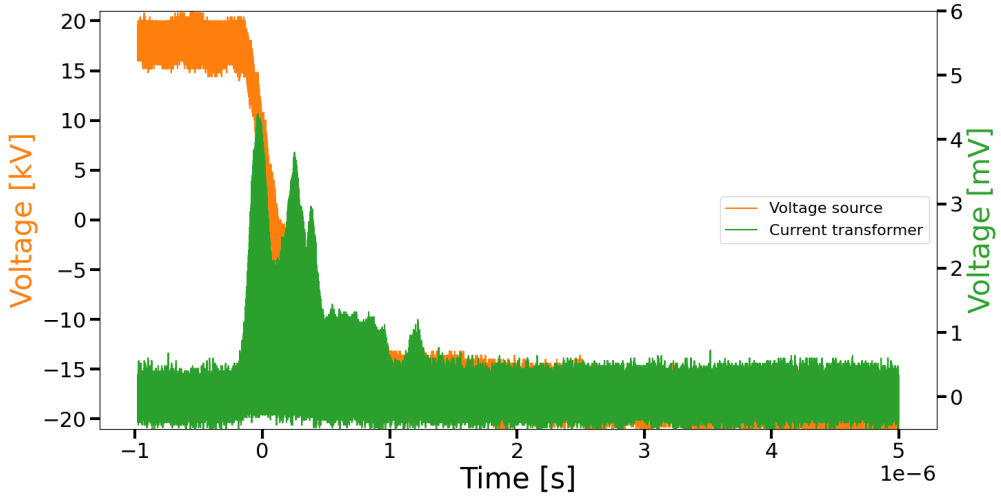


*Figure 91: Nytro 10XN impregnated insulation system. 18 $kV_{peak}$ applied voltage, negative voltage pulse. The signal from the PMT is not included. The signals were collected using the envelope function on the oscilloscope for 1 minute.*

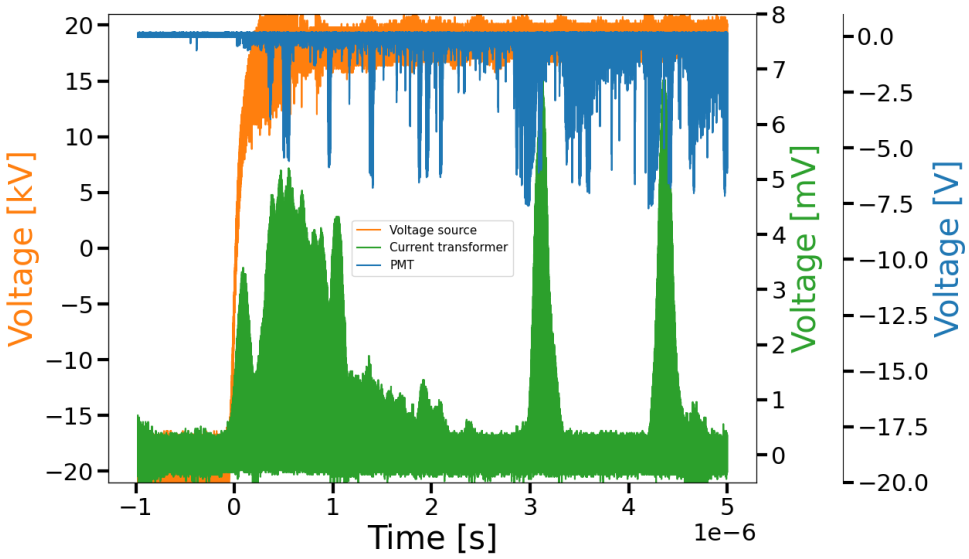


*Figure 92: Nytro 10XN impregnated insulation system. 19 $kV_{peak}$ applied voltage, positive voltage pulse. The signals were collected using the envelope function on the oscilloscope for 1 minute.*

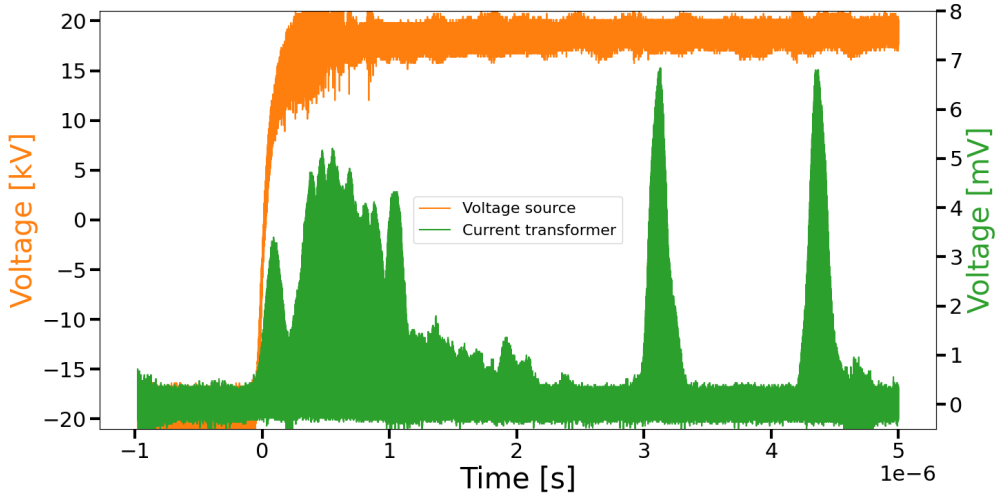


*Figure 93: Nytro 10XN impregnated insulation system. 19 $kV_{peak}$ applied voltage, positive voltage pulse. The signal from the PMT is not included. The signals were collected using the envelope function on the oscilloscope for 1 minute.*

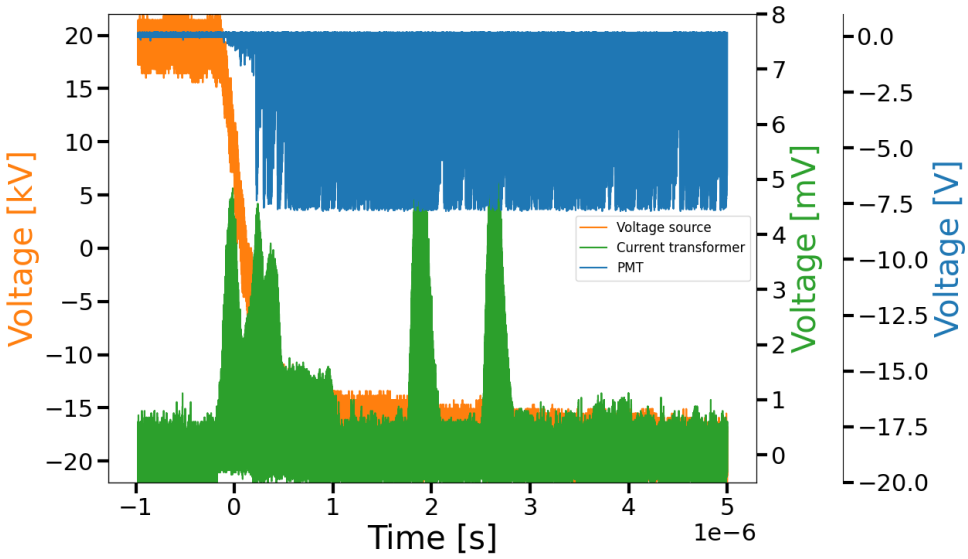


*Figure 94: Nytro 10XN impregnated insulation system. 19 $kV_{peak}$ applied voltage, negative voltage pulse. The signals were collected using the envelope function on the oscilloscope for 1 minute.*

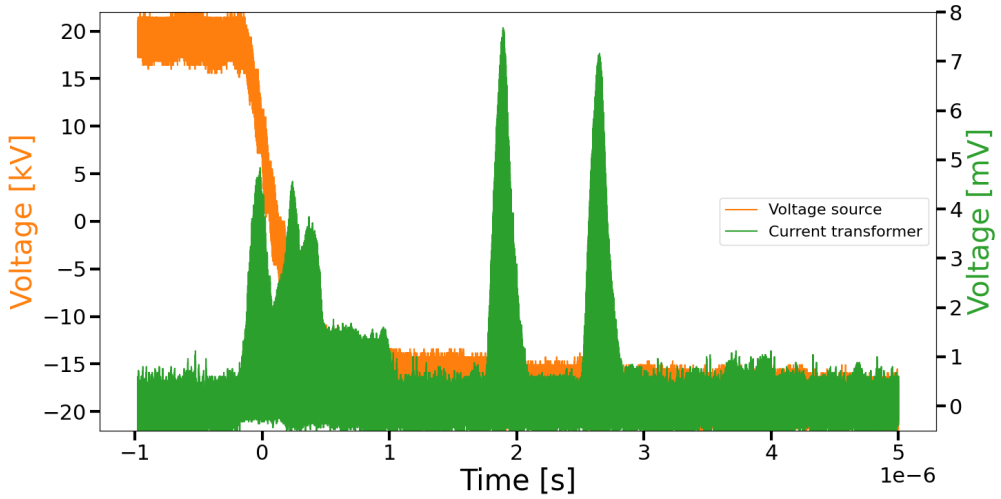


*Figure 95: Nytro 10XN impregnated insulation system. 19 $kV_{peak}$ applied voltage, negative voltage pulse. The signal from the PMT is not included. The signals were collected using the envelope function on the oscilloscope for 1 minute.*

# D Midel 7131 impregnated system, bipolar voltage pulse

## D.1 The switching transient

The switching transient when the Midel 7131 impregnated insulation system was stressed by a 5 $kV_{peak}$ voltage is depicted in Figure 96. Figure 97 shows the same signal after it has been shifted 4 µs to the left in order to compensate for the signal delay.

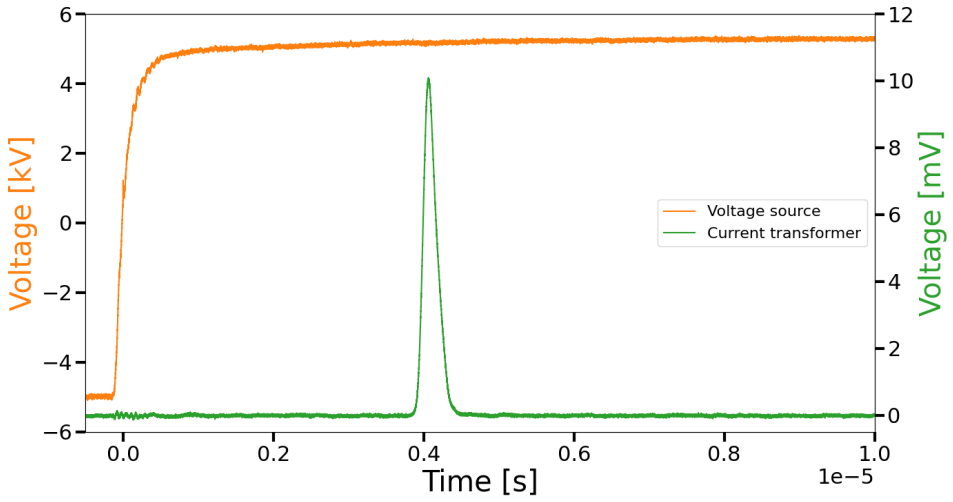


*Figure 96: The capacitive switching transient registered by the current transformer (green curve). The applied voltage is represented by the orange curve. There is a 4 µs delay in the signal from the current transformer. The test was performed on a Midel 7131 impregnated pressboard sample.*

## D.2 PDs detected by the current transformer and the PMT

The PDs detected by the current transformer and the PMT when the applied voltage had amplitudes at 8 - 9 $kV_{peak}$, 11 - 15 $kV_{peak}$, and 17 - 19 $kV_{peak}$, for both positive and negative voltage pulses, are included in this appendix. These plots are from the measurements on the Midel 7131 impregnated system stressed by a bipolar voltage pulse. The signal from the current transformer was filtered using a spectrum analyzer, see section 3.3. The resulting current transformer signal was then shifted 4 µs to the left during the post processing in order to compensate for the signal delay, as explained in section 4.2.1.2.

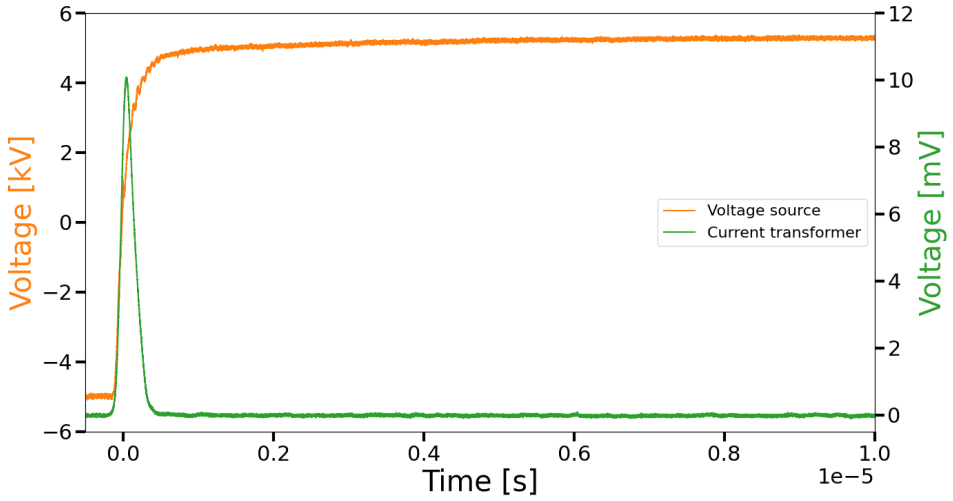


*Figure 97: The capacitive switching transient registered by the current transformer (green curve). The applied voltage is represented by the orange curve. The test was performed on a Midel 7131 impregnated pressboard sample.*

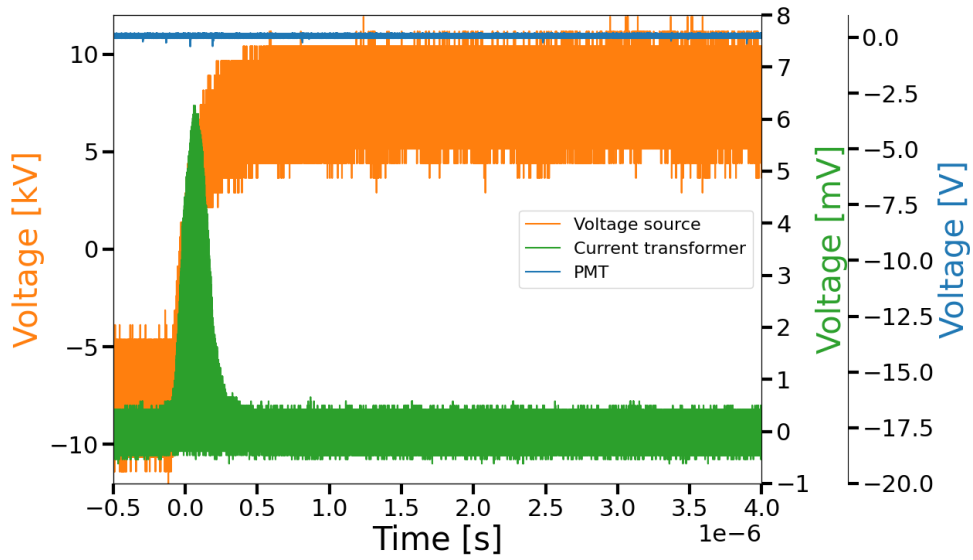


*Figure 98: Midel 7131 impregnated insulation system. 8 $kV_{peak}$ applied voltage, positive voltage pulse. The signals were collected using the envelope function on the oscilloscope for 1 minute.*

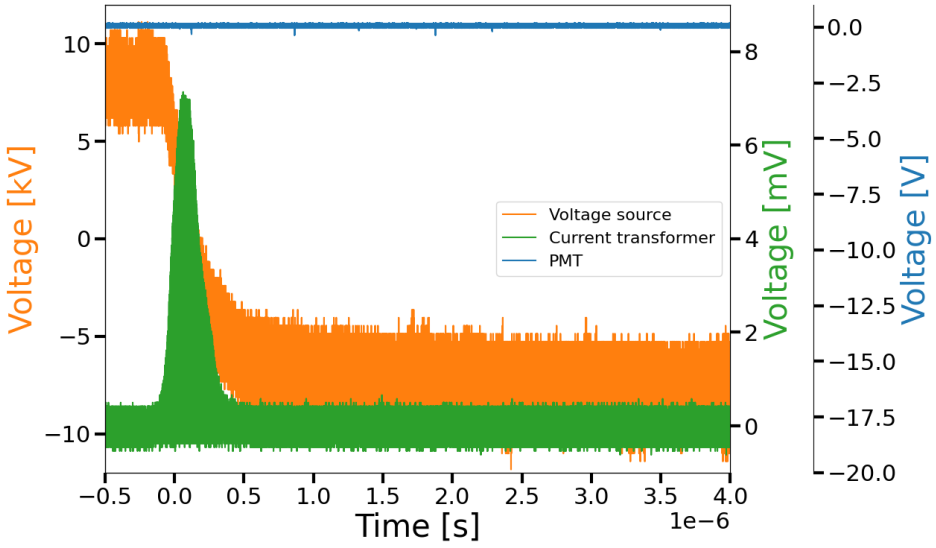


*Figure 99: Midel 7131 impregnated insulation system. 8 $kV_{peak}$ applied voltage, negative voltage pulse. The signals were collected using the envelope function on the oscilloscope for 1 minute.*

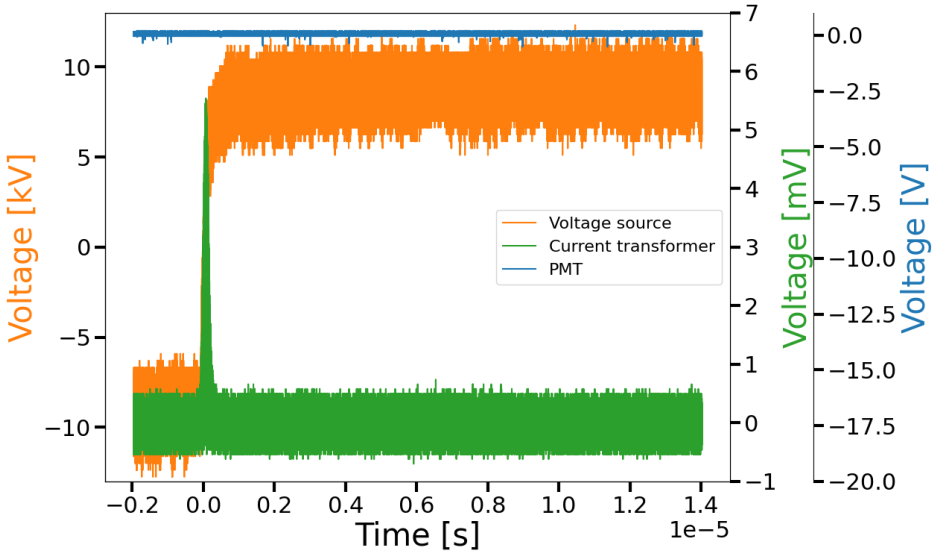


*Figure 100: Midel 7131 impregnated insulation system. 9 $kV_{peak}$ applied voltage, positive voltage pulse. The signals were collected using the envelope function on the oscilloscope for 1 minute.*

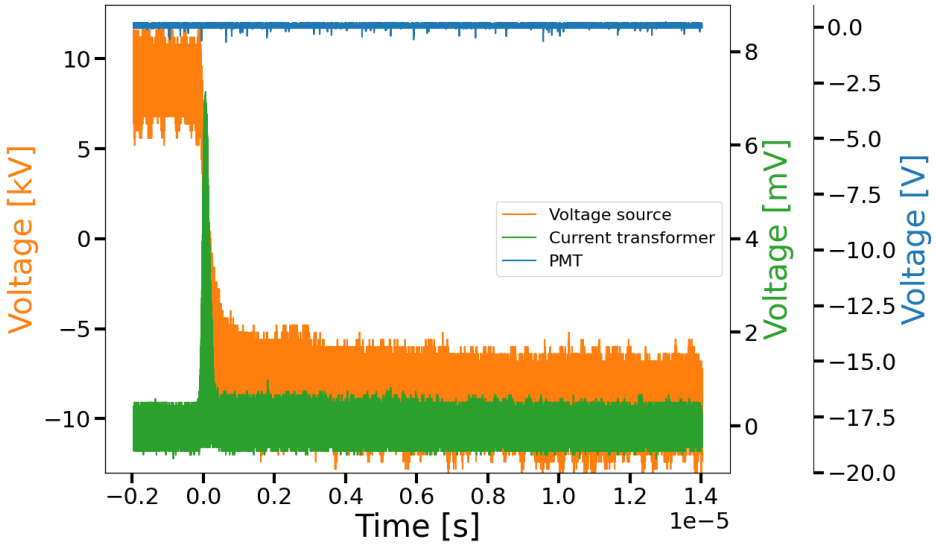


*Figure 101: Midel 7131 impregnated insulation system. 9 $kV_{peak}$ applied voltage, negative voltage pulse. The signals were collected using the envelope function on the oscilloscope for 1 minute.*

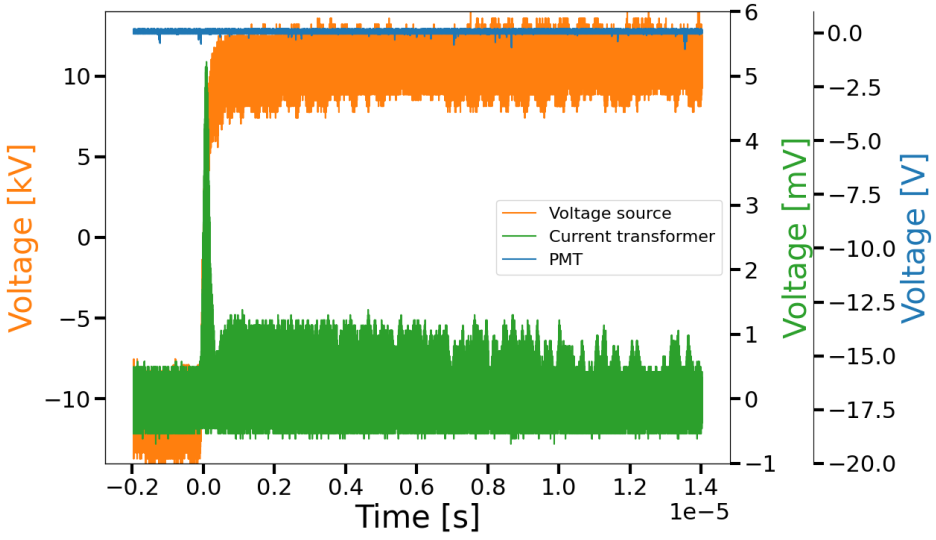


*Figure 102: Midel 7131 impregnated insulation system. 11 $kV_{peak}$ applied voltage, positive voltage pulse. The signals were collected using the envelope function on the oscilloscope for 1 minute.*

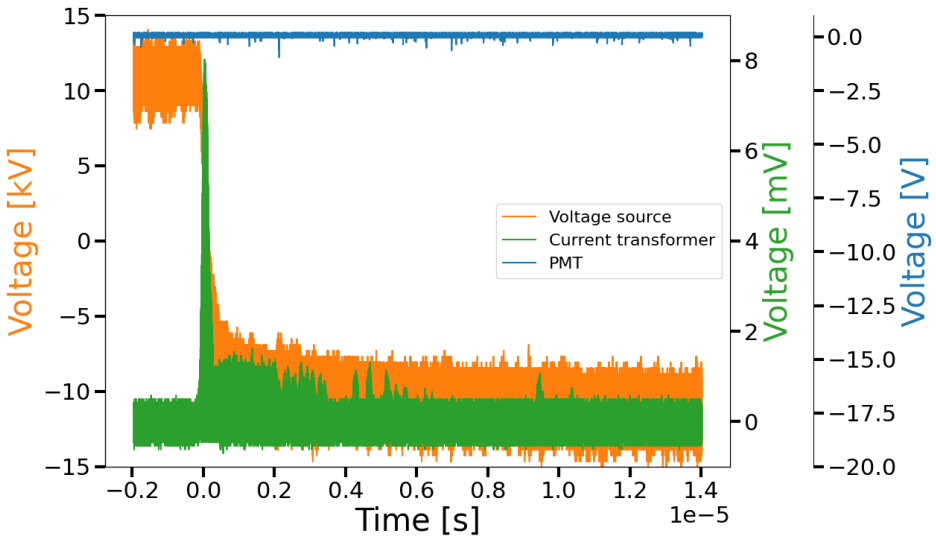


*Figure 103: Midel 7131 impregnated insulation system. 11 $kV_{peak}$ applied voltage, negative voltage pulse. The signals were collected using the envelope function on the oscilloscope for 1 minute.*

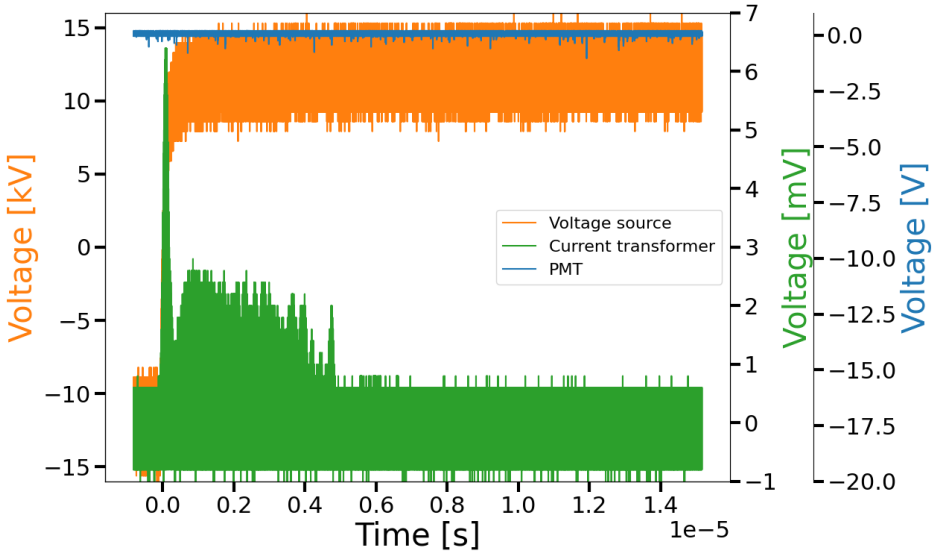


*Figure 104: Midel 7131 impregnated insulation system. 12 $kV_{peak}$ applied voltage, positive voltage pulse. The signals were collected using the envelope function on the oscilloscope for 1 minute.*

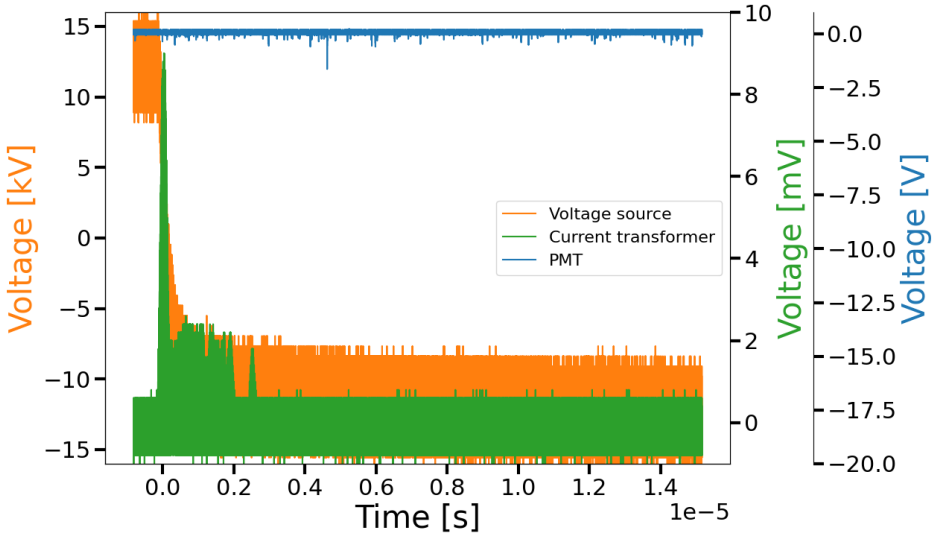


*Figure 105: Midel 7131 impregnated insulation system. 12 $kV_{peak}$ applied voltage, negative voltage pulse. The signals were collected using the envelope function on the oscilloscope for 1 minute.*

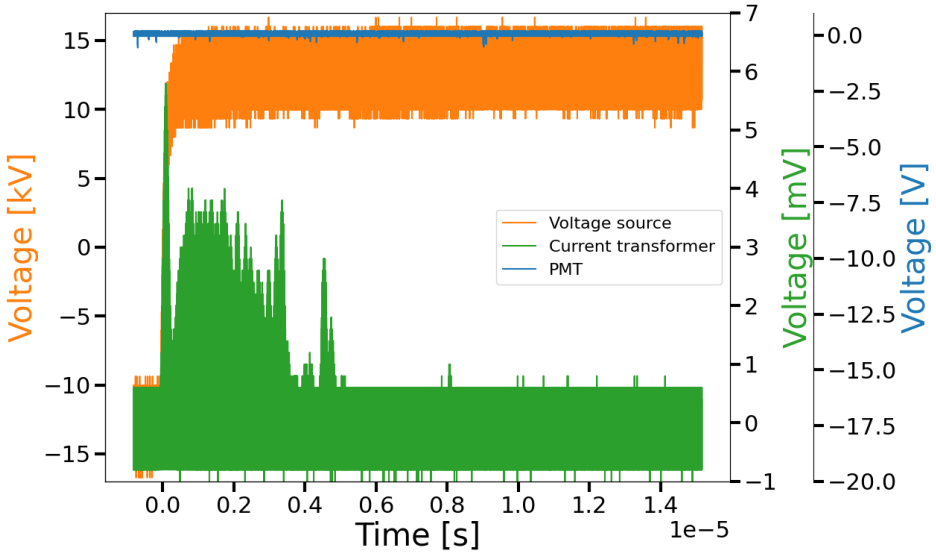


*Figure 106: Midel 7131 impregnated insulation system. 13 $kV_{peak}$ applied voltage, positive voltage pulse. The signals were collected using the envelope function on the oscilloscope for 1 minute.*

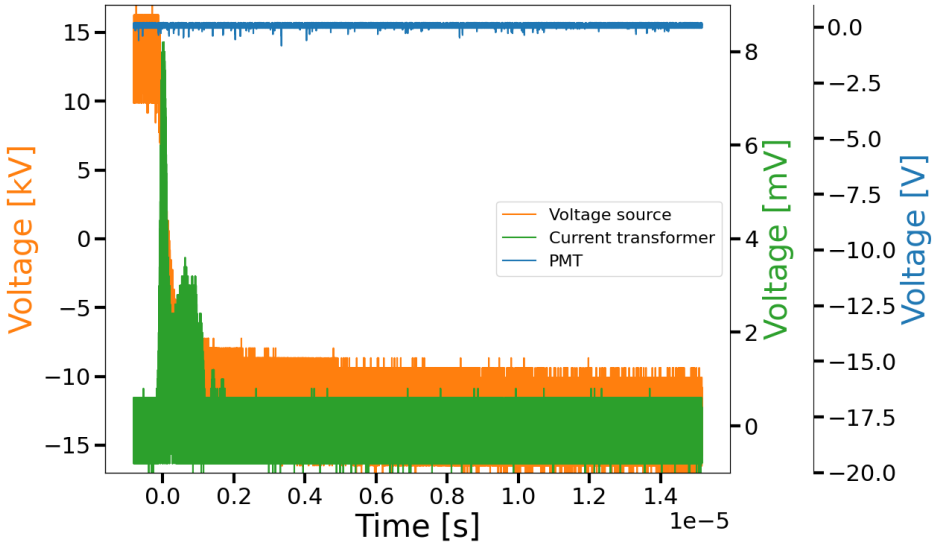


*Figure 107: Midel 7131 impregnated insulation system. 13 $kV_{peak}$ applied voltage, negative voltage pulse. The signals were collected using the envelope function on the oscilloscope for 1 minute.*

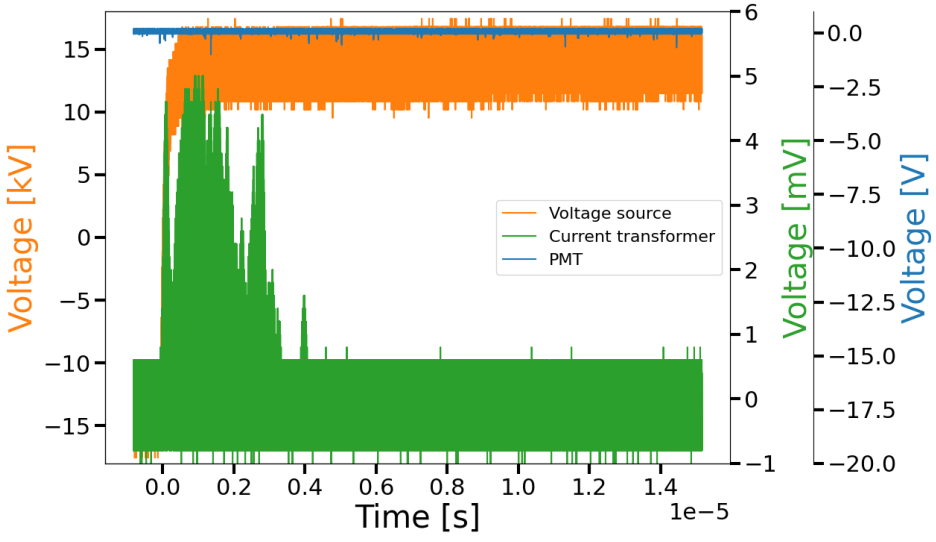


*Figure 108: Midel 7131 impregnated insulation system. 14 $kV_{peak}$ applied voltage, positive voltage pulse. The signals were collected using the envelope function on the oscilloscope for 1 minute.*

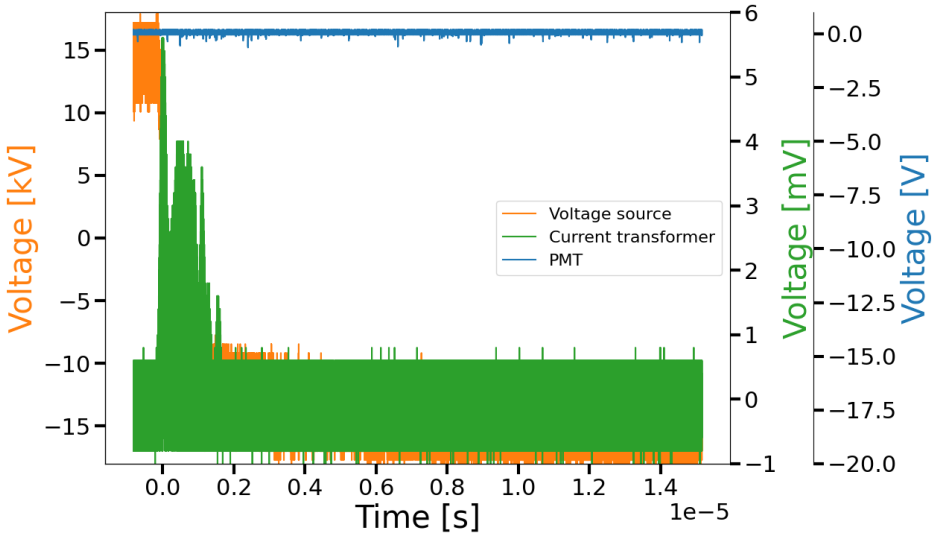


*Figure 109: Midel 7131 impregnated insulation system. 14 $kV_{peak}$ applied voltage, negative voltage pulse. The signals were collected using the envelope function on the oscilloscope for 1 minute.*

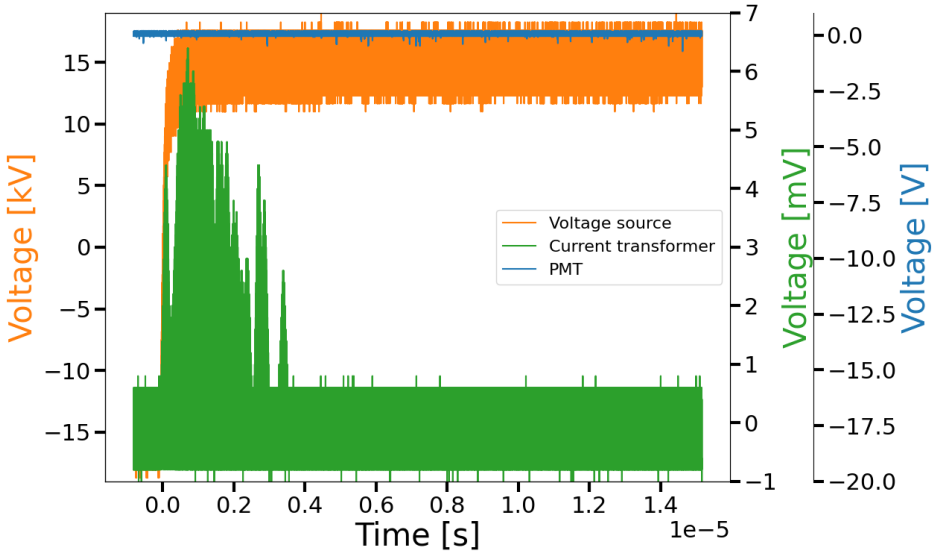


*Figure 110: Midel 7131 impregnated insulation system. 15 $kV_{peak}$ applied voltage, positive voltage pulse. The signals were collected using the envelope function on the oscilloscope for 1 minute.*

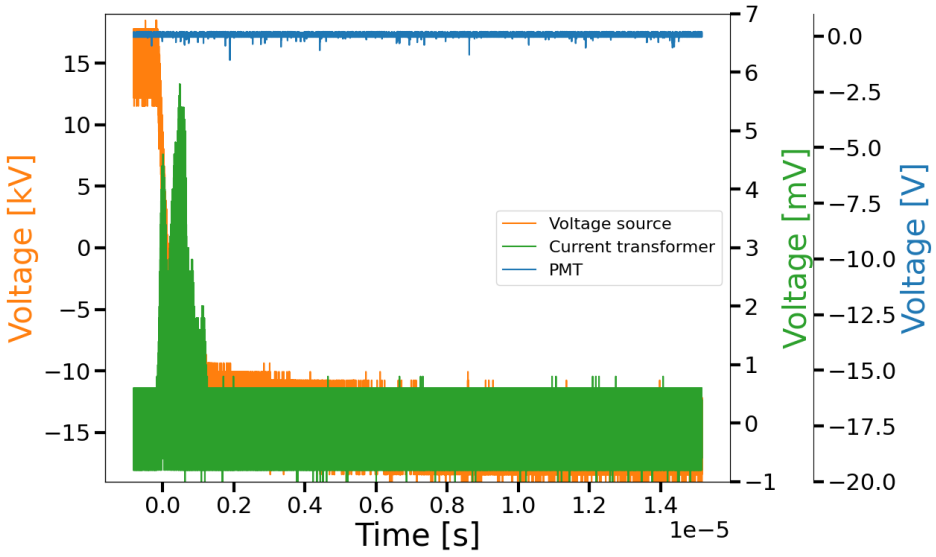


*Figure 111: Midel 7131 impregnated insulation system. 15 $kV_{peak}$ applied voltage, negative voltage pulse. The signals were collected using the envelope function on the oscilloscope for 1 minute.*

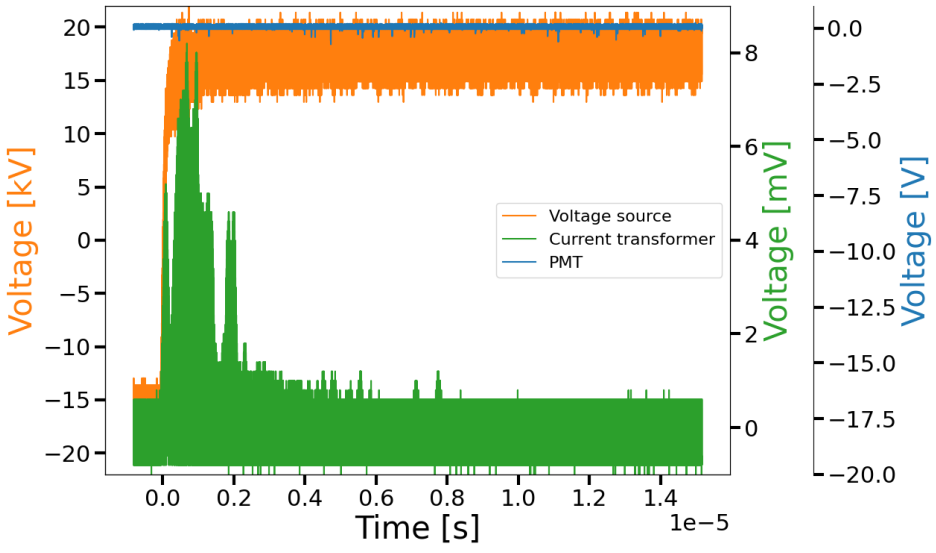


*Figure 112: Midel 7131 impregnated insulation system. 17 $kV_{peak}$ applied voltage, positive voltage pulse. The signals were collected using the envelope function on the oscilloscope for 1 minute.*

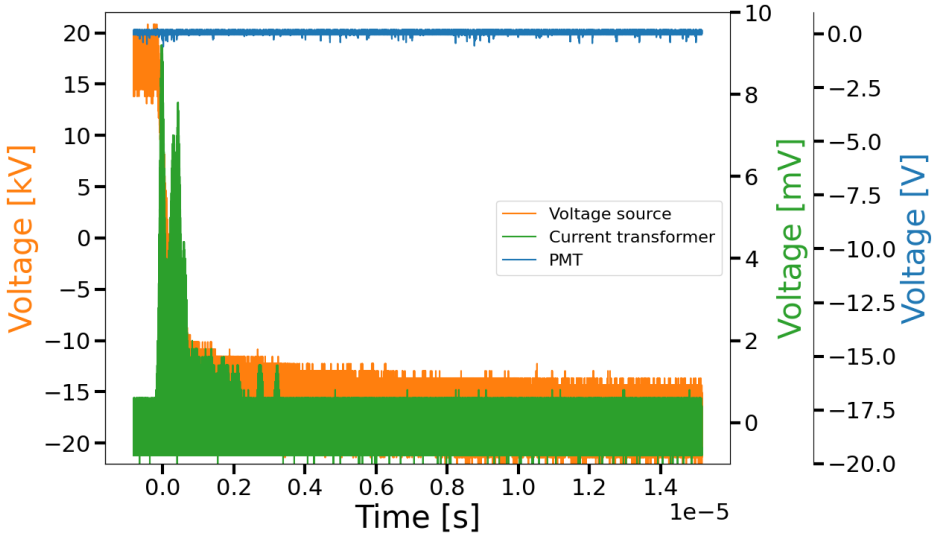


*Figure 113: Midel 7131 impregnated insulation system. 17 $kV_{peak}$ applied voltage, negative voltage pulse. The signals were collected using the envelope function on the oscilloscope for 1 minute.*

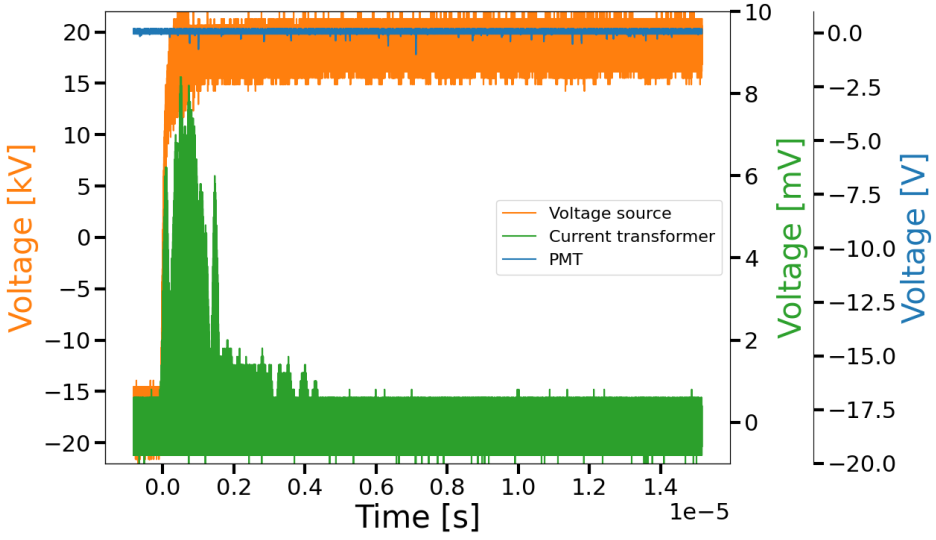


*Figure 114: Midel 7131 impregnated insulation system. 18 $kV_{peak}$ applied voltage, positive voltage pulse. The signals were collected using the envelope function on the oscilloscope for 1 minute.*

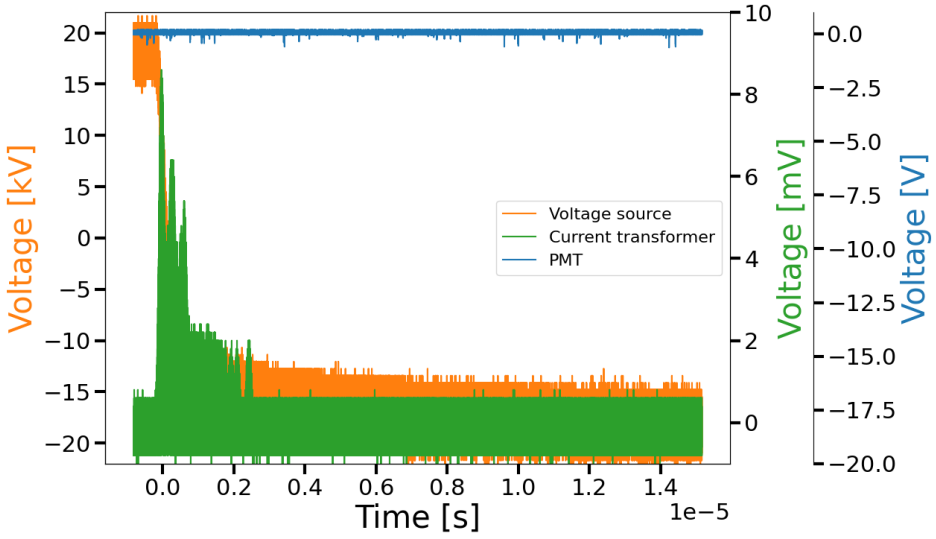


*Figure 115: Midel 7131 impregnated insulation system. 18 $kV_{peak}$ applied voltage, negative voltage pulse. The signals were collected using the envelope function on the oscilloscope for 1 minute.*

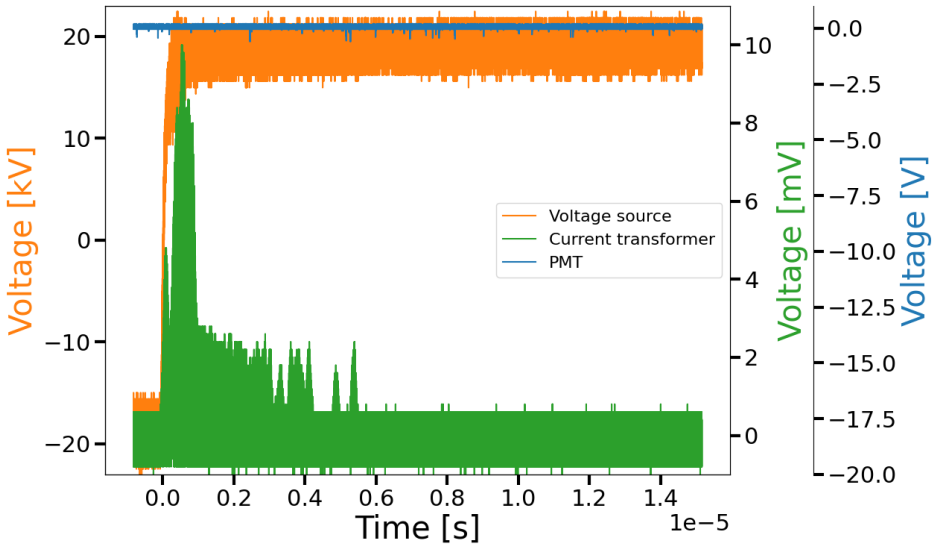


*Figure 116: Midel 7131 impregnated insulation system. 19 $kV_{peak}$ applied voltage, positive voltage pulse. The signals were collected using the envelope function on the oscilloscope for 1 minute.*

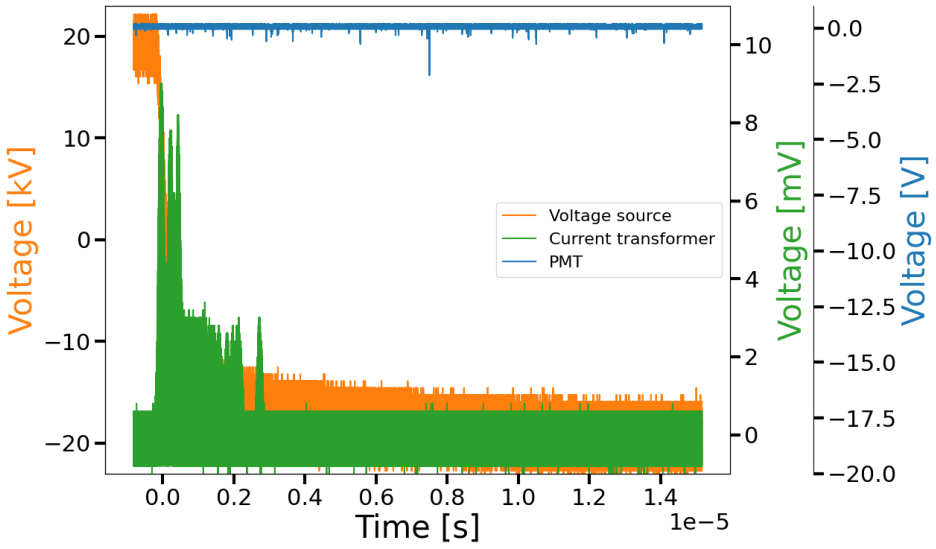


*Figure 117: Midel 7131 impregnated insulation system. 19 $kV_{peak}$ applied voltage, negative voltage pulse. The signals were collected using the envelope function on the oscilloscope for 1 minute.*

Fanny Skirbekk

# Transformer insulation stressed by power converters

NTNU
Norwegian University of
Science and Technology